

27744  
NATIONAL LIBRARY  
OTTAWA



BIBLIOTHÈQUE NATIONALE  
OTTAWA

NAME OF AUTHOR.....

NEED SHEK-HUNG

TITLE OF THESIS.....

Thermodynamics study of  
strong acid cation exchange

UNIVERSITY.....

Alberta

DEGREE FOR WHICH THESIS WAS PRESENTED.....

Ph.D.

YEAR THIS DEGREE GRANTED.....

1976

Permission is hereby granted to THE NATIONAL LIBRARY  
OF CANADA to microfilm this thesis and to lend or sell copies  
of the film.

The author reserves other publication rights, and  
neither the thesis nor extensive extracts from it may be  
printed or otherwise reproduced without the author's  
written permission.

(Signed).....

PERMANENT ADDRESS:

1026 38 Ave

Edmonton Alberta

DATED.....

26-4-

1976

NL-91 (1C-68)

## INFORMATION TO USERS

THIS DISSERTATION HAS BEEN  
MICROFILMED EXACTLY AS RECEIVED

This copy was produced from a microfiche copy of the original document. The quality of the copy is heavily dependent upon the quality of the original thesis submitted for microfilming. Every effort has been made to ensure the highest quality of reproduction possible.

PLEASE NOTE: Some pages may have indistinct print. Filmed as received.

Canadian Theses Division  
Cataloguing Branch  
National Library of Canada  
Ottawa, Canada K1A 0N4

## AVIS AUX USAGERS

LA THESE A ETE MICROFILMEE  
TELLE QUE NOUS L'AVONS RECUE

Cette copie a été faite à partir d'une microfiche du document original. La qualité de la copie dépend grandement de la qualité de la thèse soumise pour le microfilmage. Nous avons tout fait pour assurer une qualité supérieure de reproduction.

NOTA BENE: La qualité d'impression de certaines pages peut laisser à désirer. Microfilmée telle que nous l'avons reçue.

Division des thèses canadiennes  
Direction du catalogage  
Bibliothèque nationale du Canada  
Ottawa, Canada K1A 0N4

THE UNIVERSITY OF ALBERTA

THERMODYNAMIC STUDY OF STRONG ACID CATION EXCHANGE  
RESINS

(C)

by

JOSEPH SHEK-HUNG TANG

A THESIS

SUBMITTED TO THE FACULTY OF GRADUATE STUDIES AND RESEARCH  
IN PARTIAL FULFILLMENT OF THE REQUIREMENTS FOR THE DEGREE  
OF DOCTOR OF PHILOSOPHY

DEPARTMENT OF CHEMISTRY

EDMONTON, ALBERTA

SPRING 1976

THE UNIVERSITY OF ALBERTA  
FACULTY OF GRADUATE STUDIES AND RESEARCH

The undersigned certify that they have read,  
and recommend to the Faculty of Graduate Studies and  
Research, for acceptance, a thesis entitled THERMO-  
DYNAMIC STUDY OF STRONG ACID CATION EXCHANGE RESINS.

submitted by JOSEPH SHEK-HUNG TANG  
in partial fulfilment of the requirements for the degree  
of Doctor of PHILOSOPHY

B. Kratochvil  
B. Kratochvil, Supervisor

F.F. Cantwell

G. Horlick

J.S. Martin

F.D. Otto

D.J. Pietrzyk, External  
Examiner

Date February 26, 1974



This thesis is dedicated to my parents, without whose help this work would never have been started, and to my wife, Connie, whose faith and understanding made this presentation possible.

# ABSTRACT

The exchange constant for the reaction between hydrogen ion in solution and the strongly acidic resin Dowex 50W X8 in a mixture of the sodium and hydrogen forms was measured at 21°C by a modified stoichiometric method. This method consists of measuring the concentrations of any two species in the external solution, and from these measurements obtaining the concentrations of the remaining species in the resin and solution phases. Values agreed with those previously reported by other methods. A detailed analysis of the precision and accuracy of the exchange constant obtained by this method showed the optimum resin loading factor to be 0.4 or greater. The procedure is rapid and resin shrinkage, non-additivities of volume, and the presence of traces of water in the resin are all implicitly accounted for.

It was found that there is an increased uptake of  $H^+$  by Dowex 50W X8 at low hydrogen ion concentrations in the presence of  $NaCl$  in the external solution, which results in an approximately doubled retention volume in ion exchange chromatography. This behavior was studied by a dynamic method, and found to be specific for  $H^+$ . Three models, one heterogeneous and the other two homogeneous, were considered in an attempt to explain this behavior. The heterogeneous model, which arbitrarily distinguishes between two sites for  $H^+$

(i.e. ordinary  $-\text{SO}_3^-$  exchange sites, and sites due to Donnan sorption) was first excluded, owing to the failure of this model to interpret adequately the finding of a special affinity of Donnan sorption sites for  $\text{H}^+$ . The two homogeneous models are both based on association theory, and differ in the nature of the sites of association. The first proposes association between  $\text{H}^+$  and  $-\text{SO}_3^-$  in the resin, while the second is between  $\text{H}^+$  and  $-\text{CO}_2^-$  present as an impurity in the resin. Both models show the same sorption isotherm, and cannot be distinguished mathematically, but the one involving association between  $\text{H}^+$  and  $-\text{CO}_2^-$  is more realistic because the number of sorption sites found in this work is comparable to the number of carboxylate groups found to be present in this resin by earlier workers. Carboxylate groups appear primarily responsible for the extra uptake of  $\text{H}^+$ , although the possibility of a contribution to sorption by association between  $\text{H}^+$  and  $-\text{SO}_3^-$  cannot be excluded.

The sorption of weak organic acids on strong acid cation-exchangers was also studied. Using Reichenberg's data for the system  $\text{H}^+ \text{R}^- - \text{HA} - \text{H}_2\text{O}$  ( $\text{HA}$  = benzoic acid, butyric acid, propionic acid, or acetic acid), it was shown that the weak acid-dissociation equilibrium in external solution also exists in the resin phase, with the internal

dissociation constant  $K_1$  being of the same order of magnitude as  $K_1$  in solution. The molecular acid may be sorbed by both surface adsorption and true dissolution mechanisms; only the latter is in true equilibrium with  $\overline{HA}$  and  $\overline{A^-}$ .

The system  $Na^+R^- - HA - NaCl - H_2O$  ( $HA$  = chloroacetic acid, benzenesulfonic acid, phenylacetic acid) was also studied experimentally. The same conclusions as described above can be drawn, or correction for the additional hold-up of  $H^+$ .

#### ACKNOWLEDGEMENT

The author would like to express his appreciation to Dr. B. Kratochvil for his guidance and encouragement throughout this project; and to Dr. E. Cantwell for valuable advice.

Financial assistance from the National Research Council of Canada and the University of Alberta is gratefully acknowledged.

# TABLE OF CONTENTS

Page	Page
CHAPTER I INTRODUCTION	1
Liquid Ion Exchange	1
Membrane Ion Exchangers	2
Organic Ion Exchangers	3
Applications of Ion Exchangers	10
Mechanisms	10
Chromatography	10
Nonchromatographic Analytical Applications	13
Isotopic Applications	13
Catalysis	16
CHAPTER II SPECTROPHOTOMETRIC DETERMINATION OF THE ION EXCHANGE CONSTANT FOR SODIUM AND HYDROGEN ON DEXTRANSOULFONATE SULFONIC ACID FILMS	19
Background	19
Experimental	26
Treatment of Data	29
Precision and Reliability	32
The Magnitude of Measurement Errors	34
Results and Discussion	40

Title	Page
CHAPTER III SORPTION OF TRACE AMOUNTS OF HCl IN THE PRESENCE OF NaCl ON DOWEX 50W x 8 CATION EXCHANGE RESIN	49
Background	49
Models of Resin	54
1) Quasi-homogeneous Model	54
2) Quasi-heterogeneous Model	56
Purpose	59
Experimental	62
Determination of Single Electrolyte Sorption	62
Determination of Ion Exchange Equili- brium Constants by a Dynamic Method	63
Determination of Trace Amounts of HCl on Dowex 50W x 8 in the Presence of NaCl	64
Results and Discussion	66
Sorption of Electrolyte	66
Ion Exchange equilibrium Constant $K$ and Total Exchange Capacity $C$	71
Proposed Mechanism for Additional Hold-up of $H^+$	76
Comments on the Two Models	87
Chromatography	93
CHAPTER IV FURTHER STUDIES OF THE HOMOGENEOUS MODEL	96
Sorption of Trace NaCl from Solutions of HCl on Dowex 50W x 8	96

Page	Title
	CHAPTER IV (Cont'd)
96	Experimental Procedure
96	Measurement of $K_{Na/H}$
98	Flame Photometric Determination of Na
99	Measurement of $K_{Na/H}$
104	Results and Discussion
105	Sorption of NaCl in KCl on Dowex 50W-8
105	Experimental Procedure
109	Results and Discussion
112	Sorption of HCl in NaCl on Dowex 50W-2
113	Experimental Procedure
114	Results and Discussion
123	Sorption of HCl in NaCl on Amberlyst 15 Macroreticular Resin
124	Experimental Procedure
125	Results and Discussion
132	Sorption of HCl in the Presence of Large Quantities of NaCl on an Empty Column
133	Experimental Procedure
134	Results and Discussion
136	CHAPTER V SORPTION OF WEAKLY DISSOCIATED ELEC- TROLYTES ON THE SULFONIC ACID ION EXCHANGE RESIN DOWEX 50W-8
136	Sorption of Nonelectrolytes
136	Simple Dissolution of Neutral Solutes in the Interior Solvent of the Resin Phase



# Title

## CHAPTER V. (Cont'd)

London Dispersion Interactions	140
Salting-out Effect	141
Polar Interactions	143
Specific Interactions: Salting-in Effect	144
Simultaneous Sorption and Exchange of Weakly Dissociated Electrolytes: Organic Ions as Counter Ions in the System $\text{H}^+\text{A}^- - \text{HA} - \text{H}_2\text{O}$	145
Simultaneous Sorption and Exchange of Weakly Dissociated Electrolytes: Organic Ions as Corons and Hydrogen Ions as Counter Ions in the System $\text{H}^+\text{P}^- - \text{HA} - \text{H}_2\text{O}$	146
Thermodynamic Model	149
Scheme 1	151
Scheme 2	152
Interpretation of Previous Work	153
Simultaneous Sorption and Exchange in the System, $\text{HA} - \text{NaCl} - \text{H}_2\text{O} - \text{Dowex 50W-X8}$	154
Experimental	156
Reagents	156
Preparation of Solutions	156
Procedure	157
Determination of HA and $\text{A}^-$ by UV Spectrophotometry	158
HBSA	158
HPAA	159
HCAA	170
Results and Discussion	171

<u>Title</u>	<u>Page</u>
CHAPTER V (Cont'd)	
HBSA-NaCl-H <sub>2</sub> O-Dowex 50W x 8 System	172
HPAA-NaCl-H <sub>2</sub> O-Dowex 50W x 8 System	176
HCAA-NaCl-H <sub>2</sub> O-Dowex 50W x 8 System	187
CONCLUSIONS	191
GLOSSARY	194
BIBLIOGRAPHY	197
APPENDIX I	206
APPENDIX II	214
APPENDIX III	220

# LIST OF TABLES

Table		Page
1a	Measurement of H	38
1b	Measurement of Cl	38
1c	Measurement of $V_a$	39
1d	Measurement of C	39
1e	Measurement of $H_o$	40
2	Comparison of values for $AK/k$ as measured and as calculated by emr equation (8) Experiment (A) $\alpha = 0.516$ Experiment (B) $\alpha = 0.999$	44 45
3	Comparison of K values obtained by stoichiometric method and dynamic method	48
4	Variation of $K$ with $\overline{X}_{Na}$ at ionic strengths 0.2 and 0.07	75
5	Total sorption of HCl at various concentrations of HCl and NaCl	78
6	Data for measurement of total $H^+$ in resin phase by column equilibration at various $Na^+$ and $H^+$ concentrations in external solution	84
7	Values for ratio of intercept to slope and of total $H^+$ in resin phase to $H^+$ concentration in external solution as a function of $Na^+$ concentration	85
8	Variation of $K_{Na/H}$ with ionic strength and concentration ratio for Dowex 50w x 8 at 21°C	101
9	Total sorption of $Na^+$ as a function of [HCl] and [NaCl] on Dowex 50w x 8 at 21°C	103

10	Total sorption of NaCl at various concentrations of KCl and NaCl on Dowex 50w x 8	108
11	Variation of $K_H/Na$ of Dowex 50w x 2 with ionic strength and concentration ratio at 21°C	116
12	Total sorption of $H^+$ as a function of [HCl] and [NaCl] on Dowex 50w x 2	117
13	Intercept and slope of lines in Figure 18	117
14	Variation in $K_H/Na$ with ionic strength and concentration ratio for the macroreticular resin Amberlyst 15 at 21°C	127
15	Total sorption of $H^+$ as a function of [HCl] and [NaCl] on Amberlyst 15 at 21°C	128
16	$H^+$ sorption on empty Pyrex column at 20°C	135
17	Internal dissociation constant $\bar{K}_i$ of organic acids in 1 g of dried (5.3 meq) 10% DVB sulfonated polystyrene resin in the hydrogen form at 25°C	160
18	Spectrophotometric determination of benzene sulfonic acid HBSA on Dowex 50w x 8	173
19	Coulometric determination of $H^+$ sorbed on Dowex 50w x 8 in HBSA/NaCl mixture	174
20	Coulometric and spectrophotometric determination of HPAA sorbed on Dowex 50w x 8, HPAA <sub>1</sub> in HPAA/NaCl mixture at 25°C	179
21	Calculation of internal dissociation constant $\bar{K}_i$ for phenylacetic acid, HPAA, in Dowex 50w x 8	181

# LIST OF FIGURES

<u>Figure</u>		<u>Page</u>
1	Plots of relative uncertainty $\Delta K/K$ against, $\alpha$	41
2	Arrangement of electrodes for monitoring pH of ion exchange column effluent	65
3	Plots of the ratio of amount of ion sorbed to ion concentration against concentration for $\text{Na}^+$ and $\text{H}^+$ as NaCl and HCl	69
4	Plots of ion exchange constant K for $\text{Na}^+ - \text{H}^+$ exchange on Dowex 50w x 8 as function of the mole fraction of resin in the $\text{Na}^+$ form at ionic strengths 0.2 and 0.07	74
5	Plots of ratio of total $\text{H}^+$ in resin phase over $[\text{H}^+]$ against $[\text{H}^+]$ at varying concentrations of $\text{Na}^+$ in the external solution	79
6	Plots of ratio of total $\text{H}^+$ in resin phase over $\text{H}^+$ concentration against reciprocal of $\text{Na}^+$ concentration at varying concentrations of $\text{H}^+$ in the external solution	80
7	Plots of $\text{H}^+$ concentration in external solution over sorbed $\text{H}^+$ against $\text{H}^+$ concentrations in external solution at several concentrations of $\text{Na}^+$ in external solution	82
8	Plots of the ratio of the intercept to slope from Table 7 against $\text{Na}^+$ concentration in external solution	86
8a	Plots of $\text{Na}^+$ sorption due to Donnan invasion against the effective capacity $\alpha$	88
9	Comparison of 3 methods for determining the ratio of total $\text{H}^+$ in resin phase over $\text{H}^+$ concentration at different $\text{Na}^+$ concentrations in external solution	95

10	Plots of ion exchange constant $K$ for $\text{Na}^+ - \text{H}^+$ exchange on Dowex 50w x 8 as function of the mole fraction of resin in the $\text{H}^+$ form at ionic strengths of 0.1, 0.2, 0.5 and 1	102
11	Plots of ratio of total $\text{Na}^+$ in resin phase over $\text{Na}^+$ concentration against $\text{Na}^+$ concentration at varying concentrations of $\text{H}^+$ in the external solution	<u>104</u>
12	Plots of ratio of total $\text{Na}^+$ in resin phase over $\text{Na}^+$ concentration against reciprocal of $\text{H}^+$ concentration at zero concentrations of $\text{Na}^+$ in the external solution	106
13	Plots of ratio of total $\text{Na}^+$ in resin phase over $\text{Na}^+$ concentration against $\text{Na}^+$ concentration at varying concentrations of $\text{K}^+$ in external solution	110
14	Plots of ratio of total $\text{Na}^+$ in resin phase over $\text{Na}^+$ concentration against the reciprocal of $\text{K}^+$ concentration at varying concentrations of $\text{NaCl}$ in external solution	111
15	Plots of ion exchange constant $K$ for $\text{H}^+ - \text{Na}^+$ exchange on Dowex 50w x 2 as a function of the mole fraction of resin in the $\text{Na}^+$ form at ionic strengths of 1, 0.5 and 0.1	115
16	Variation of ion exchange constant $K$ for $\text{H}^+ - \text{Na}^+$ exchange on Dowex 50w x 2 in $\text{Na}^+$ form with ionic strength	118
17	Plots of ratio of total $\text{H}^+$ in the resin phase of 16.9 meq Dowex 50w x 2 over $\text{H}^+$ concentration against $\text{H}^+$ concentration at varying concentrations of $\text{Na}^+$ in the external solution	120
18	Plots of $\text{H}^+$ concentration in external solution over sorbed $\text{H}^+$ on Dowex 50w x 2 against $\text{H}^+$ concentration in external solution at several concentrations of $\text{Na}^+$ in the external solution	121

19	Plots of the ratio of the intercept to slope from Table 13 against $\text{Na}^+$ concentration in the external solution	122
20	Plots of ion exchange constant $K$ for $\text{H}^+ - \text{Na}^+$ exchange on Amberlyst 15 as function of the mole fraction of resin in the $\text{Na}^+$ form at ionic strengths of 1, 0.5, and 0.1	126
21	The variation of ion exchange constant $K$ for $\text{H}^+ - \text{Na}^+$ exchange on Amberlyst 15 in $\text{Na}^+$ form with ionic strength	129
22	Plots of ratio of total $\text{H}^+$ in the resin phase of Amberlyst 15 over $\text{H}^+$ concentration against $[\text{HCl}]$ at varying concentrations of $\text{Na}^+$ in the external solution.	130
23	The sorption of organic weak acids on Dowex 50w x 8 in $\text{H}^+$ form at various organic acid concentrations in external solution	161
24	Comparison of the ratio of total sorbed HBSA on Dowex 50w x 8 over $\text{H}^+$ concentration in equilibrium with HBSA in external solution at various $\text{H}^+$ and $\text{NaCl}$ concentrations and with that of $\text{HCl}$ in Figure 5	175
25a, b	The total sorption of HPAA on Dowex 50w x 8 at various concentrations of HPAA and $\text{NaCl}$	182 183
26	Comparison of the ratio of total sorbed HCAA on Dowex 50w x 8 over $\text{H}^+$ concentration in equilibrium with HCAA in external solution at various $\text{H}^+$ concentration and with that of $\text{HCl}$ in Figure 5.	189

## CHAPTER 1

### Introduction

That many products in nature, such as cellulose, coal and clay, exhibit ion-exchange behavior as was discovered centuries ago. However, because of a number of undesirable properties possessed by these natural ion exchangers, including low capacity and poor physical form, they have only limited use. In recent years, synthetic ion exchangers have been developed and marketed that overcome the handicaps of the natural materials and that are tailor-made for special purposes.

Synthetic ion exchangers can be divided roughly into three kinds - liquid, solid inorganic and solid organic.

#### Liquid Ion Exchangers

Liquid anion exchangers are prepared by dissolving long chain aliphatic amines (containing on the order of 15 to 18 carbon atoms) in a nonaqueous solvent that is completely immiscible with water. The amine itself may be primary, secondary or tertiary, or even quaternary in spite of the large solubility of the ionic form in water. Amberlite LA-1 (dodecenyl-[trialkylmethyl] amine,  $RR'R''C-NH-CH_2CH=CHCH_2C(Me)_2CH_2C(Me)_3$ , where  $R$ ,  $R'$  and  $R''$  are side chains containing 18 to 15 carbons,



Rohm and Haas Co.) and Amberlite LA-2 (lauryl[trialkylmethyl]amine,  $RR'R''CNHCH_2(CH_2)_{10}CH_3$ , Rohm and Haas Co.) are two examples. Organic solvents typically used include chloroform and nitrobenzene.

Liquid cation exchangers are acids that are dissolved in organic solvents, such as dialkyl esters of phosphoric acid,  $(C_8H_{17}O)_2POO^-H^+$ , and monoalkyl esters of alkane phosphonic acids,  $(C_8H_{17})PO(OC_8H_{17})O^-H^+$ , in chloroform. The number of carbon atoms in the side chain is 8 to 17.

Liquid ion exchangers are compounds containing exchange sites dissolved in an organic solvent<sup>1,2</sup>. The ideal liquid ion exchanger should be insoluble in water, yet soluble in water-immiscible organic solvents in the concentration range 2 to 12%, and stable toward acids and oxidants. It should also have high selectivity, small surface activity, and large exchange capacity. Compared with solid exchangers, advantages include greater selectivity<sup>3</sup> and a higher exchange rate. Furthermore, liquid ion exchangers do not contain interstitial water; this eliminates dead volume corrections.

#### Inorganic Ion Exchangers

Inorganic ion exchangers had been reviewed by Amphlett<sup>4</sup> and can be classified into the following types:

- 1) Hydrous oxides of Cr(III), Zr(IV)<sup>5</sup>, Sn(IV), Th(IV), Si(IV), and Al(III). Owing to the amphoteric

3

character of these metal oxides, they act as weak acid cation exchangers at high pH values, as an anion exchanger at low pH values, and as both in intermediate pH ranges. They can withstand high temperatures and high levels of radiation, and in general undergo rapid exchange, but can be used only over a narrow pH range, and have relatively low capacities.

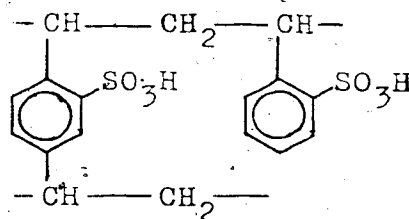
2) Gelatinous salts of multivalent metals. These include the antimonate, arsenate, molybdate or tungstate salts of Ti(IV), Sn(IV) or Sb(V). The exchange properties of these materials depend on the composition. Advantages and disadvantages are similar to the hydrous oxides listed above.

3) Zeolites. The zeolites have a crystalline structure consisting of  $\text{AlO}_2^-$  or  $\text{SiO}_2$  units containing metal ions such as  $\text{Na}^+$ ,  $\text{K}^+$ , or  $\text{Ca}^+$  sitting inside inter-~~4.1~~ tetrahedral or octahedral holes. Typically, holes of 11.4 Å diameter are interconnected through "windows" of 4.2 Å diameter. Though they exhibit cation exchange properties, zeolites are used mainly as molecular sieves in the dehydrated state<sup>6</sup> for adsorption of water or other small polar molecules from gases and liquids.

#### Organic Ion Exchangers

Organic ion exchangers are by far the most common type of those mentioned above, and have received the

greatest attention. They are composed of a cross-linked hydrocarbon polymer network on which a number of ionized or ionizable groups such as  $-\text{SO}_3^-$ ,  $-\text{CO}_2^-$ ,  $-\text{NH}_3^+$ , or  $-\text{N}^+(\text{Me})_3$  is incorporated. The first two, which bear negative charges, will exchange cations, and are called cation exchangers; the other two are anion exchangers. Organic ion exchangers are synthesized by polymerization of small monomers, either via condensation or addition steps in the presence of a catalyst. The cation exchange resin studied in this work is a sulfonated polystyrene resin with different degrees of crosslinking. It is made by addition polymerization via a free radical mechanism under the influence of a catalyst such as benzoyl peroxide and mild heat. The polymerizing mixture contains styrene, along with some divinylbenzene (DVB) to serve as a crosslinking agent between the chains. The degree of crosslinking is controlled by the percentage of DVB used. Polymerization conditions must be well controlled



because the physical form of the resin is directly affected by those conditions. The size of the drop-lets formed from the solution after polymerization is

determined chiefly by the viscosity, degree of mixing and nature of suspension stabilizer, gelatin, polyvinyl-alcohol, or sodium oleate, for example, to keep the polymer suspended in solution. A wide range of physical forms can be obtained by suitable combination of these factors. A sulfonation reaction is then carried out to add the sulfonate groups on the benzene rings with the product fully swelled in toluene or nitrobenzene.

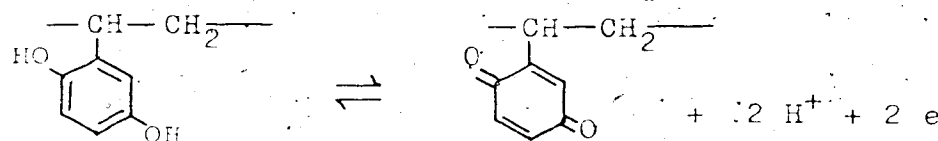
Organic ion exchanger resins can further be classified according to physical state or functional groups. With regard to the physical state, there are three types of ion exchangers, namely microreticular (the conventional gel-type of resin), macroreticular, and pellicular. Macroreticular resins<sup>7,8,9</sup> are formed in a medium which is a good solvent for the monomer, yet is a poor swelling agent for the product polymer. They are rigid, porous, and have a large surface area. Thus, they are suitable for use in nonaqueous solvents, which do not cause sufficient swelling in conventional resins to allow ions to diffuse readily into the resin pores. Pellicular ion exchange resin beads<sup>10,11</sup> consist of solid impenetrable cores of 30 to 40  $\mu$ m diameter with a thin porous layer of ion exchanger material approximately 1  $\mu$ m thick chemically bonded to the surface. They have high separating efficiency owing to reduced

mass transfer hindrance in the resin phase. The ratio of transfer resistance of a pellicular resin relative to a conventional spherical resin bead is <sup>12</sup>

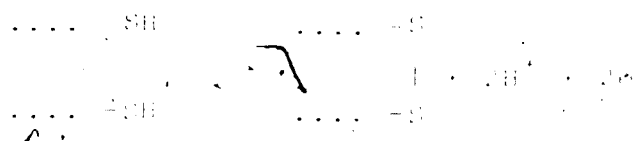
$$15\epsilon_F^3(1 - 2\epsilon_F)$$

where  $\epsilon_F$  is the fractional thickness of the layer. They are only used analytically as a column packing in modern high pressure ion exchange chromatography because of low capacity and high manufacturing costs.

A number of resins having special functional groups have also been synthesized and used for special purposes. Resins showing oxidation-reduction properties, called redox ion exchangers, redoxites, or electron exchangers, possess sites at which reversible redox reactions can be carried out <sup>13,14</sup>. The redox function may either come from the ions associated with the resin, such as  $\text{Cu}^{2+}$ ,  $\text{Fe}^{3+}$ , or  $\text{SO}_3^{2-}$ , which can act as oxidizing or reducing agents while coordinated to the resin, or from redox groups directly incorporated in the resin through synthesis. Examples include a hydroquinone electron exchanger,

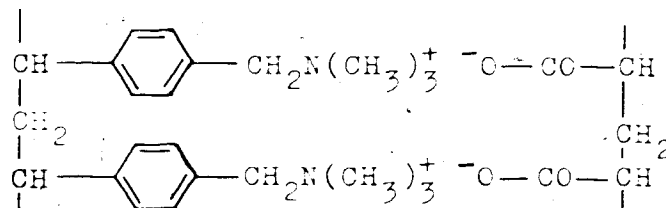


and a mercapto electron exchanger



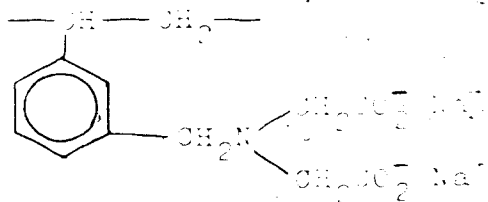
The redox strength depends on the functional group and on the ratio of oxidized to reduced form present. It is expressed quantitatively by the formal potential of the couple according to the Nernst equation. Unfortunately, redox capacities and reaction rates are usually low. Also, the resin itself is often chemically not stable. For these reasons redox resins are not used to any large extent.

Resins which have both positive and negative groups, and are held together by electrostatic forces, are designated as "snake cage" resins. They are prepared by polymerization of acrylic or methacrylic acid into different quaternary ammonium anion exchange resins<sup>15</sup>, and have the general structure shown below:



These materials attract ions in solution by electrostatic forces and, when used in column form, slow their rate

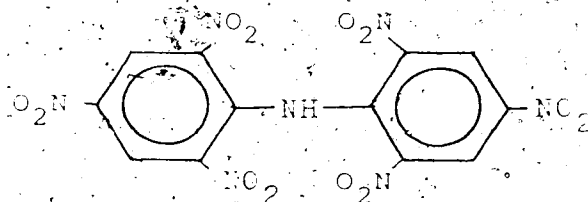
Some resins can complex heavy metal ions, either in their functional groups as coordinative ligands. These are called chelating resins<sup>12</sup>. The most known commercial product of this type is an aminodiacetate ion-exchanger (Dowex A-1, Dow Chemical Co.). The aminodiacetate group, a good complexing agent, is directly attached to a polystyrene matrix.



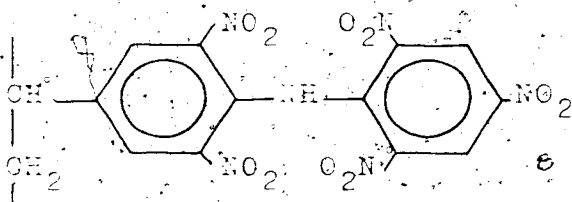
polyvalent metal ions such as  $\text{Cu}^{2+}$  form stable chelates with iminodiacetate and thus can be separated from

monovalent ions or ions which do not form strong complexes<sup>18,19</sup>.

In addition to the various resins described above, numerous other kinds have been synthesized for special purposes, and come under the general name of specific resins. One example is the incorporation of dipicrylamine,



a precipitating agent for  $K^+$ , into a polystyrene matrix to form a resin containing the group.



This material shows excellent uptake of  $K^+$ .

An optically active ion exchange resin<sup>20,21</sup> can facilitate the separation of racemates similar to the use of optically active natural products such as lactose and starch as adsorbent materials. For example, chloromethylated polystyrene resins react with optically active tertiary amines to yield an optically active strong base anion exchanger, on which the separation of



the d and l isomers of mandelic acid is feasible.

### Applications of Ion Exchangers

Ion exchange resins have a wide range of applications in analytical chemistry as well as in industry on a larger scale. The applications can roughly be classified according to whether the resin exchanges ions or catalyzes reaction without changing itself. Examples of each type of application are listed below.

#### Exchange

##### A) Chromatography (displacement, elution, and frontal)

Chromatography is by far the most important application of ion exchange resins in analytical chemistry, especially after the development of improved resin materials. The theory of ion exchange elution chromatography was developed in 1941 by Martin and Synge<sup>22</sup> using a plate concept, and modified by Glueckauf in 1955<sup>23,24</sup>. Of the various chromatographic parameters, the resolution R and the retention volume V<sub>R</sub> (time t<sub>R</sub>) are of prime importance in determining the separating efficiency of a column. Resolution is expressed as a function of ratio of partition coefficients and their absolute magnitude<sup>23,25</sup>. The retention volume depends on pH, ionic strength, composition of eluant, ion exchange constant, and specific interactions. In the

ideal case of a linear exchange isotherm and no interaction (solute-solute, solute-mobile phase, solute-stationary phase) other than exchange, values of  $V_R$ ,  $R$ , and the elution profile can be predicted quite accurately by theory. In reality most systems are far from ideal, especially for large molecules and ions which interact appreciably with the resin; in these instances  $V_R$  and  $R$  can only be estimated empirically. Pellicular ion exchange resins are especially adapted to modern high pressure liquid chromatography systems, and can separate virtually every kind of compound ranging from nonpolar molecules to fully ionized electrolytes. Because of rapid recent advances being reported in this area a complete description is impossible. Only significant examples are given.

---

In the area of polar compounds, the separation of nucleic acids<sup>26</sup> in the early 1950's with conventional resins required 16 hrs, while amino acids<sup>27</sup> required 22 hrs.. Through the use of pellicular resins the same separations now can be achieved in 1 hr<sup>28</sup> and 2 hrs<sup>29</sup>. Complex body fluids<sup>30</sup> such as urine, blood serum, and cerebrospinal fluid can be analyzed by high pressure exchange chromatographic techniques which were not feasible in the past.

Separation of inorganic compounds has also become faster and simpler. For example, the separation

of the lanthanides is possible by use of sulfonated polystyrene resins in 2 M acid<sup>31</sup>. The lanthanide and actinide elements can also be separated in weakly acidic solution by sorption on a strongly acidic cation exchanger, followed by sequential elution with an anionic complexing agent<sup>32</sup>. Alkali metals may be separated with an HCl/EtOH mixture as eluent on a cation exchanger resin<sup>33</sup>.

Another area, ion exclusion chromatography<sup>34</sup>, involves the separation of electrolytes from non-electrolytes. Electrolytes having the same counter ions as the resin phase are excluded from the resin due to Donnan potential (p. 66) and thus come out first from the column.

---

The technique of salting out chromatography<sup>35</sup> is used for the separation of nonelectrolytes using a salt solution as eluant. Addition of a salt such as  $(\text{NH}_4)_2\text{SO}_4$  to the eluting solution may influence the distribution of nonelectrolyte between mobile phase and resin phase as a consequence of the salting out effect. The effective concentration of nonelectrolyte increases with increasing salt concentration owing to the tying up of free water by the salt. The amount of nonelectrolyte sorbed on the resin is enhanced correspondingly. Nonelectrolytes have a larger retention volume and so are more readily separated in the presence of electrolyte.

To further facilitate the separation of mixtures, a number of techniques, such as use of nonaqueous and mixed solvents, two-step elution, gradient programming, and so on have been employed. These are powerful aids in achieving satisfactory separation conditions.

B) Nonchromatographic analytical applications.

Ion exchange resins are used in a variety of other applications. These include the demineralization of water, determination of total salt content of a mixture<sup>36</sup>, separation of interfering ions prior to a determination, changing the ions present in an electrolyte, concentrating ions of a salt in solution, dissolution of precipitates through shifting of equilibria, and measuring complex formation constants<sup>37</sup>.

Liquid ion exchangers are used in ion selective electrodes<sup>38</sup>.

C) Industrial applications

Ion exchangers are well-known for the desalination and softening of water. Either conductivity or drinkable water can be prepared. In waste water treatment, ion exchange is the most effective method known for the quantitative (up to 99.99%) removal of radioactive ions from waste solutions of nuclear reactors<sup>39</sup>. Even poliomyelitis virus in contaminated water can

be inactivated by an ion exchange process<sup>40</sup>. Ion exchange technology is also important in hydrometallurgical practice including winning, purification, and concentration of metal ions and in the recovery of metals from hydrometallurgical effluents. For example, uranium can be recovered from low grade uranium ores as  $\text{UO}_2(\text{SO}_4)_n^{2-2n}$  ( $n = 1, 2, 3$ ) by use of an anion-exchange resin (Porter-Arden process), a liquid ion exchanger of the weak base amine type (Amex process), or a combination of the two (Eluex process<sup>41</sup>). The yields approach 98%<sup>42</sup>. Thorium, which occurs simultaneously with uranium, can be extracted in a similar way by a liquid ion exchanger<sup>43</sup>. Gold<sup>44</sup> and platinum are removed from waste leach solutions in ore processing in the forms of  $[\text{Au}(\text{CN})_2]^{-1}$  and  $[\text{PtCl}_6]^{-2}$  by anion exchange resins which are later incinerated to recover the metals. Chromium-containing effluents can be treated by anion exchange to remove chromic acid<sup>45</sup>. Nickel from the rinse cycle of nickel-plating baths is recovered in a similar way. Copper<sup>46</sup>, zinc<sup>47</sup> and iron<sup>48</sup> in waste effluents are readily removed by cation exchange resins. Ion exchange resins are widely used in the treatment of cane sugar juice, the refining of cane sugar and the production of sugar syrup. In this application, the ion exchanger serves a dual purpose - metal ions such as  $\text{Mg}^{2+}$ ,  $\text{Ca}^{2+}$ ,  $\text{Fe}^{3+}$ , and anionic components such as

inorganic anions, fats, waxes, and organic acids, are either demineralized by passage through a column of cation exchanger in  $\text{Na}^+$  or  $\text{NH}_4^+$  form, or removed by a combination of strong base anion exchanger and weak acid cation exchanger. The remaining colored components in sugar syrup after treatment with activated charcoal can also be removed by the above process. The wine industry<sup>49, 50</sup> uses cation exchangers to remove  $\text{K}^+$  (to improve stability on storage), a portion of the nitrogen compounds (to reduce turbidity due to albumin) and  $\text{Na}^+$  (to remove a soapy flavor); excess acid also can be reduced by anion exchangers.

Ion exchangers are valuable in the milk industry, where they can increase the calcium content in dairy products, reduce the sodium level to prolong shelf life and remove radioactive fallout products, particularly <sup>90</sup>Sr. In industrial chemical processes, such as the preparation of formaldehyde, glycol, phenol, acrylic acid, and citric acid, ion exchangers are used to eliminate impurities in products. Ion exchangers of large surface area (macroporous or macroreticular resins) are effective as drying agents and as adsorbents<sup>51</sup> comparable to silica and activated charcoal. These materials also have a wide range of application in drug manufacturing and medicine, where they are used to purify and concentrate products, or to convert products

into the desired ionic form. Finally, ion exchangers have been proposed to remove excess stomach acid and to reduce electrolyte leach in the blood and other body fluids.

### Catalysis

Ion exchange resins in the appropriate form serve as catalysts for several reactions<sup>52</sup>. The mechanism chiefly involves the counter ions associated with the exchange sites. Cation exchangers in the hydrogen form can catalyze dehydration, hydrolysis<sup>53,54</sup>, hydration<sup>55</sup>, esterification<sup>56</sup>, cracking of hydrocarbons, sugar inversion, and other reactions requiring active hydrogen ion to form intermediates. Exchangers loaded with  $\text{Hg}^{2+}$ ,  $\text{CN}^-$  or  $\text{OAc}^-$  exhibit the catalytic properties of these ions in solution. The reactions can be carried out in gas-solid or liquid-solid state. Since conventional organic resins tend to collapse in an anhydrous state, the efficiency may be greatly diminished under such conditions. In these cases, the use of an inorganic exchanger such as a zeolite is more profitable. The advantages of ion exchangers as catalysts

as follows:

The reactions are highly specific, and side reactions are suppressed.

The catalyst is readily separable from the products.

- iii) Ions of unusual oxidation state, such as Mn(III), which can serve as an active species in some reactions, may be stabilized.
- iv) Ion exchangers can be used for reactions which require a high concentration of the catalyst ion. The internal counter ion concentration can be as high as 6 N. Such high concentrations can cause trouble in conventional homogeneous solutions.

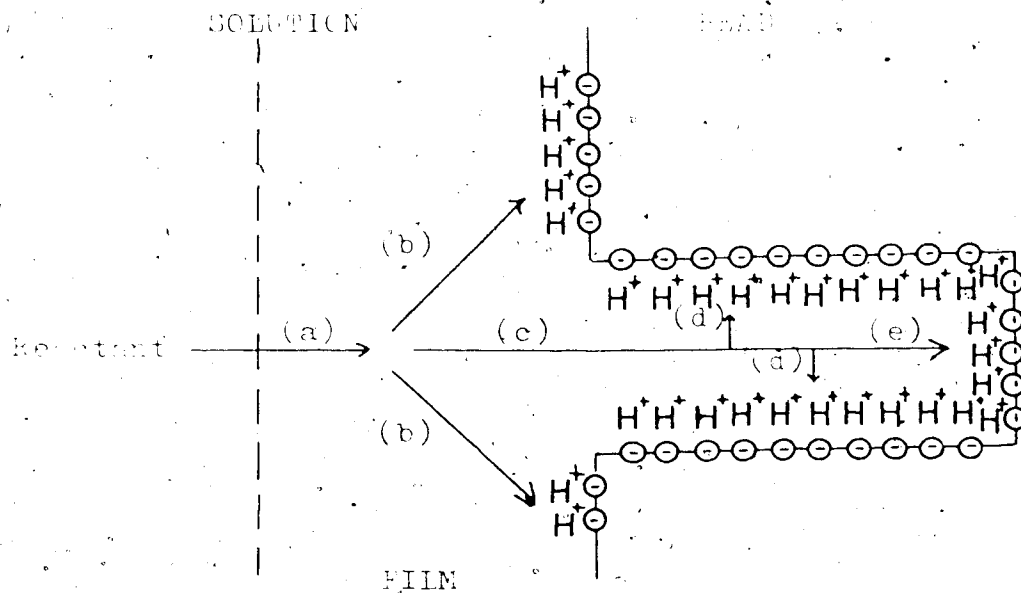
Stability in a thermal, chemical, and radio-chemical sense generally sets the limits on the use of ion exchangers as catalysts.

The theory<sup>57</sup> of catalysis by ion exchangers has not yet been fully developed. The catalytic behavior is believed to lie somewhere between homogeneous catalysis

and heterogeneous catalysis. The transport of reactants and products to and from the exchange sites is definitely heterogeneous in nature<sup>58</sup>, while the intrinsic reaction between the counter ion and reactant is homogeneous. The whole process can be broken down into several simple transport and reaction steps and treated separately. This is shown schematically as follows:

Film diffusion  $\xrightarrow{(b)}$  surface reaction  
 (a)  $\xrightarrow{(c)}$  diffusion into inner pores  $\xrightarrow{(d)}$  outer volume reaction  
 $\xrightarrow{(e)}$  intraparticle diffusion and internal reaction





An exact solution can be obtained for a first order reaction where the rate is directly proportional to the solute concentration, but the rate of overall reaction, which is a series or parallel combination of transfer and reaction steps, is determined by parameters such as particle size, flow rate, surface area, and so on. The effect of these parameters can be predicted quantitatively once the rate-determining step is known.

## CHAPTER IV

### STOICHIOMETRIC DETERMINATION OF THE ION EXCHANGE CONSTANT FOR SODIUM AND HYDROGEN ON DOWEX 50W · 8 SULFONIC ACID RESIN

#### Background

The ion exchange constant  $K$  is one of the important physical properties that must be known accurately for useful applications of ion exchangers to analytical or industrial problems. Methods for the determination of  $K$  fall into two types: batch and column. In the batch method<sup>59</sup>, the resin is immersed in a mixed salt solution containing the same co-ion as the resin. The solution is stirred at constant temperature until equilibrium is attained. The concentrations of both counter ions present in solution are then measured, the solution is drained from the resin, and the resin is washed several times with distilled water. The counter ions in the resin phase are now eluted by another electrolyte, the presence of which will not interfere with measurement of the counter ion concentration, and the concentration of counter ions displaced from the resin measured. From these data, the apparent ion exchange constant  $K$  for the reaction  $\bar{A} + B \rightleftharpoons A + \bar{B}$  can be calculated as:

$$K_{B/A} = \frac{[\bar{B}][A]}{[\bar{A}][B]}$$

The bar denotes the species in the resin phase.

The column method is faster than the batch method, because all the steps can be carried out continuously.

There are two different procedures by which an ion exchange constant can be measured in a column, the dynamic approach<sup>60,61</sup> and the chromatographic approach<sup>62</sup>.

In the dynamic method, a solution containing two salts is passed through a column of resin until the resin is completely equilibrated with the solution. The column is then rinsed with distilled water, the counter ions displaced from the resin by a solution containing a second electrolyte, and the displaced species measured. The ion exchange constant then can be obtained readily by the equation above.

The chromatographic method is also popular for the measurement of  $K$  if high accuracy is not required. The advantages are that attainment of equilibrium is not necessary and the data can be recorded automatically<sup>63</sup>.

Thus it is rapid and convenient. Rachinskii<sup>64</sup> gives a detailed discussion of the various kinds of ion exchange chromatographic methods available for the determination of  $K$  using radioisotope techniques. In the first method, named by the author eluted dynamic chromatography, the ionic species is measured directly in the column. For

the exchange of monovalent ions, it can be shown that

$$K = \left( \frac{XQ}{V - XQ} \right) \left( \frac{q_O s_O}{LQC_O} \right)$$

where  $X$  is the distance from the top of the column,

$L$  the column length,

$Q$  the cross sectional area of column,

$V$  the volume of solution passed,

$q_O$  the weight of ion exchanger in column,

$s_O$  the sorption capacity per unit weight, and

$C_O$  the solution concentration.

The second method is elution chromatography, which is the conventional mode of operation. The radioactivity is measured at the outlet of the column.

$$K = \left( \frac{LQ}{V_R - LQ} \right) \left( \frac{q_O s_O}{LQC_O} \right)$$

where  $V_R$  is the retention volume.

The third method is frontal chromatography, which is essentially identical to the dynamic method except that the amount of sorbed counter ion  $A$ ,  $S_A^O$ , is measured directly in the column by radioactivity counting

$$K = \frac{C_B}{C_A} \left( \frac{S_A^O}{S^O - S_A^O} \right)$$

Chromatography is often used when the solution consists of a complex mixture in which the batch and column methods are no longer applicable. For example,

For example, constant values of  $K$  and distribution ratios for the chlorides of Cu, Cd, Pb, Ni, Fe, Co, Mn, and Th, have been obtained. In a few cases,  $K$  with a low concentration of eluting water, which is then changed to 50 ml, the constant values are obtained. However, then values of  $K$  were used by calculation and not reliable. This is typically the case for ions possessing a high charge.

The dynamic method is by far the most convenient method for measuring values of  $K$ . It is more efficient than the batch method because the operation is continuous, which saves labor and requires less attention. It also provides rapid equilibrium and allows more complete rinsing. A large number of analytical applications of ion exchangers are performed in the chromatographic mode, therefore where a column is to be used for a later application, it is desirable to use the same column to determine  $K$  in situ under the same operating conditions. Furthermore, because the solution in the column is continuously being renewed during the measurement step, any contaminant in the resin phase, such as ions or soiled organic compounds, which could shift the equilibrium as well as interfere with the concentration measuring step, can be washed out by the eluting solution, and thus will not affect the measurement of  $K$ . No matter what the initial state of the resin, the same equilibrium

23  
state and  $K$  can be obtained for a given eluting solution.

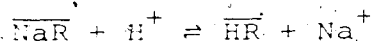
Finally, the apparent ion exchange constant  $K$  depends strongly on experimental conditions such as ionic strength and concentration ratio of counter ions in solution (mole fraction of counter ion in resin phase). Therefore  $K$  can be used to predict equilibrium concentrations only when these conditions are specified. If the value of  $K$  under specified conditions of ionic strength or concentration ratio  $[A]/[B]$  is desired, then only the dynamic method is applicable because only in this method is the resin in the final state in equilibrium with a solution of known ionic strength and composition. The equilibrium solution in a batch measurement will change composition at constant ionic strength due to redistribution of counter ions between the solution phase and the resin phase, making it difficult to obtain  $K$  at a specified solution composition unless the resin is washed successively with portions of solution until the solution composition does not change further<sup>66</sup>. This is by no means convenient. The dynamic method also has the peculiar feature that the whole isotherm can be calculated from the effluent history of one single column experiment<sup>67</sup>. However, it requires extreme control of experimental conditions as well as rapid local equilibrium between the solution and resin.

phases. This latter condition is not met adequately by inorganic ion exchangers or by moderately cross linked organic ion exchange resins and therefore this method is not recommended generally. But even though less convenient and efficient than the column method, the batch method still is important because it can be applied to ion exchanger materials in any physical form<sup>66</sup>, such as membranes, tubes or rods, whereas the column method can only be applied to beads possessing high fluid permeability. In the application of ion exchangers to industry, tubular column reactors<sup>68</sup> are by far the most commonly used, for example in counter-current<sup>69</sup> and fluidized processes<sup>70</sup>. The batch reactor<sup>71</sup> and CSTR (constant stirred tank reactor) are also used in some cases as in uranium recovery<sup>68</sup> and in mining processes<sup>72</sup> owing to cheaper construction costs and better isothermality<sup>73</sup>.

To maximize efficiency, minimize resin costs, allow monitoring of the activity of the exchanger, and allow calculation of exchange times for a given system, the exchange equilibrium constant  $K$  must be known. It is desirable where feasible to measure  $K$  in situ, as this involves the least expense of time and effort. The batch method is the only one that meets the above requirements; the drawback is that it involves a series of steps such as phase separation, washing, displacing

and determining four concentrations, which are quite tedious and time consuming.

A modified batch method, called the stoichiometric method, which is simple to handle yet accurate enough for industrial purposes has been proposed by Ghate, Gupta and Shankar<sup>74</sup>. Unfortunately these workers made use of this method without taking into account the change in water content of the dry resin when it was equilibrated with salt solution. This introduces error, especially when the volume of the equilibrating solution is small. Because air drying of samples of resin to constant weight is time consuming, a way of avoiding this step is desirable. The method described below does not require drying of the resin, and yet allows correction for the water remaining in the resin. It involves calculation of counter ion distribution in both phases by material balance after measuring the concentration of any two ions in solution. This method is faster than the others because phase separation and successive washing is not required, and is highly suitable to routine analysis. In this work, the desalination of sea water by ion exchange was studied, and the apparent ion exchange constant  $K_{H/Na}$  for the reaction



was measured.



Three species are present in solution at equilibrium;  $\text{Na}^+$ ,  $\text{H}^+$  and  $\text{Cl}^-$ . Only the concentrations of two ions are required, as the third can be obtained by charge balance.  $\text{Na}^+$  can be determined by flame photometry while  $\text{H}^+$  and  $\text{Cl}^-$  are most conveniently determined by acid-base and precipitation titration. The analysis of solutions for  $\text{H}^+$  and  $\text{Cl}^-$  were chosen because the titration procedure was more convenient than flame photometry. The value of  $K$  can then be calculated as shown in the next section.

### Experimental

#### Reagents

The resin selected for study was Dowex 50W-8 cation exchange (Dow Chemical) resin, 50 to 100 mesh. The properties of this resin as given by the manufacturer are: total exchange capacity (wet volume), 1.8 meq/ml; total exchange capacity (dry basis), 5.2 meq/g; moisture content, 54.7%; wet screen analysis, retained on US No. 35 sieve, 1.3%; passing through US No. 70 sieve, 3.8%. All other chemicals were of analytical grade, which met ACS specifications and were used as received without further purification. The sources were:  $\text{AgNO}_3$  (Johnson, Matthey and Mallory Ltd., Toronto),  $\text{NaOH}$  (Fisher Scientific Company),  $\text{K}_2\text{Cr}_2\text{O}_7$  (The British

Drug House Ltd., England), HCl (Baker Analyzed), and NaCl (Fisher Scientific Company).

#### Preparation of Standard Solutions

Standard solutions were prepared by the following procedures. Solutions of 0.3 M, 0.1 M, and 0.06 M NaOH were made by dissolving 24 g, 8 g and 4.8 g of NaOH pellets in distilled water in 2-litre volumetric flasks, and then standardized in duplicate against potassium hydrogen phthalate using phenolphthalein as indicator. The average concentrations were found to be 0.3014, 0.1023 and 0.06219 M. A solution of silver nitrate was prepared by weighing accurately about 34 g  $\text{AgNO}_3$ , dissolving in distilled water and diluting to volume in a 2-litre volumetric flask. The concentration was calculated to be 0.1001 M. Solutions of 0.1 M and 0.2 M HCl were prepared by diluting 15.9 ml and 31.8 ml of concentrated HCl (12.6 M) in distilled water in 2-litre volumetric flasks, and were standardized against 0.1 M NaOH phenolphthalein as indicator.

#### Procedure

About 40 meq of resin were used per run. The resin was allowed to stand in distilled water for a day to ensure complete swelling, then washed in an 800-ml beaker, first with 300 ml 6 M HCl and then with 300 ml distilled water to remove impurities, especially heavy

metals. The exchange capacity of the portion of resin was measured by direct titration of the  $H^+$  form with 0.3 M NaOH to the phenolphthalein end point in the 800-ml beaker. The resin was first converted to the  $H^+$  form by washing 3 times with 300 ml 6 M HCl, then the excess acid was removed by rinsing with several portions of distilled water until the equilibrated wash liquid was neutral as tested by pH paper. After decanting the excess water, 200 ml of 1 M NaCl solution and 5 drops of phenolphthalein indicator were added, the batch stirred and the suspension titrated with 0.3 M NaOH with vigorous stirring. A sharp end point was obtained.

After measuring the total capacity of the batch in this way, the resin was converted to the  $Na^+$  form by washing with three 200-ml portions of 1 M NaCl, and then with distilled water until a test of a portion of the equilibrated solution for  $Cl^-$  by  $AgNO_3$  was negative. The resin next was transferred quantitatively to a 500-ml volumetric flask. After excess water had been decanted, 200 ml of 0.1 M HCl were pipetted into the flask, the exact volume being measured by weighing the flask and contents before and after the acid was added, then dividing the weight by the density of 0.1 M HCl solution. The concentration of 0.1 M HCl added was measured by titration of a 25-ml solution with 0.1 M NaOH. The flask was tightly stoppered and the solution

stirred with a Micro V Magnetic Stirrer (Cole-Parmer, Chicago) for four hours at 22°C, at which time it was assumed equilibrium was obtained.

Two 25-ml portions of the liquid phase were pipetted into each of two flasks. The first was titrated with 0.06 M NaOH for  $H^+$ , the second with 0.1 M  $AgNO_3$  for  $Cl^-$  by the Mohr method<sup>75</sup>. The procedure, starting from measurement of total capacity of the resin in the 500-ml volumetric flask, was repeated 5 times. The experiment then was repeated using 0.2 M HCl in place of 0.1 M.

#### Treatment of Data

##### Definitions of Symbols Used

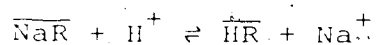
- $V_o$  volume of water retained with the resin, ml.
- $V_a$  volume of acid added, ml.
- $H_o$  concentration of acid added, M.
- $H$  concentration of hydrogen ion present in external solution at equilibrium, M.
- $Na$  concentration of sodium ion present in external solution at equilibrium, M.
- $Cl$  concentration of chloride ion present in external solution at equilibrium, M.
- $c$  capacity of resin sample used per experiment, meq.

$\underline{c}$  =  $c/(\underline{V}_a + \underline{V}_o)$  capacity per unit volume of external solution,  $\underline{M}$ .

$\overline{HR}$  total amount of hydrogen ion present in resin phase, meq.

$\overline{NaR}$  total amount of sodium ion present in resin phase, meq.

For the reaction



the equilibrium constant is given by

$$\underline{K} = \frac{\overline{HR}}{\overline{NaR}} \frac{Na}{H} \quad (1)$$

the charge balance is

$$Na + H = Cl \quad (2)$$

and the material balance is

$$\underline{c} = \overline{HR} + \overline{NaR} \quad (3)$$

At equilibrium, the concentrations are given by

$$H = H_o \left( \frac{\underline{V}_a}{\underline{V}_a + \underline{V}_o} \right) - Na \quad (4)$$

$$\overline{NaR} = \underline{c} - Na \left( \frac{\underline{V}_o + \underline{V}_a}{\underline{V}_o} \right) \quad (5a)$$

$$\overline{HR} = Na \left( \frac{\underline{V}_o + \underline{V}_a}{\underline{V}_a} \right) \quad (5b)$$

Since  $Cl$  and  $H$  can be measured, Equations (4) and (5) can be solved for  $Na$  and  $\underline{V}_O$

$$Na = Cl - H \quad (6a)$$

$$\underline{V}_O = \left( \frac{H_O - Cl}{Cl} \right) \underline{V}_a \quad (6b)$$

Substituting Equations (4) and (5) into (1) gives

$$K = \frac{Na}{H_O \left( \frac{\underline{V}_a}{\underline{V}_a + \underline{V}_O} \right) - Na} \cdot \frac{Na (\underline{V}_O + \underline{V}_a)}{C - Na (\underline{V}_O + \underline{V}_a)} = \frac{(Na)^2}{(B - Na) (C - Na)} \quad (7)$$

where

$$B = H_O \left( \frac{\underline{V}_a}{\underline{V}_a + \underline{V}_O} \right)$$

Then  $K$  can be calculated by inserting values for  $\underline{V}_O$  and  $Na$ , obtained from Equation (6), into Equation (7).

An important point to be noted is that it is not necessary to assume volume additivity and constant water content in the resin, because these factors have already been taken account of in the term  $\underline{V}_O$ . Actually,  $\underline{V}_O$  is the sum of three terms: the volume of external water adhering to the resin  $\underline{V}_O'$ ; the change in internal water content of the resin  $\Delta V_w$ , and any deviation from volume additivity  $\Delta V_v$ . Thus

$$\underline{V}_O = \underline{V}_O' + \Delta V_w + \Delta V_v$$

$\underline{V}_O'$  is always positive, while  $\Delta V_w$  and  $\Delta V_v$  may be positive

or negative. The magnitude of  $V_O$  is not necessarily greater than zero; especially if little water is carried along with the resin (i.e.  $V_O$  is small), and the volume shrinks and the resin swells tremendously upon the addition of acid (i.e.  $V_w$  and  $\Delta V_v \neq 0$ ).

### Precision and Reliability

It is of interest to consider the level of precision and reliability expected for  $K$  from these stoichiometric calculations. Since two material balances, one in the resin and one in the solution phase, are involved, along with a charge balance and several subtraction steps, the precision cannot be expected to be as great as for equilibrium values measured directly. Indeed, this method is not applicable to those experimental regions in which the subtraction of two nearly equal numbers is required. Because its usefulness depends on how precisely the value of  $K$  must be known, it is important to be able to predict at least semi-quantitatively the precision of  $K$  obtained, so that it can be compared with the precision desired. Values of  $K$  obtained by this method should not be used for subsequent calculations if the desired precision is insufficient; under these conditions, measurement by the batch method is the only choice.

Also, once the parameters affecting the precision have been identified and their magnitude estimated, one can avoid measurements in those regions which give the least precision. Indeed, a valid estimate of precision is an important criterion in all stoichiometric methods.

The uncertainty in  $K$  can be derived from error propagation theory<sup>76,77,78</sup>, the derivation of which is given in Appendix I. This theory can be applied to any stoichiometric system. The system considered here is assumed to be in complete equilibrium and all errors are assumed to arise only from the measurements, which are random in nature. As revealed from Equation (7), the uncertainty in  $K$  is determined by five independent measurement errors  $H_o$ ,  $V_a$ ,  $H$ ,  $Cl$ , and  $c$ ; that is,  $K = f(H_o, V_a, H, Cl, c)$ . If the measurement errors are not large, then the random error (variance) in  $K$  due to random errors in the variables is

$$s_K^2 = \left(\frac{\partial K}{\partial Cl}\right)^2 s_{Cl}^2 + \left(\frac{\partial K}{\partial H}\right)^2 s_H^2 + \left(\frac{\partial K}{\partial H_o}\right)^2 s_{H_o}^2 + \left(\frac{\partial K}{\partial V_a}\right)^2 s_{V_a}^2 + \left(\frac{\partial K}{\partial c}\right)^2 s_c^2$$

where  $s_x$  is the standard deviation of the quantity concerned,  $x$  ( $Cl, H, \dots$ ). From Appendix I, this equation can be written in relative error form as

$$\begin{aligned} \left(\frac{\Delta K}{K}\right)^2 &= \left(\frac{\Delta H}{H}\right)^2 (1+\alpha)^4 + \left(\frac{\Delta Cl}{Cl}\right)^2 (1+\alpha)^2 (2+\alpha)^2 \\ &+ (1+\alpha)^2 \left\{ \left(\frac{\Delta c}{c}\right)^2 + \left(\frac{\Delta V_a}{V_a}\right)^2 + \left(\frac{\Delta H_o}{H_o}\right)^2 \right\}, \quad \alpha = \frac{B}{c} \end{aligned} \quad (A8a)$$



and in absolute error form as

$$\left(\frac{\Delta K}{K}\right)^2 = (\Delta H)^2 \frac{(1+\alpha)^6}{\alpha^2 C'^2} + (\Delta C1)^2 \frac{(2+\alpha)^2 (1+\alpha)^2}{\alpha^2 C'^2} + (\Delta C')^2 \frac{(1+\alpha)^2}{C'^2} + \frac{(\Delta V_a)^2}{V_a^2} + \frac{(\Delta H_o)^2}{H_o^2} (1+\alpha)^2 \quad (A8b)$$

### The Magnitude of Measurement Errors

Measurement errors can be classified as nonrandom or random<sup>76,78</sup>. Nonrandom error, also called determinate error or systematic error, is generally in one direction and tends to be reproducible from measurement to measurement. It is caused by bias in the procedure from the operator, apparatus, or method. These can be avoided by modification of technique, equipment, or procedure. The other type, random error, is inherent to the measurement, and cannot be eliminated completely for a given system. Assuming there is no determinate error, then the measurement errors will follow a Gaussian distribution. By making several measurements  $\underline{X}_i$ ,  $i=1, \dots, N$ , and taking the average  $\bar{X}$ , the true value is best approximated. The standard deviation  $s_X$  for this set corresponds to the uncertainty of a single measurement  $\Delta X$ .

$$s_X = \sqrt{\frac{\sum (\underline{X}_i - \bar{X})^2}{N-1}} = \Delta X$$

If all measurement errors are random and their variance is known, the total uncertainty can be obtained either by (A8a) or (A8b).

Measurement errors can also be estimated by other means. For example, a precision of 1 ppt can be estimated with confidence in many aliquoting and titration procedures. Use of such values is convenient in predicting the uncertainty  $\Delta K/K$  for a typical experimental result. On the other hand, the probable error of an operation for a given individual is quite easily obtained by inserting into (A8a) or (A8b) the measurement errors of that individual as calculated from his daily work. In this way the precision of  $K$  can be estimated readily through (A8a) or (A8b) from only one set of measurements.

The variation in the uncertainty expression  $\Delta K/K$  with parameters  $a$  and  $c$  can be gotten only if the relationship between measurement errors and sample size is known. This relationship is usually too complicated to be evaluated. Measurement errors may vary or not with sample size depending on the source of the errors. For simplicity, only two of the most common cases will be considered: constant relative error (proportional error) and constant absolute error (constant error). These cases outline the general shape of the error curve. The former indicates a first

order linear relationship between error and sample size, while the latter does not depend on sample size at all.

For a volumetric titration, when the quantity of sample to be titrated is relatively large, the precision of the measurement is limited by buret reading error, by aliquoting error (if the sample is measured out by an aliquoting procedure), by weighing errors and by end point error<sup>79</sup>. In this instance, a constant relative error is likely. For strong acid-base titrations as well as for the Mohr method for chloride the overall relative error is on the order of 1 ppt. On the other hand, when the concentration of the sample to be titrated is low, a constant absolute error, determined by indicator sensitivity, initial concentration, and the magnitude of concentration change at the end point, is likely. A typical value for this error is about  $1 \cdot 10^{-4}$  M (1 ppt of 0.1 M solution).

The error in volume measurement  $V_a$  for the experimental work done in this thesis is likely to be a constant relative error, and is estimated to be 1 ppt. As for  $\xi$ , the error can be estimated as follows: The resin was titrated with 0.3 M NaOH, and the error in end point selection owing to the strong acid-base reaction, estimated to be 0.015 ml<sup>79</sup>, must be included with the error in buret reading and sample measurement. The

overall uncertainty in volume is estimated to be about 0.1 to 0.2 ml, giving an absolute error of around 0.04 meq. The uncertainty of  $H_0$  is also estimated to be 1 ppt. In all experiments  $c$  was held at 40 meq, with  $H_0 \geq 0.1 M$  and  $V_a \approx 200$  ml. Thus  $\Delta c/c = 0.04/40 = 10^{-3}$ ,  $\Delta V_a/V_a = 10^{-3}$ , and  $\Delta H_0/H_0 = 10^{-3}$ . The following values can be inserted then into (A8a) and (A8b):  $c = 40$  meq,  $V_a + V_0 \approx 200$  ml (since  $V_a \gg V_0$ ),  $K = 1$ ,  $\Delta H_0/H_0 = 10^{-3}$ ,  $\Delta c/c = 10^{-3}$  and  $\Delta V_a/V_a = 10^{-3}$ . For (A8a),  $\Delta H/H = 10^{-3}$  and  $\Delta Cl/Cl = 10^{-3}$ , while for (A8b),  $\Delta H = 10^{-4} M$ , and  $\Delta Cl = 10^{-4} M$ . Then

$$\left(\frac{\Delta K}{K}\right)^2 = 10^{-6}(1+\alpha)^4 + 10^{-6}(1+\alpha)^2(2+\alpha)^2 + 3 \times 10^{-6}(1+\alpha)^2 \quad (8a)$$

$$\left(\frac{\Delta K}{K}\right)^2 = 10^{-6} \left[ \frac{(1+\alpha)^6}{\alpha^4 c^2} \right] + 10^{-8} \left[ \frac{(2+\alpha)^2 (1+\alpha)^2}{\alpha^2 c^2} \right] + 3 \times 10^{-6} (1+\alpha)^2 \quad (8b)$$

### Results and Discussion

The standardization of solutions and all measurement data are shown in Tables I a to e. Equations (8a) and (8b) are plotted in Figure 1 on the same scale. Curve I in Figure 1 shows that the constant relative titration error (Equation (8a)) increases as a function of  $\alpha$ . The uncertainty  $\Delta K/K$  in the measurement is low at small  $\alpha$ , that is, when the ratio of acid added to the total capacity is small. Since it has been assumed that the relative titration errors  $\Delta H/H$  and  $\Delta Cl/Cl$  are

Table 1a

Measurement of H<sub>2</sub>O. 25-ml portions of equilibrated solution titrated with 0.06219 M NaOH to phenolphthalein end point.

Experiment A H <sub>2</sub> O=0.1 M			Experiment B H <sub>2</sub> O=0.2 M		
trial	vol. of NaOH, ml	H <sub>2</sub> , M	trial	vol. of NaOH, ml	H <sub>2</sub> , M
1	15.78	0.03925	1	41.36	0.1029
2	15.83	0.03938	2	41.45	0.1031
3	15.77	0.03922	3	41.33	0.1028
4	15.85	0.03944	4	41.36	0.1029
5	15.82	0.03936	5	41.36	0.1029

Table 1b

Measurement of Cl<sub>2</sub>. 25-ml portions of equilibrated solution titrated with 0.1001 M AgNO<sub>3</sub> (blank correction: 0.02 ml).

Experiment A			Experiment B		
trial	(corrected for blank), vol. AgNO <sub>3</sub> , ml.	Cl <sub>2</sub> , M	trial	(corrected for blank), vol. AgNO <sub>3</sub> , ml.	Cl <sub>2</sub> , M
1	24.76	0.09915	1	46.95	0.1880
2	24.80	0.09929	2	46.88	0.1877
3	24.81	0.09933	3	46.93	0.1879
4	24.78	0.09920	4	46.80	0.1874
5	24.82	0.09938	5	46.80	0.1874

Table 1c

Measurement of  $V_a$ .

Experiment A $H_2O=0.1M$ density at $20^\circ C=1.0019^a$			Experiment B $H_2O=0.2M$ density at $20^\circ C=1.0037^a$		
trial	wt. of HCl solu- tion added, g	vol. = $\frac{wt}{D}$ , ml	trial	wt. of HCl solu- tion added, g	vol. = $\frac{wt}{D}$ , ml
1	200.580	200.20	1	200.901	200.10
2	200.500	200.12	2	200.630	199.85
3	200.390	200.01	3	200.770	200.03
4	200.320	199.94	4	200.579	199.84
5	200.230	199.85	5	200.931	200.19

<sup>a</sup> Interpolated values from Handbook of Chemistry and Physics, 47th Ed., Chemical Rubber Publishing Co., Cleveland, U.S.A., p. B-1967.

Table 1d

Measurement of  $c$  by titration with  $0.3014 M$  NaOH to phenolphthalein end point.

Experiment A $H_2O=0.1M$			Experiment B $H_2O=0.2M$		
trial	vol. of NaOH, ml	$c$ , meq	trial	vol. of NaOH, ml	$c$ , meq
1	134.32	40.48	1	134.64	40.58
2	134.44	40.52	2	134.53	40.55
3	134.31	40.48	3	134.31	40.48
4	134.64	40.58	4	134.34	40.49
5	134.51	40.54	5	134.54	40.55

Table 1c

Measurement of  $H_O$  by titration of 25-ml portions of equilibrated solutions with 0.1023 M NaOH to phenolphthalein end point.

Experiment A $H_O = 0.1 M$			Experiment B $H_O = 0.2 M$		
trial	vol. of 0.1 M NaOH, ml	$H_O$ M	trial	vol. of 0.1 M NaOH, ml	$H_O$ M
1	25.56	0.1046	1	49.46	0.2024
2	25.54	0.1045	2	49.44	0.2023
3	25.55	0.1046	3	49.54	0.2027
4	25.61	0.1048	4	49.41	0.2022
5	25.54	0.1045	5	49.43	0.2023

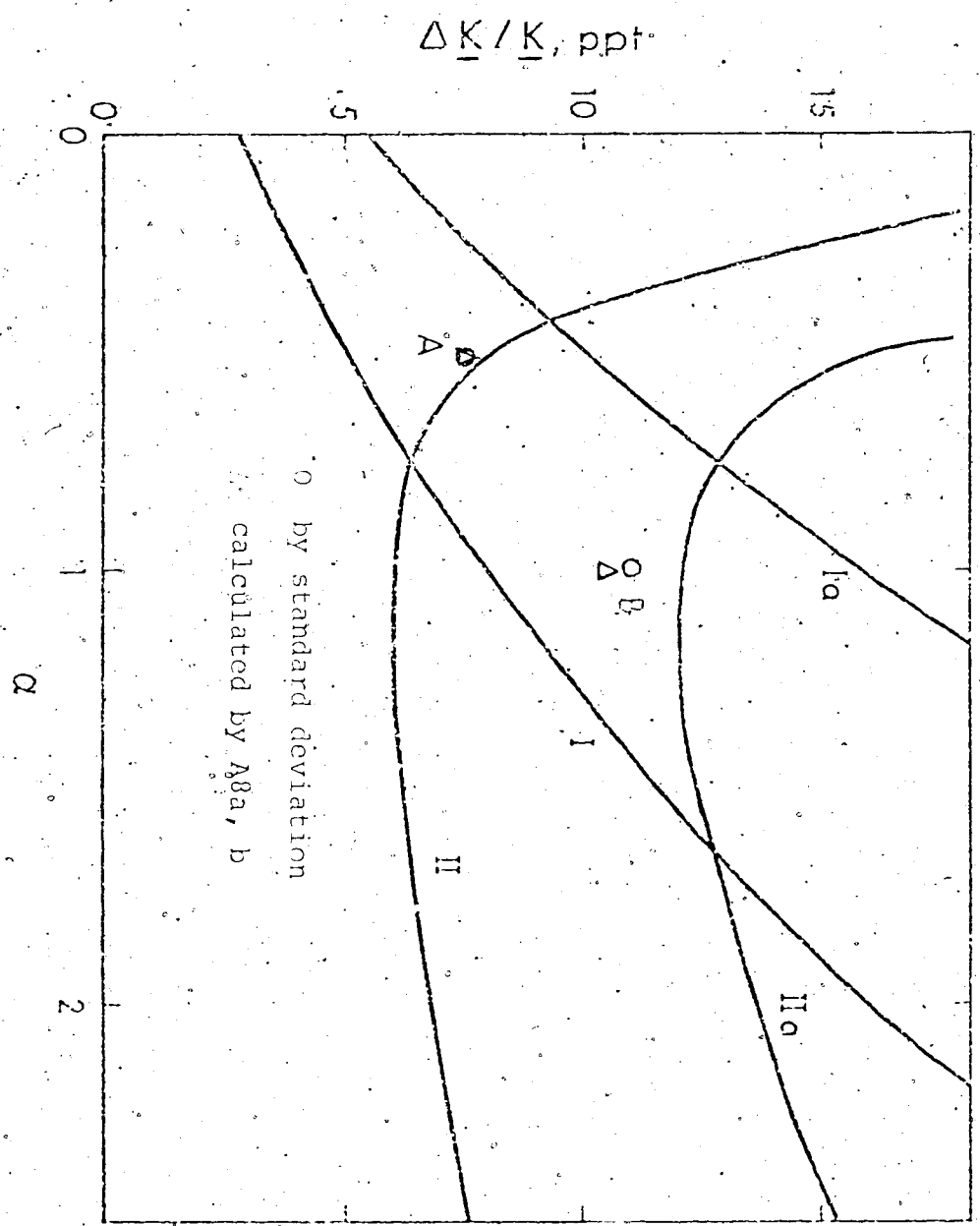


Figure 1. Plots of relative uncertainty  $\Delta K / K$  against  $\alpha$ . Curve I, constant relative measurement errors as calculated by Equation 8a; II, constant absolute errors by Equation 8b; Ia, IIa, with measurement errors double that of I, II.



constant and do not depend on sample size, the precision of  $\bar{H}$  and  $\bar{Cl}$  will be the same whether  $\underline{B}$  is large or small. Nevertheless, values of  $\bar{NaR}$  obtained from  $(\underline{c}/\underline{NaV})$  will have higher precision at low values of  $\underline{B}$ , where  $\underline{c} \gg \underline{NaV}$ . The limiting uncertainty when  $(\underline{B}/\underline{c}')$  approaches zero is

$$\lim_{\underline{B} \rightarrow 0} \left( \frac{\Delta \underline{K}}{\underline{K}} \right)^2 = 10^{-6} + 4 \times 10^{-6} + 3 \times 10^{-6} = 8 \times 10^{-6}$$

$$\therefore \left( \frac{\Delta \underline{K}}{\underline{K}} \right)_{\lim} = 2.8 \times 10^{-3} = 2.8 \text{ ppt}$$

As  $\underline{B}$  increases, and the resin is converted to the  $\text{H}^+$  form,  $(\Delta \underline{K}/\underline{K})$  becomes large because of the difficulty in obtaining accurate values of  $\bar{NaR}$ .

On the other hand, curve II for constant absolute titration error (Equation (8b)) shows a quite different shape. The minimum in the region of 1.1 to 1.15 for  $\alpha$  corresponds to half conversion at  $\underline{K} = 1$  and depends on  $\underline{c}'$  as well as  $\alpha$ . The tremendous uncertainty observed at low values of  $\alpha$ , where the addition of acid is small, is caused by the large relative error in the measurement of  $\text{H}^+$  and  $\text{Cl}^-$  ( $\Delta \bar{H}/\bar{H}$ ,  $\Delta \bar{Cl}/\bar{Cl}$ ). This is because a constant absolute titration error ( $\Delta \bar{H}$ ,  $\Delta \bar{Cl}$ ) is assumed. If 13 is the maximum uncertainty in  $\underline{K}$  that can be tolerated, measurements should not be made at values of  $\alpha < 0.4$ . The increasing uncertainty at large  $\alpha$  comes in the

measurement of  $\bar{N}K$ , again because of the large relative error in the measurement of  $H^+$  and  $Cl^-$  under these conditions. Compared with curve I at moderate values of  $\alpha$ , curve II has a smaller value for  $\Delta K/K$  because the relative error in the measurement of  $H^+$  and  $Cl^-$  at high concentrations is small.

The uncertainties in the values of  $\Delta K/K$  obtained experimentally as the standard deviation for five measurements by the stoichiometric method and by calculation from Equations (A8a) and (A8b) using the experimental standard deviations are compared in Table 2, and are plotted in Figure 1. The excellent agreement between the experimental points and the calculated points supports the validity of (A8a) and (A8b). The small difference observed may be caused by one or more of the following:

- i) The presence of determinate error in one or more measurement steps.
- ii) Even when the measurement errors all are random in nature, the error in  $K$  is not necessarily random due to nonlinear propagation of error<sup>76</sup>. However the bias thus produced is usually small and can be neglected, so that  $\Delta K$  can still be approximated by a Gaussian distribution.
- iii) If the value of  $\Delta K$  is large, then<sup>77</sup>.

$$\left(\frac{\Delta K}{\Delta X}\right)_X \neq \left(\frac{\partial K}{\partial X}\right)_X$$

Table 2

Comparison of values for  $\Delta K/K$  as measured and as calculated by error Equation (8).Expt. (A)  $\alpha = 0.516$ 

Run	Measured quantities					Calculated		
	H, M	Cl, M	V <sub>a</sub> , ml	$\Sigma$ , meq	H <sub>2</sub> O, M	Na, by Eq. (6a)	V <sub>2</sub> , by Eq. (6b)	$\frac{K}{\text{by Eq. (7)}}$
1	0.03925	0.09915	200.20	40.48	0.1046	0.05990	11.00	0.6938
2	0.03938	0.09929	200.12	40.52	0.1045	0.05991	10.50	0.6880
3	0.03922	0.09933	200.01	40.48	0.1046	0.06011	10.61	0.6975
4	0.03944	0.09920	199.94	40.52	0.1048	0.05976	11.29	0.6841
5	0.03936	0.09938	199.85	40.54	0.1045	0.06002	10.30	0.6887
Ave, $\bar{X}$	0.03933	0.09927	200.02	40.52	0.1046			0.6904
$S_x = \Delta X$	$0.92 \times 10^{-4}$	$0.94 \times 10^{-4}$	0.14	$4.2 \times 10^{-2}$	$1.2 \times 10^{-4}$			$5.25 \times 10^{-3}$
$\Delta \bar{X} / \bar{X}$	$2.3 \times 10^{-3}$	$0.95 \times 10^{-3}$	$0.7 \times 10^{-3}$	$1.0 \times 10^{-3}$	$1.2 \times 10^{-3}$			$7.63 \times 10^{-3}$

 $\Delta K/K$  (calculated by Equation (8b)) =  $7.63 \times 10^{-3}$

Table 2 (cont'd)

Expt. (B)  $\alpha = 0.999$ 

Run	Measured quantities					Calculated		
	H, M	Cl, M	V <sub>a</sub> , ml	C, meq	H <sub>2</sub> O, M	K <sub>a</sub> , by Eq. (6a)	V <sub>0</sub> , by Eq. (6b)	K by Eq. (7)
1	0.1029	0.1880	200.16	40.58	0.2024	0.0851	15.33	0.6619
2	0.1031	0.1877	199.89	40.55	0.2023	0.0846	15.55	0.6699
3	0.1028	0.1879	200.03	40.48	0.2027	0.0851	15.76	0.6873
4	0.1029	0.1874	199.84	40.49	0.2022	0.0845	15.78	0.6719
5	0.1029	0.1874	200.19	40.55	0.2023	0.0845	15.92	0.6726
Ave, $\bar{X}$	0.1029	0.1877	200.03	40.53	0.2024			0.6768
$\bar{S}_X (\Delta X)$	$1.1 \times 10^{-4}$	$2.8 \times 10^{-4}$	0.15	$4.3 \times 10^{-2}$	$1.9 \times 10^{-4}$			$7.8 \times 10^{-3}$
$\Delta X / \bar{X}$	$1.1 \times 10^{-3}$	$1.5 \times 10^{-3}$	$0.75 \times 10^{-3}$	$1.1 \times 10^{-3}$	$0.94 \times 10^{-3}$			$11.0 \times 10^{-3}$

 $\Delta K / K$  (calculated by Equations (8a) and (8b)) =  $10.5 \times 10^{-3}$

- iv) Number of measurements is so small that the average value is not equal to the true value, and  $\Delta X \neq \underline{s}_X$ .
- v) The assumption that  $K = 1$ , used in deriving (A8a) and (A8b), is not valid.

As mentioned before, the absolute titration error is likely to be constant at low concentrations of  $H^+$  and  $Cl^-$  (low  $\alpha$ ). The variation in uncertainty with  $\alpha$  is probably best represented by curve II at  $\alpha < 0.7$ , and by curve I at  $\alpha > 0.9$ . This is supported by the fact that measurement A at  $\alpha = 0.5$  lies on curve II while measurement B at  $\alpha = 1$  is "closer" to curve I than curve II even though the deviation from both curves is large. This large deviation is due to greater measurement errors than the estimated values used in (A8a) and (A8b), especially in the sensitive term  $\Delta Cl/Cl$  where the measurement error (standard deviation of 5 measurements) is  $1.5 \times 10^{-3}$  instead of the previously assumed value of  $1 \times 10^{-3}$ .

The uncertainty  $\Delta X/X$  can be reduced if more measurements are taken and the average is used instead of a single value, since

$$\underline{s}_n = \frac{\underline{s}}{\sqrt{N}}$$

where  $\underline{s}$  is the standard deviation for a single measurement and  $\underline{s}_n$  is the standard deviation for the average

of  $N$  measurements.

For example, the error in  $H$  is estimated to be 1 ppt for a single measurement, but reduces to  $1 \text{ ppt} / \sqrt{10} = 0.3 \text{ ppt}$  for ten measurements. Thus it is advantageous to use large volumes of equilibrating solution (large  $V$ ), either by increasing  $V_a$  or  $V_o$ , and do the titration three times or more so that  $K$  calculated by the average will have a higher precision.

Values of  $K$  obtained by the stoichiometric method are compared with those by the dynamic method in Table 3. The reasonable agreement indicates that the stoichiometric method is a valid method of measuring  $K$ . Assuming measurement errors to be known, Schartz<sup>80</sup> used a Monte Carlo simulation to generate numbers which could be processed by a computer program to obtain the value of the uncertainty numerically without the necessity of solving the error equation explicitly. Use of an approximation method of this type is the only resort when the error equations (A8a) and (A8b) become too complicated to be solved analytically.

Table 3

Comparison of  $K$  values obtained by stoichiometric method and dynamic method.

	$X_{\text{ad}}$	$K$ stoichiometric method	$K^a$ dynamic method	$K^b$ batch
0.2	0.56	0.677	0.67	
0.1	0.56			0.66
0.1	0.68	0.69	0.68	0.69

a. From p. , interpolated value.

b. From ref. 59, fig. 1.

## CHAPTER III

### SORPTION OF TRACE AMOUNTS OF HCl IN THE PRESENCE OF NaCl ON DOWEX 50W x 8 CATION EXCHANGE RESIN

#### Background

##### Solvent Uptake and Osmotic Pressure

When a conventional gel-type resin is in contact with water, either in the form of water vapor or liquid (water or aqueous solution), it will take up a certain amount of water and swell in volume until equilibrium has been achieved. The driving force for water (solvent) uptake is the solvation of mobile and fixed ionic sites in the resin, and the tendency of ions in the resin phase to undergo dilution. The behavior of an ion exchange resin can be compared to a semipermeable membrane separating pure water and an aqueous salt solution in which water will pass from one side to dilute the salt solution, creating an osmotic pressure on the solution side to counterbalance the solvent flow. A similar high osmotic pressure is developed in an ion exchange resin. Because the resin is relatively rigid, the volume increase of the resin due to water sorption results in a significant strain in the resin. This internal osmotic pressure may reach 500 to 1000 atmospheres depending on the degree of crosslinking, so that the



swelling resin can burst a sealed container. The thermodynamic treatment of membrane equilibrium involves use of the concept of chemical potential. A similar treatment can also be applied to a batch of resin brought into contact with water. The equilibrium between resin and water in various states can be written as <sup>809</sup>:

$$RT \ln \frac{P_w}{P} = \bar{V}_w \pi + RT \ln a_w \quad \text{Resin-water vapor} \quad (9a)$$

$$\bar{V}_w \pi = RT \ln \frac{a_w}{a_w^0} \quad \text{Resin-water} \quad (9b)$$

$$\bar{V}_w \pi = RT \ln \frac{a_w}{a_w^0} a_w \quad \text{Resin-solution} \quad (9c)$$

where  $\pi$  is the osmotic pressure,

$\bar{V}_w$  the partial molal volume of water,

$a_w$  the water activity in the resin phase,

$a_w^0$  the water activity in the solution phase,

$P_w$  the partial pressure of water, and

$P$  the atmospheric pressure where the standard state is defined.

Upon sorption of water, the resin will show a volume increase owing to the volume of water sorbed and the stretching of coiled chains of polymer matrix as a result of decreasing interaction between chains with water sorption. An increase in resin volume is counteracted by the elastic force of the matrix, which tends to contract the resin, as well as by the configurational entropy which tends to increase also on contraction of

the resin. The equivalent volume of the swelling resin,  $\bar{V}$ , water sorption, and osmotic pressure can be inter-related by Equations (9a) to (9c), and the empirical equation<sup>80a</sup>

$$\bar{V} = \underline{a} + \underline{b}$$

where  $\underline{a}$  is the elasticity of the resin, and  $\underline{b}$  is the volume of unstrained resin. The magnitude of  $\underline{a}$  increases with the degree of crosslinking, while that of  $\underline{b}$  is independent of crosslinking.

Since water molecules in the resin phase are under the influence of a region of high charge density, the physical properties of sorbed water are quite different from those of external water. This has been shown by NMR measurement<sup>81</sup>, where three peaks<sup>82</sup> are obtained for resins suspended in water; one is attributed to external water (water located at the resin surface), one to internal water, and one to bulk water (water not affected by the resin). The last peak is not observed in measurements made on settled resin.

The chemical shift with respect to external water,  $[\delta = (\text{ext. H}_2\text{O} - \text{int. H}_2\text{O})/60 \text{ ppm}]$ , is greater than zero<sup>83</sup>, that is, the internal water peak is shifted upfield with respect to the external water peak. This indicates that hydrogen bond breakage has taken place in the internal water. Internal water tends to cluster around the polar

groups of the resin and form domains of different sizes. Hydrogen bonding is thus not so extensive as in external water, especially when the extent of water sorption is small, e.g., the resin is highly crosslinked.

The line width<sup>84,85</sup> of the internal water peak is greater than that of pure water. This is probably due to magnetic field inhomogeneities in the resin and to restricted internal water motion which causes a decrease in both transverse and longitudinal relaxation times. The exchange lifetime of internal and external water is approximately 13 sec and depends on resin particle size<sup>86</sup>.

The water-vapor sorption isotherm<sup>87</sup> of ion exchange resins at different crosslinkings indicates that two types of water in the resin phase can be distinguished. In the first water uptake step, the sorption of water does not depend on the degree of crosslinking, but does depend on the nature of the counter ions on the resin. The volume of the hydrated resin is less than the sum of the volumes of water sorbed and the anhydrous resin. Also, the heat of sorption is on the order of 4 kcal/mole. Both of these observations indicate strong interaction. The quantity of water sorbed in this step is 4 moles<sup>88</sup> per equivalent or less, depending on the ion. It is believed that the water entering the resin at this stage is

chiefly water of hydration, which hydrates the counter ions in the resin and, to a lesser extent, the fixed ionic groups<sup>89</sup>. In the next stage additional water, when added enters the resin as free water. The result of free water uptake is to dilute the high concentration of ions in the resin phase, build up osmotic pressure, and swell the resin. This uptake of free water is affected by crosslinking, in that a low degree of crosslinking permits increased water sorption. The absence of interaction between free water and resin is confirmed by the additivity of volumes and the low heat of sorption. Because exchange is rapid on the NMR time scale, NMR cannot distinguish between these two types of internal water. Nevertheless, Ismatullayev<sup>90</sup> was able to distinguish among three different kinds of water in a sulfonic acid resin by differential thermometric analysis (DTA). Three endothermic peaks were found for a resin which had previously been dried in a desiccator. The first peak at 50-55°C corresponded to osmotic water (free water), the second at 105-115°C to adsorbed water, and the third at 175-185°C to hydrated water. The bonding of adsorbed water and hydrated water to the resin is so strong that it is not affected by ultrasonic oscillation, whereas free water absorbs ultrasonic energy readily<sup>90</sup>. Yamabe<sup>91</sup> even reported a desulfonation peak at 300°C which can be used for the determina-

tion of the capacity and ion exchange constant of a sulfonic acid resin involving  $H^+$ .

### Models of Resins

The behavior of resins can be treated thermodynamically without assuming any model; nevertheless, the use of a model is helpful in elucidating abstract thermodynamic ideas, and also in simplifying the problem by incorporation of the particular properties of a specific model. Because none of the various models used to describe ion exchange resins is satisfactory in all respects, it is sometimes advantageous to combine the non-contradictory aspects of several models. It may also happen that one model can account reasonably for resin behavior under one set of conditions, while another model must be used for another. For example, the homogeneous model can be applied to resins that have high solvent sorption and slight specific interactions, whereas the heterogeneous model is better for the opposite case of low sorption and appreciable specific interactions.

#### 1) Quasi-homogeneous model

In this model the resin is regarded as consisting of only one active phase, a liquid phase containing internal water, counter ions and fixed charge groups,

which behaves like a concentrated solution. A second phase, consisting of a solid matrix which normally is considered to be inert, does not take part in any reactions, and therefore is not involved in the calculations.

i) Gregor's model<sup>92,93</sup>

Gregor's model assumes that there is no interaction in the resin other than osmotic pressure, and all ions in the resin are hydrated. Then

$$RT \ln K_{B/A} = -(\bar{V}_{Ah} - \bar{V}_{Bh}) \quad (10a)$$

where  $\bar{V}_{Ah}$  and  $\bar{V}_{Bh}$  are the partial molal volumes of the hydrated ions A and B. The ion exchange constant is directly related to the difference in the hydrated volume of the two ions.

ii) Glueckauf's model<sup>94,95</sup>

The lack of knowledge of hydration parameters has led to a modified Gregor model in which an unhydrated counter ion is used as the standard state. In this model, the swelling effect is less significant.

$$RT \ln K_{B/A}^* = -(\bar{V}_A - \bar{V}_B) \quad (10b)$$

where  $\bar{V}_A$  and  $\bar{V}_B$  are the partial molal volumes of the dehydrated ions A and B.  $K_{B/A}$  and  $K_{B/A}^*$  are correlated through activity coefficients in the resin phase.

There are also models which drop the osmotic pressure term by choosing a standard state for the ion in the resin that is the same as that in solution. The choice of standard state is quite arbitrary and will not be considered here.

## 2) Quasi-heterogeneous model

In this model the resin is regarded as a single solid phase possessing fixed groups on its surface in a manner similar to the active sites present on the surface of an adsorbent material. Counter ions are localized at individual fixed groups and held by electrostatic force.

## 1) Harris and Rice model<sup>96</sup>

This is based on the earlier Katchalsky model<sup>97</sup> in which the configurational free energy of a charged polymer and the free energy of interaction along the chain, both treated in terms of polyelectrolyte theory, are used to account for selectivity, osmotic pressure, and internal activity coefficients. Harris and Rice modified this model by adding a third free energy term that depended on the ion pairing of counter ions with fixed ionic groups. They assumed that some counter ions are bound to the exchange sites in the form of ion pairs, and that different counter ions have different bounding abilities, described in terms of binding

constants  $\bar{K}_i$ . The overall energy of reaction, then, is defined by

$$\underline{G} = \underline{G}_{\text{conf}}(\bar{V}) + \underline{G}_{\text{interaction}}(\bar{V}, \bar{N}_i) + \sum_{i \neq 0} \bar{N}_i RT (\ln \bar{K}_i - \ln \bar{C}_i)$$

where  $\bar{N}_i$  is the number of sites bound in ion pairs with ion  $i$ , and  $\bar{C}_i$  is the external concentration of ion  $i$ . Equilibrium is determined by minimizing  $\underline{G}$  with respect to  $\bar{N}_i$ . This model is not satisfactory in explaining reversal ( $\bar{K}_{A/B}$  changes from greater than 1 to less than 1 with percentage of loading) and lacks a mechanistic point of view.

The ion pair concept was also adopted by Arkhangel'skii<sup>98</sup> to develop a similar model in terms of bond energy and thermal energy. Comparisons of IR<sup>81</sup> spectra of resins in the dry and swollen (wet) state show that sulfonate groups are completely dissociated in the swollen state and that no sign of binding can be seen. Ion pairing implies a kind of labile interaction and is highly non-realistic.

ii) Pauley<sup>99</sup> and Eisenman model<sup>100,101,102</sup>, with Ling's<sup>103,104</sup> modification.

This model emphasizes the electrostatic interaction,  $\underline{G}_E$ , between hydrated counter ions and fixed charge groups which can be treated as non-compressible point charges by Coulomb's law. As a counter ion



approaches a fixed group, the hydrated water may be partially stripped to allow closer contact. The additional free energy required to remove the hydrated water,  $\Delta G_s$ , is nearly equal to the hydration energy, but opposite in sign.

$$\Delta G = \Delta G_D + \Delta G_s$$

$$\Delta G_{A \rightarrow B} = -RT \ln K_{A \rightarrow B} = (\Delta G_D)_A - (\Delta G_D)_B + (\Delta G_s)_A - (\Delta G_s)_B$$

$$= \frac{e^2}{r_C + r_A} - \frac{e^2}{r_C + r_B} + (\Delta G_s)_A - (\Delta G_s)_B$$

where  $r_C$ ,  $r_A$  and  $r_B$  are the effective radii after water stripping of the fixed group, ion A, and ion B. The selectivity depends on the relative magnitude of the hydration energy and electrostatic attraction. For large fixed groups (large  $r_C$ , as sulfonate groups), selectivity is determined solely by the hydration energy, the resin preferring ions of lower hydration energy. In this event a normal affinity sequence,  $\text{Cs} > \text{K} > \text{Na} > \text{Li}$ , results. On the other hand, when  $r_C$  is small, as in a carboxylate resin, electrostatic attraction is the key factor in determining affinity. The resin may then prefer small bare ions and a reversed sequence,  $\text{Li} > \text{Na} > \text{K} > \text{Cs}$ , results. This crude model has been modified by Ling to take into account the effect of ion-induced dipoles, dipole-induced dipoles, and London dispersion interaction.

Changes in dielectric constant in the resin phase have also been considered. Effective radii were calculated by the equilibrium distance between two ions using the Born equation. Kurnetsova<sup>105</sup> has greatly simplified the various expressions and has provided an explicit form.

#### (ii) Miscellaneous models

Russian workers have worked out a couple of models which are useful in explaining some resin phenomena. A loose quasi crystal model<sup>106,107</sup>, which states that counter ions are highly localized near the exchange sites and can only migrate to other exchange sites by an activated jump over a period  $T_1$ , is good for explaining the temperature dependence of internal diffusion coefficients. A two-dimensional model<sup>108</sup>, making use of the analogy of a resin to a two-dimensional surface, can predict selectivity by means of the Zhukhovitskii-Evans-Guggenheim equation for a two-dimensional surface. The surface tension of the resin phase is involved.

#### Purpose

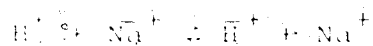
Ion exchange chromatography is widely used as a technique for separating mixtures of electrolytes. Among other factors, the apparent ion exchange constant

$\bar{H}^+$  and the exchange capacity  $c$  are of prime importance in determining the retention of individual ions in a column.

In the elution of small quantities of HCl from a strong acid cation exchange resin with NaCl solutions at various concentrations, the retention volume  $\underline{V}_R$  of HCl can be described by the formula,

$$\underline{V}_R = \underline{V}_M \left( 1 + \frac{\text{amount of solute in stationary phase}}{\text{amount of solute in mobile phase}} \right)$$

where  $\underline{V}_M$  is the volume of mobile phase (void volume) in the column. This assumes the distribution constant  $\underline{K}_D$  does not change with solute concentration. Thus, for the exchange reaction



the apparent equilibrium constant for the ion exchange reaction  $K$  is equal to

$$\frac{\bar{H}^+ [\text{Na}^+]}{\text{Na}^+ [\bar{H}^+]}$$

and the retention volume  $\underline{V}_R$  of HCl is

$$\underline{V}_R = \underline{V}_M \left( 1 + \frac{\bar{H}^+}{[\text{H}^+] \underline{V}_M} \right) = \underline{V}_M + \frac{\bar{K}c}{[\text{Na}^+]} \quad (11)$$

where  $\bar{H}^+$  is the milliequivalents of  $\text{H}^+$  in the resin (the bar denoting resin phase) and  $c$  is the total

exchange capacity of the resin in the column,  $\overline{Na}^+ + \overline{H}^+$ , in milliequivalents.

A similar equation has been derived by Rachinski<sup>104</sup>. Under conditions where the amount of  $H^+$  solute present is small compared with the amount of eluting  $Na^+$  electrolyte, the column is virtually completely in the  $Na^+$  form. The apparent equilibrium constant  $K$  can thus be defined as,  $K(\overline{X}_{Na} - 1)$  and should be independent of the concentration of  $[H^+]$  over a considerable range. In this case the shape of the elution peak should be Gaussian, and the retention volume is predicted by Equation (11), provided the flow rate is sufficiently slow relative to the exchange rate that the dynamic capacity<sup>109</sup> does not differ significantly from the static capacity.

Experimentally a severely skewed elution peak is observed with a retention volume on the order of twice that predicted by Equation (11). Thus a mechanism other than exchange must be taking place. The purpose of this work was to investigate the nature of the mechanism. This was done through use of both a chromatographic method and a column equilibration method (called here a dynamic method) to measure independently values of  $\overline{H}_t^+$ . The results of the measurements are discussed in terms of the quasi-heterogeneous and quasi-homogeneous models described previously.

## Experimental

### Determination of Single Electrolyte Sorption

The general method used has been previously described<sup>110</sup>. A 20 cm x 0.5 cm i.d. glass column was used. The resin was washed in the column with 3 M NaCl for 1 hour, then with distilled water for another half hour. Next an NaCl solution of known concentration was passed through the column for about 45 min. The solution in the void volume was removed by vacuum suction for 10 min, then the column was washed with distilled water; a stirrer of stainless steel wire was used to remove air bubbles. Suction times of more than 10 min did not change the amount of chloride found. About 60 ml of eluate was collected and the total chloride determined by coulometric generation of silver<sup>111</sup>. The coulometer cell consisted of a silver indicator electrode, a silver generating electrode, a 1 M calomel reference electrode, a platinum wire in 0.5 M HNO<sub>3</sub> as counter electrode, and a 0.5 M KNO<sub>3</sub> salt bridge. The electrolyte was 0.4 M NaNO<sub>3</sub> and 0.05 M HClO<sub>4</sub>. An equal volume of ethanol was added to the eluate to decrease the solubility of AgCl. The Ag anode and counter electrode were connected to a Leeds and Northrup coulometric analyzer and the indicator electrode and calomel electrode to a Metrohm Model E-436 automatic titrator for

recording potential vs. time. The NaCl molarities used in the column equilibrations were 0.08994, 0.1501, 0.2403, 0.2499, 0.3076 and 0.3298 M.

The void volume  $V_m$  was measured at each NaCl concentration by bringing the NaCl solution level to just above the resin, and then washing with water. The washings were collected and analyzed for Cl; the results were corrected for sorbed  $Cl^-$  as measured previously.  $V_m$  was then calculated by dividing the corrected  $Cl^-$  content by its concentration. The sorption of HCl was determined in a similar fashion, except that the resin was converted initially to the hydrogen form with 3 M HCl instead of to the sodium form.

#### Determination of Ion Exchange Equilibrium Constants by a Dynamic Method

This method has also been previously described<sup>112</sup>. The column was first equilibrated with a mixture of NaCl and HCl of varying molarities, but with the ionic strength held constant at either 0.07 or 0.2. The pH of the eluate was monitored with a glass electrode, then the column was washed with 50 ml  $H_2O$ , followed by 0.77 M NaCl until the effluent tested neutral. The HCl in the NaCl solution was titrated with 0.15 M NaOH. The total exchange capacity of the resin in the column was determined by an indirect

method<sup>74</sup>. The column was converted to the hydrogen form with 3 M HCl; after washing with water, the  $H^+$  was replaced by  $Na^+$  with 0.77 M NaCl, and the HCl titrated with 0.15 M NaOH.

Determination of Trace Amounts of HCl on Dowex 50W in the Presence of NaCl

Both a chromatographic method<sup>64</sup> and a column equilibration method were used. In the first method, varying volumes of 0.062 M HCl were placed on a column that had previously been converted to the sodium form, and the HCl eluted with NaCl. The pH of the effluent was measured using a pH meter and recorder, with the glass electrode arranged as shown in Figure 2. The retention volume was obtained from the pH vs. volume of eluent tracing.

In the second method, mixtures of NaCl and HCl in water were passed through the column until the pH of the eluate reached a steady value equal to that of the mixture being added. The level of solution at the column head was then brought just to the top of the resin and the acid in the column washed out with 0.77 M NaCl. Approximately 60 ml of eluate were collected and the hydrogen ion titrated coulometrically in 0.04 M NaBr<sup>113</sup>. A large platinum gauze working electrode

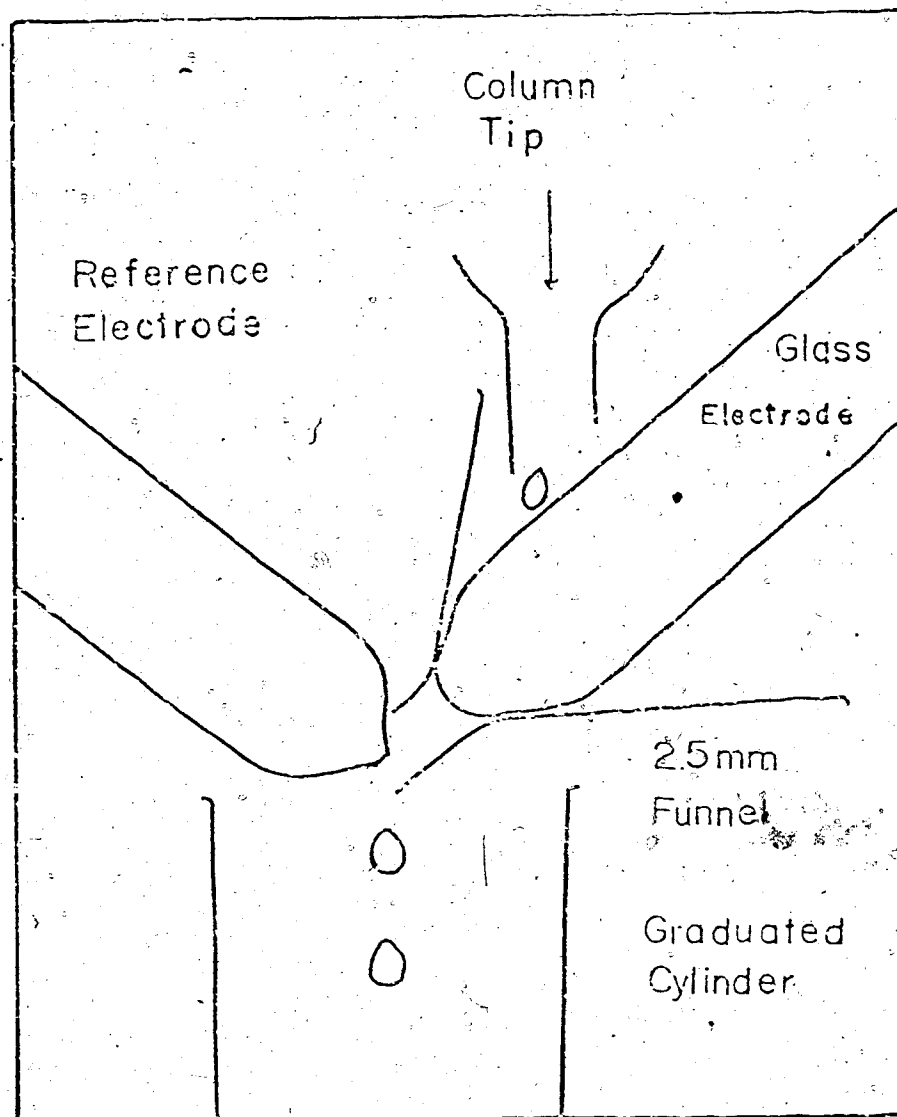


Figure 2. Arrangement of electrodes for monitoring pH of ion exchange column effluent



10

## Results and Discussion

The sorption of strong electrolytes has been measured by Pepper, Reichenberg, and Hale using a batch method with phase separation<sup>114</sup>. The distribution constant  $E_{D,Y}$  can be satisfactorily described by the expression<sup>115,116</sup>

$$\frac{E_{D,K}}{E_{K,K}} = \frac{E_{Y,K}}{E_{K,K}} = \frac{E_{Y,K}}{E_{R,K}} = \frac{E_{Y,K}}{E_{W,K}} = \frac{V_{AY}}{V_{AW}} = \frac{V_{Y,K}}{V_{W,K}} \quad (12)$$

where  $\bar{m}_Y$  is the molality of colon  $Y^-$  in the resin

phase;

$\bar{m}_Y$  is the molality of electrolyte in solution,

$z_Y$  is the charge on the colon

$\bar{m}_R$  is the molality of the fixed charge groups in the resin,

$\bar{\gamma}_Y, \bar{\gamma}_R$  are the mean ionic activity coefficients of the electrolyte in solution and resin,

$\bar{a}_w, a_w$  are the activities of water in resin and solution,

$\bar{V}_{AY}, V_w$  are the partial molal volumes of electrolyte AY and of water.

At room temperature,  $\bar{a}_w a_w \bar{V}_{AY} V_w$  varies only from 0.1 to 1, depending on the swelling pressure, so it can be treated as constant over a considerable concentration range. Unexpectedly, Pepper and coworkers found that  $\bar{\gamma}_Y$  tends to go to a small value at infinite dilution of AY. This anomaly was explained by Freeman<sup>117</sup> in terms of incomplete phase separation, non-Donnan sorption and inhomogeneity of the resin<sup>118</sup>. However, Boyd and Bunzl<sup>119</sup>, using radioisotopes and a stoichiometric method that did not require resin-liquid separation, demonstrated that  $\bar{\gamma}_Y$  increased to a constant value close to unity in dilute solution.

In the experiments reported here, sorption was studied under conditions closely resembling chromato-

graphy. Coulometric titration enabled measurements to be carried out using small quantities of hydrogen ion.

Molality is not a suitable unit to express electrolyte sorption in the column because only the total amount of sorbed species, and not the concentration, determines the retention of solute. If internal molality is to be used, the amount of solvent taken up by the resin at different external electrolyte concentrations has to be known exactly. This can be measured either by NMR<sup>120</sup> or by weighing before and after drying over  $P_2O_5$ , but the procedures are not simple. Use of units of milliequivalents of electrolyte sorbed per milliequivalent of exchangeable groups in the resin is convenient and practical for chromatography.

As compared with Soyda *et al*<sup>119</sup> and Pepper *et al*<sup>114</sup>, the milliequivalents of sorbed electrolyte found in this work are significantly larger, though the isotherm is still of the same shape. The higher value may come in part from adsorption on the glass walls of the columns or the resin matrix, and also from the thin film of liquid remaining on the surface of the resin beads after the solution was removed. The film on the bead contains about 4 to 5% of the total amount of electrolyte present in the solution outside the resin particles<sup>110</sup>. Plots of amount sorbed against concentration (Figure 3) gives straight lines for both

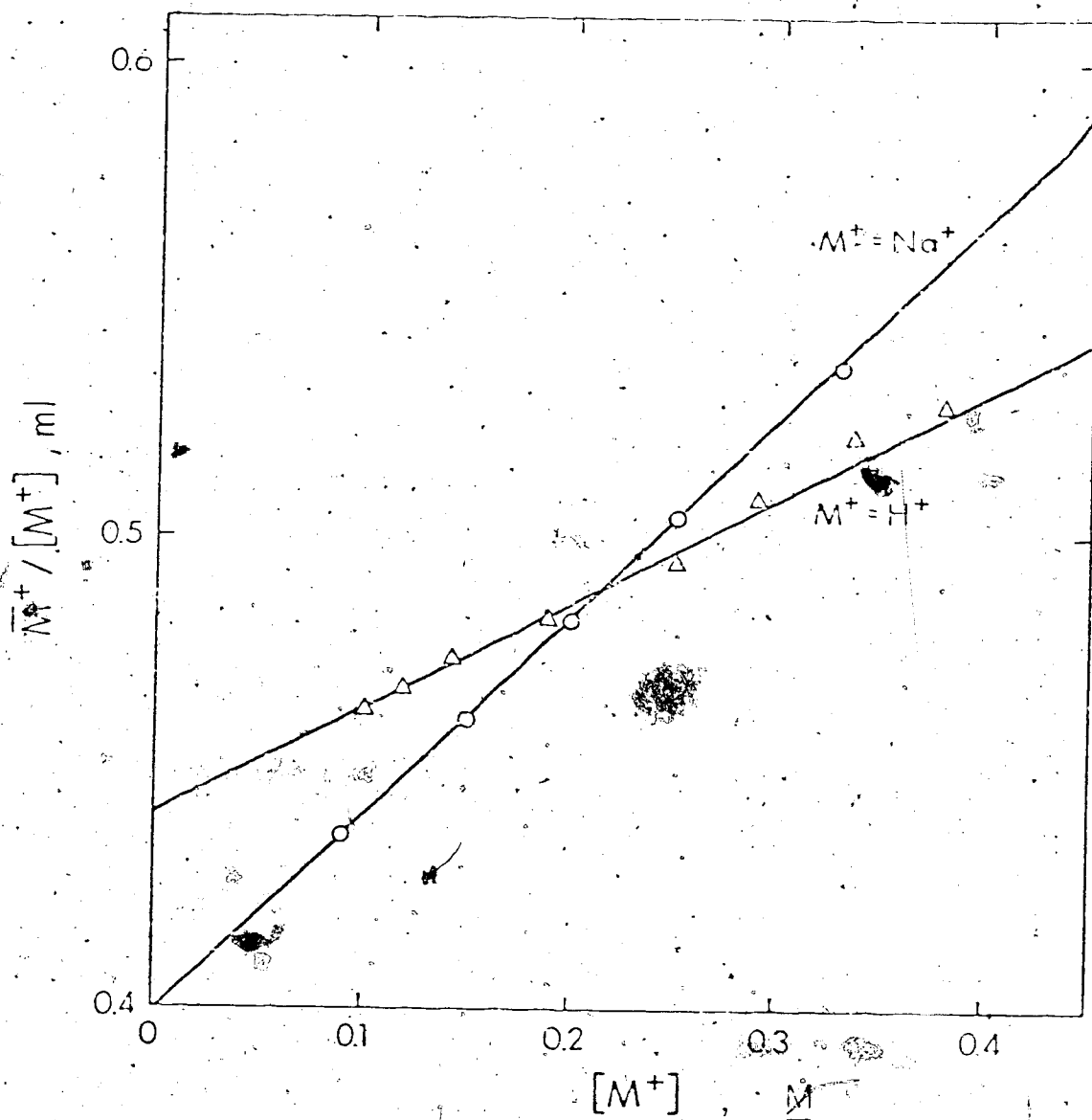


Figure 3. Plots of the ratio of amount of ion sorbed to initial concentration against concentration for  $Na^+$  and  $H^+$  as  $NaCl$  and  $HCl$ .

NaCl and HCl, with non-zero intercepts. By least-squares analysis the data fit the empirical equations

$$\frac{\bar{H}^+}{[H^+]^2} = 0.221 [H^+] \left( 1 + \frac{2.0}{[H^+]} \right) = 0.221 [H^+] + 0.442 \quad (13)$$

$$\frac{\bar{Na}_D}{[Na^+]} = 0.418 [Na^+] \left( 1 + \frac{0.95}{[Na^+]} \right) = 0.418 [Na^+] + 0.398 \quad (14)$$

In these equations  $\bar{H}_D^+$  and  $\bar{Na}_D$  are expressed in meq/lb. of resin and  $[Na^+]$  and  $[H^+]$  in  $M$  (meq/ml). It has been illustrated by Boyd and Bunt<sup>119</sup> that the sorption of electrolyte is governed by a Donnan equilibrium where  $\bar{v}$  increases to 1 in dilute solutions, and sorption increases with the square of the external concentration if the error due to incomplete phase separation is eliminated. A power of less than 2 and a value for  $\bar{v}$  of less than 1 had been obtained by previous authors<sup>114</sup>. These results were attributed to a small volume of solution adhering to the resin, rather than to inhomogeneity and to impurities in the resin. In the sorption experiment, the phases are separated by vacuum suction under reproducible conditions. The thin film remaining on the resin is assumed to be the same for every run, and thus constitute a constant background to the  $\bar{M}_D^+ [M^+]$  term. This is confirmed by the constant and nearly equal values of the last term on the right

hand side of (13) and (14). Thus, 0.442 and 0.398 represent the volume of the film remaining on the resin. This volume can easily be corrected for by shifting the lines in Figure 3 so that they pass through the origin, in effect deleting the two terms 0.442 and 0.398. Then (13) and (14) can be written as

$$\frac{H_D^+}{[H^+]} = 0.221 [H^+] \quad (13a)$$

and

$$\frac{Na_D^+}{[Na^+]} = 0.418 [Na^+] \quad (14a)$$

Equation (13a) agrees with previous work<sup>119</sup> within experimental error, which is on the order of  $\pm 10\%$ . Therefore the vacuum suction method of determining electrode sorption is considered to be valid.

$\frac{V}{m}$  was found to vary slightly with sodium ion concentration over the concentration range studied. An average value of 3 ml was used for all calculations in this chapter.

#### Ion Exchange Equilibrium Constant $K$ and Total Exchange Capacity $C$

The apparent equilibrium constant  $K$  can be determined in a column or batch-wise by replacing the counter ions present under equilibrium conditions

by a third ion, and retaining the two replaced ions. Only one titration is required if the total exchange capacity of the resin is known, the amount of the second ion being found by difference. This method is fast and accurate as long as the difference is not too small. Use of a glass electrode monitor to determine when equilibrium has been obtained is critical, since equilibration takes at least an hour and the time required for equilibrium increases to three or four hours with decreasing HCl concentration.

The total exchange capacity is found by titrating the displaced hydrogen ion. This method is more reliable than that of direct titration of the resin in the hydrogen form with NaOH, which may give an early end point due to slow exchange, especially near the end point, or to indicator adsorption. All measurements were made in situ, so the resin did not have to be taken out of the column and the chromatographic parameters were not affected. When measuring  $K$ , redistribution of  $\text{Na}^+$  and  $\text{H}^+$  may occur during the washing step and the composition of resin thus change. Gorshkov<sup>110</sup> has shown that redistribution errors are most serious when counter ions have different charges, when sorption capacity is high, and when the flow rate is large. For  $\text{Na}^+ - \text{H}^+$  exchange at low flow rates and low levels of ionic strength, the redistribution error is negligible.

Three measurements of total exchange capacity gave values of 16.89, 16.90 and 16.92 for an average of  $16.90 \pm 0.01$ . The ion exchange constant  $K$  was measured for various ratios of  $\text{Na}^+$  to  $\text{H}^+$  at two ionic strengths, 0.07 M and 0.2 M (Table 4) and plotted against the mole fraction of  $\text{Na}^+$  in the resin,  $\bar{X}_{\text{Na}}$ , in Figure 4. It is seen that  $K$  depends on both the ionic strength of the eluting solution and the percentage of  $\text{Na}^+$  in the resin. This change of  $K$  with  $\bar{X}_{\text{Na}}$  has been investigated by several workers. Recently Meares and Thain<sup>121</sup> used a rigorous thermodynamic approach proposed by Gaines and Thomas<sup>122</sup> to calculate thermodynamic  $K$  values. This approach tacitly assumes the quasi-homogeneous model, which is weak in dealing with the variation of  $K$  with percentage loading. Kuznetsova<sup>123</sup> used an electrostatic model and Logenchenko<sup>124</sup> a statistical model, both heterogeneous, to offer a plausible picture of what takes place in the resin, and predicted qualitatively the variation of  $K$  with  $\bar{X}_{\text{Na}}$ . Of these models, that of Logenchenko provides the best explanation for the curve in Figure 4 by expressing  $K$  as

$$\log K = a + b\bar{X}_B + c\bar{X}_B^2$$

This approach assumes that extra stability is gained by formation of clusters of counter ions in the resin.



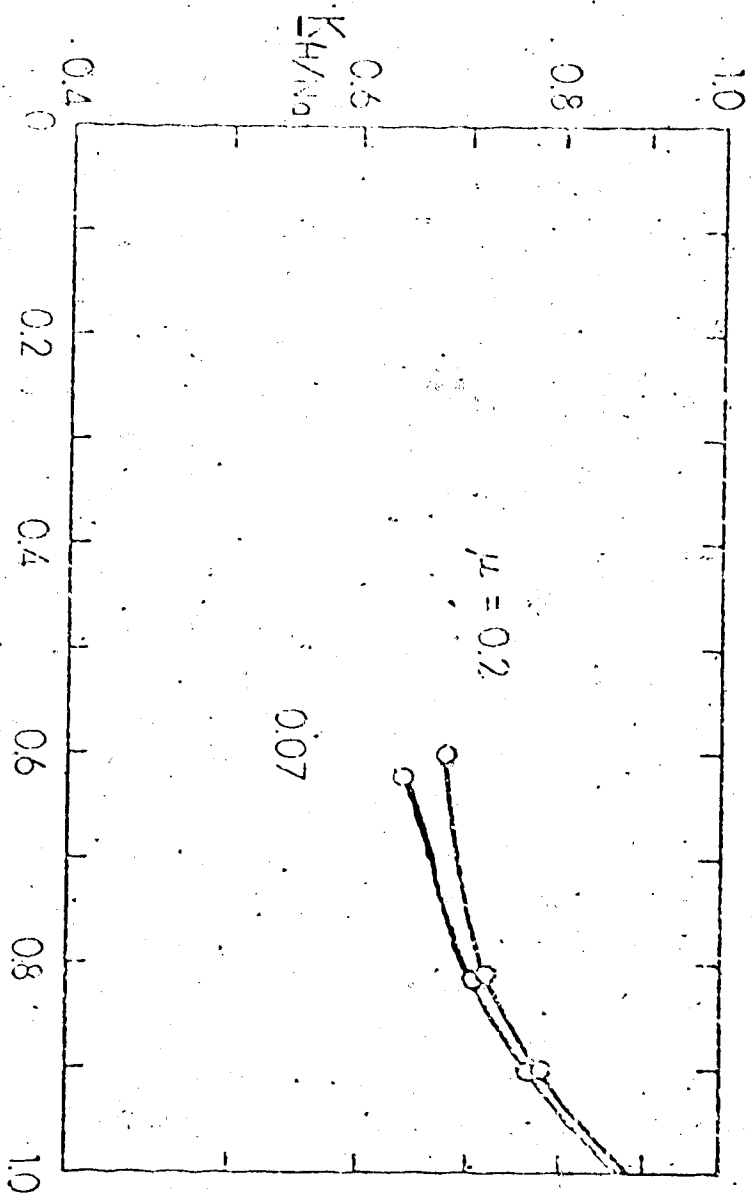


FIGURE 4. Ratio of ion exchange constant  $K_{H/N_0}$  for Dowex 5W-X 8 as function of mole fraction of resin in the ion exchange resin mixture 0.2 and 0.07.

Table 4. Variation of  $K$  with  $\bar{X}_{Na}$  at ionic strengths 0.2 and 0.07

$\frac{[Na^+]}{[H^+]}$	Ionic strength 0.2				Ionic strength 0.07			
	$\bar{H}^+$ meq	$\bar{Na}^+$ meq	$\bar{X}_{Na}$	$K$	$\bar{H}^+$ meq	$\bar{Na}^+$ meq	$\bar{X}_{Na}$	$K$
7.179	1.661	15.24	0.902	0.783	1.613	15.29	0.905	0.758
3.088	3.194	13.71	0.811	0.720	3.159	13.74	0.813	0.710
1.044	6.679	10.22	0.605	0.683	6.417	10.48	0.620	0.640
0.362	10.90	6.00	0.355	0.660	9.510	7.39	0.437	0.467
0.168	13.19	3.71	0.220	0.600	10.98	5.92	0.350	0.31

Both curves extrapolate to nearly the same intercept at  $X_{Na} = 1$ , so  $K_{X_{Na}=1}$  varies only slightly with total ionic strength under the experimental conditions used. The value of  $K_{X_{Na}=1}$  found in this work, 0.87, compares well with values of 0.84 obtained previously by Myers and Boyd<sup>12b</sup> and 0.87 by Bonner and Rhett<sup>12c</sup> using Dowex 50 - 8 at 25°C.

#### Proposed Mechanism for Additional Hold-up of $H^+$

In the column equilibration experiments the resin was brought to equilibrium with solutions containing  $10^{-4}$  and  $10^{-3}$  M HCl and  $10^{-4}$  to 1.2 M NaCl. Thus the resin was virtually completely in the  $Na^+$  form. Though ion exchange equilibria of this kind have been studied extensively by other workers, little information has been reported in the region near

$X_{Na} = 1$ . When  $K_{X_{Na}=1}$  is obtained by extrapolation, use of this expression to calculate  $H^+$  gives only the  $H^+$  replaced in the exchange sites by  $Na^+$ , and not the total amount of solute HCl held up by the resin. By coulometric titration of the eluted HCl, accurate measurement of the total HCl became feasible in the end regions. The quantity of HCl measured ranged from 6 to 200 neq in 80 ml of 0.77 M NaCl solution, and could be titrated accurately to 1%. No blank correction

was necessary for  $10^{-4}$  M HCl (8 neq in 80 ml).

11  
solution). The results are shown in Table 5.

Values of  $H_t^+$  can be calculated by subtracting the dead volume term  $V_m[H^+]$  from the measured value.

Plots of  $\log H_t^+/[H^+]$  against  $[H^+]$  at different concentrations of NaCl are shown in Figure 5. The

deviations from linearity indicate that the quotient

$H_t^+/[Na^+] \cdot [H^+]$  is not constant. Each curve is

extrapolated to zero  $[H^+]$ , then the values of  $H_t^+/[H^+]$

are plotted against  $[Na^+]^{-1}$  at various  $[H^+]$  levels to

give a series of parallel curves (Figure 6). The

measured value of  $H_t^+/[H^+]$  is greater than the value

of  $H_t^+/[H^+]$  calculated by  $V_m + K_{Na} - 1 \cdot C/[Na^+]$ , the

difference decreasing with  $[H^+]$ . This difference,

$H_t^+/[H^+] - H_o^+/[H^+]$ , or  $H_s^+/[H^+]$ , confirms the existence

of another mechanism besides replacement of  $Na^+$  in

strongly acidic exchange sites that may hold up solute

HCl in the column. This mechanism cannot be Donnan

sorption of single electrolyte, as if HCl were present

alone, because the additional hold-up,  $H_s^+/[H^+]$ , is much

greater than that calculated by Equations (13a), (14a).

From Figure 6 it can be seen that  $H_s^+/[H^+]$  does not

change with  $[Na^+]$  when  $[Na^+]$  is less than 0.5 M, but

decreases tremendously at higher  $Na^+$  concentrations,

approaching 0 as  $[Na^+]$  approaches 1 M.

Table 5 Total Sorption of HCl at Various Concentrations

of HCl and NaCl				
$[H^+], M$	$[Na^+], M$	$\bar{H}_t^+, meq$	$\frac{\bar{H}_t^+}{[H^+]}, ml$	$\left(\frac{\bar{H}_t^+}{[H^+]}\right)_c^a, ml$
11.09	0.1000	165.	152.	156
	0.2000	90.0	85.0	87
	0.3000	71.8	64.8	64.8
	0.4000	59.8	53.9	53.9
	0.5000	50.2	45.3	46.4
	0.7748	39.5	35.6	35.6
	1.200	32.9	29.6	29.7
5.543	0.1000	88.8	163.	165.
	0.2000	47.4	88.5	95.6
	0.3000	40.1	72.5	72.5
	0.4000	34.3	61.9	61.9
	0.5000	28.9	52.2	54.3
	0.7748	23.7	42.8	42.9
	1.200	20.2	36.4	36.4
2.218	0.1000	39.3	180.	180
	0.2000	23.5	109.	113.0
	0.3000	20.4	92.3	91.0
	0.4000	17.5	78.9	77.5
	0.5000	14.8	66.9	71.0
	0.7748	12.8	58.0	58.0
	1.200	9.96	44.9	44.9
1.109	0.1000	20.6	189.	189
	0.2000	13.4	124.	125
	0.3000	11.6	107.1	104
	0.4000	10.0	90.8	90.8
	0.5000	8.84	79.7	81.7
	0.7748	7.10	64.0	64.0
	1.200	5.40	48.8	48.8
0 <sup>b</sup>	0.1000		218	
	0.2000		152	
	0.3000		132	
	0.4000		112	
	0.5000		99	
	0.7748		76	
	1.200		55	

<sup>a</sup>Corrected value taken from curves in Figure 6<sup>b</sup>By extrapolation in Figure 5.

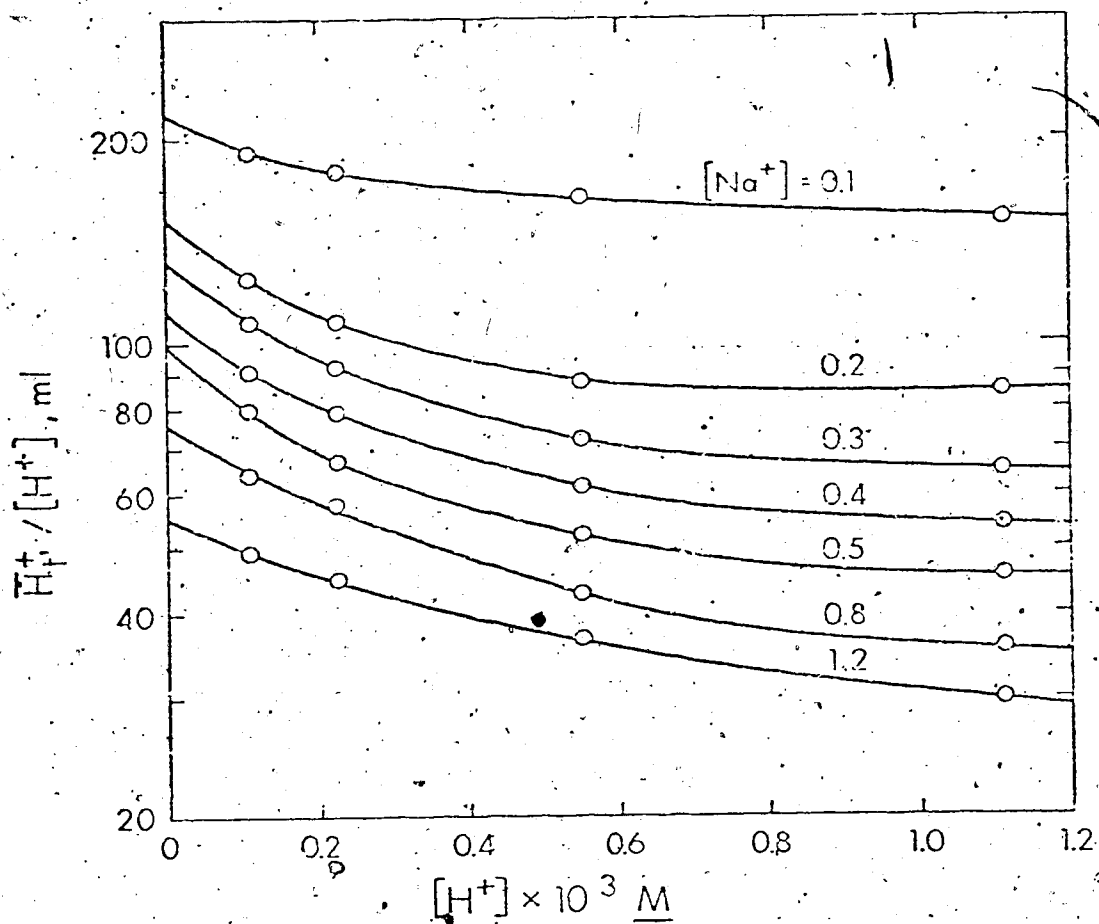


Figure 5. Plots of ratio of total  $H^+$  in resin phase over  $[H^+]$  against  $[H^+]$  at varying concentrations of  $Na^+$  in the external solution

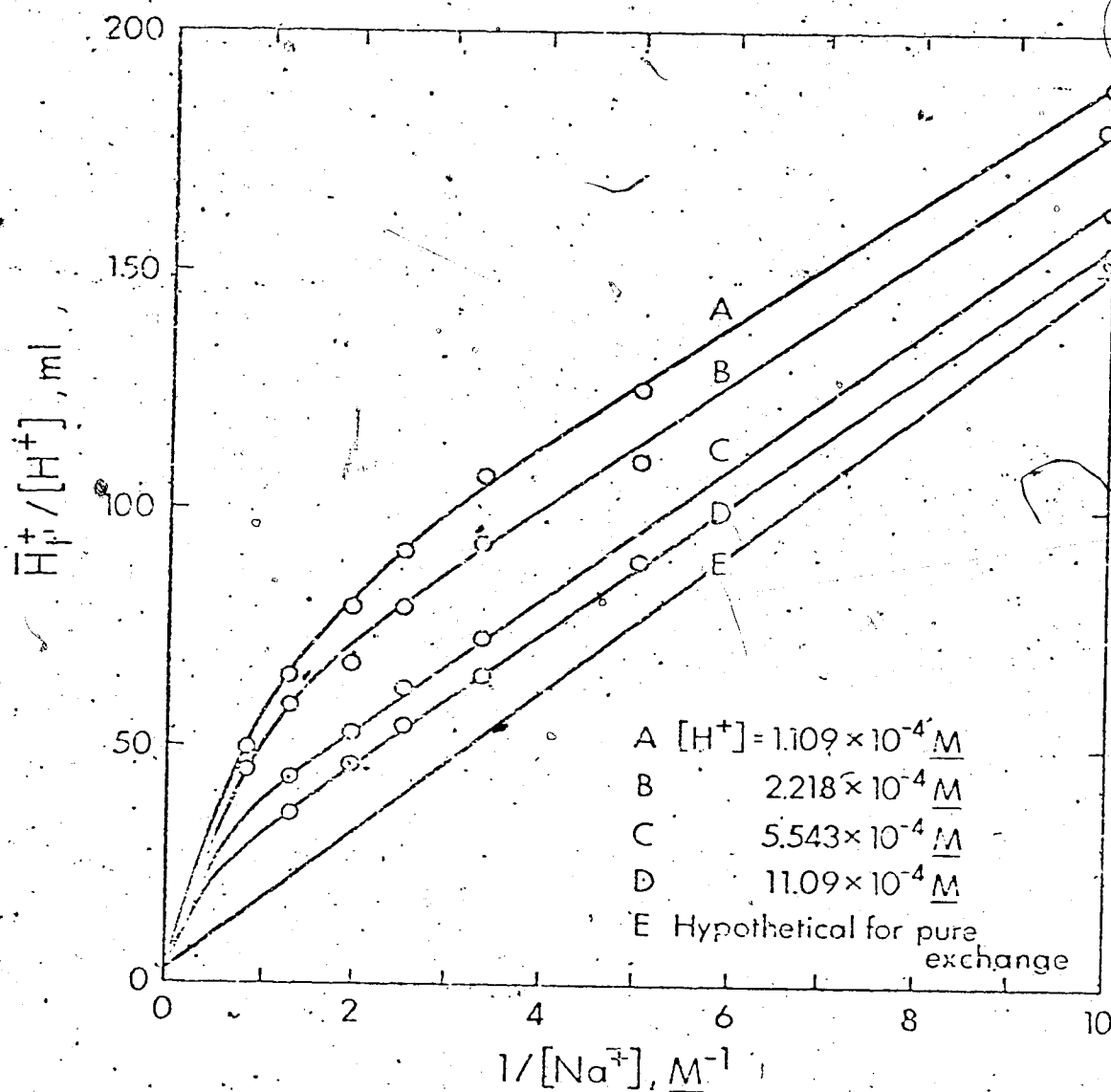


Figure 6. Plots of ratio of total  $H^+$  in resin phase over  $H^+$  concentration against reciprocal of  $Na^+$  concentration at varying concentrations of  $H^+$  in the external solution.

The extra hold-up phenomenon can be explained both in terms of heterogeneous and homogeneous models. The characteristics of these models are described in Appendix II. The isotherms representing these two models are tabulated for comparison in the table below, and show that both models serve equally well in interpreting the data with different aspects.

	heterogeneous model	homogeneous model
isotherm	$\frac{[H^+]}{\bar{H}_S} = \frac{[H^+]}{a} + \frac{k_2+k_4 [Na^+]}{k_1 a} \quad (AII6)$	$\frac{[H^+]}{\bar{H}_S} = \left( \frac{V_s + k_{Na} c}{a k_H} \right) \frac{[Na^+]}{cK} + \frac{[H^+]}{a} \quad (AII8)$
I/S	$\frac{I}{S} = \frac{k_2+k_4 [Na^+]}{k_1} \quad (AII7)$	$\frac{I}{S} = \left( \frac{V_s + k_{Na} c}{k_H cK} \right) \times [Na^+] \quad (AII9)$

The validity of Equations (AII6) and (AII8) can be tested by a plot of  $[H^+]/\bar{H}_S$  vs.  $[H^+]$  (Figure 7), where  $\bar{H}_S/[H^+]$  is calculated by Equation (AII1) from  $\bar{H}_t/[H^+]$  after subtracting the dead volume  $V_m$ . Since  $\bar{H}_S/[H^+]$  involves the difference of two nearly equal numbers, its precise estimation is difficult. Accurate value of  $\bar{H}_e/[H^+]$  can be obtained from  $K_{Na}=1$ , but obtaining accurate values for  $\bar{H}_t/[H^+]$  is difficult.



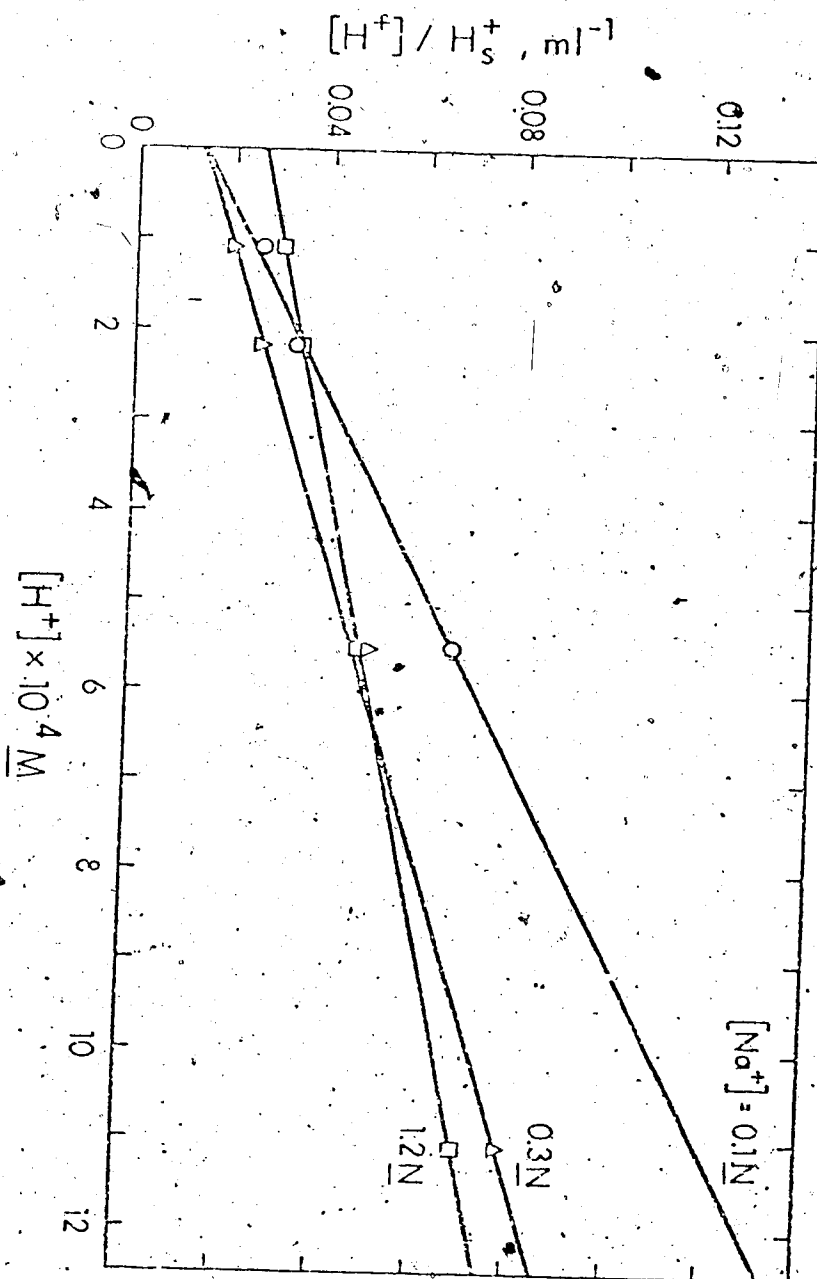


Figure 7. Plots of  $H^+$  concentration in external solution over sorbed  $H^+$  against  $H^+$  concentration in external solution at several concentrations of  $Na^+$  in external solution

The method used to minimize the effect of random scattering of individual points was to take values of  $\overline{H}_t^+ / [H^+]$  from the smooth curve joining those points rather than the measured values. In this way acceptable results were achieved (Table 6). As illustrated in Figure 7, plots of  $[H^+] / \overline{H}_S^+$  vs.  $[H^+]$  give straight lines. Both the homogeneous and heterogeneous mechanisms proposed provide a satisfactory explanation for the large amount of  $H^+$  retained in the resin. The intercepts agree with the extrapolated values in Figure 5. The values for the slopes are shown in Table 7. The heterogeneous sorption constants  $k_2/k_1$  and  $k_4/k_1$  can be determined from a plot of the ratios of the intercept  $I$  to the slope  $S$  against  $[Na^+]$  Equation (AII7) (Figure 8). These are found to vary slightly with  $[Na^+]$ ; with  $[Na^+] < 0.55 \text{ M}$ , the values found were  $k_2/k_1 = 1.05 \times 10^{-4} \text{ meq ml}^{-1}$  and  $k_4/k_1 = 3.6 \times 10^{-4}$ , while with  $[Na^+] > 0.6$ , the values were  $k_2/k_1 = 0$  and  $k_4/k_1 = 5.27 \times 10^{-4}$ . The homogeneous constant  $K_0$ , which is equal to  $(V_S + k_{Na}c) / k_H cK$ , can similarly be estimated from Figure 8, using Equation (AII9), and was found to range from  $14.4 \times 10^{-4}$  to  $5.27 \times 10^{-4}$ .

Table 6

Data for measurement of total  $H^+$  in resin phase by column equilibration at various  $Na^+$  and  $H^+$  concentrations in external solutions.

$[Na^+]$	$[H^+]$ $\times 10^{-4} M$	$\left( \frac{H^+}{[H^+]} \right)_c$	$\frac{H^+}{[H^+]} + \frac{V_m}{V_s}$	$\frac{[H^+]}{H^+}$
0.1	1.109	189.2	150	0.0255
	2.218	180.3		0.0330
	5.543	165.0		0.0667
	11.09	156.5		0.1540
0.2	1.109	125.5	76.5	0.0204
	2.218	113.0		0.0274
	5.543	95.6		0.0525
	11.09	87.5		0.0909
0.3	1.109	104.1	52.0	0.0192
	2.218	91.0		0.0256
	5.543	72.5		0.0488
	11.09	64.8		0.0781
0.4	1.109	90.8	39.8	0.0196
	2.218	77.5		0.0265
	5.543	61.9		0.0452
	11.09	53.9		0.0708
0.5	1.109	81.7	32.4	0.0203
	2.218	71.0		0.0260
	5.543	54.3		0.0458
	11.09	46.4		0.0717
0.7748	1.109	64.0	22.0	0.0238
	2.218	58.0		0.0278
	5.543	42.9		0.0479
	11.09	35.6		0.0733
1.2	1.109	48.8	15.3	0.0298
	2.218	44.9		0.0337
	5.543	36.4		0.0472
	11.09	29.7		0.0693

Table 7

Values for ratio of intercept to slope and of total  $H^+$  in resin phase to  $H^+$  concentration in external solution as a function of  $Na^+$  concentration.

$[Na^+]$ , M	Intercept, $I$ $10^{-4}$ ml $^{-1}$	Slope, $S$ meq $^{-1}$	$\frac{a}{Na_D}$ meq	$\frac{I}{S}$ $M \times 10^{-4}$	Calc. <sup>b</sup> $(H_t^+ / [H^+]_0)$	Extrap. c.	Measured <sup>d</sup>
0.1	137	94.9	10.5	4.18	1.44	223.0	218
0.15	-	-	-	-	-	-	213
0.2	129	70.6	14.1	16.7	1.82	154.0	152
0.25	-	-	-	-	-	-	151
0.3	127	59.1	16.9	37.6	2.19	132.0	132
0.33	-	-	-	-	-	-	136
0.4	138	56.4	17.7	66.9	2.45	112.0	112
0.5	146	51.5	19.4	105	2.83	101.0	99
0.7748	183	45.0	22.2	251	4.08	76.5	76
0.8	-	-	-	-	-	-	65
1.2	252	39.8	25.1	602	6.32	55.1	55

<sup>a</sup>Calculated by Equation (14a).

<sup>b</sup>Calculated by  $H_e^+ / [H^+] + \bar{V}_m + I^{-1}$ .

<sup>c</sup>Extrapolated values from Table 5 and Figures at  $[H^+] = 0$ .

<sup>d</sup>Chromatographic values.

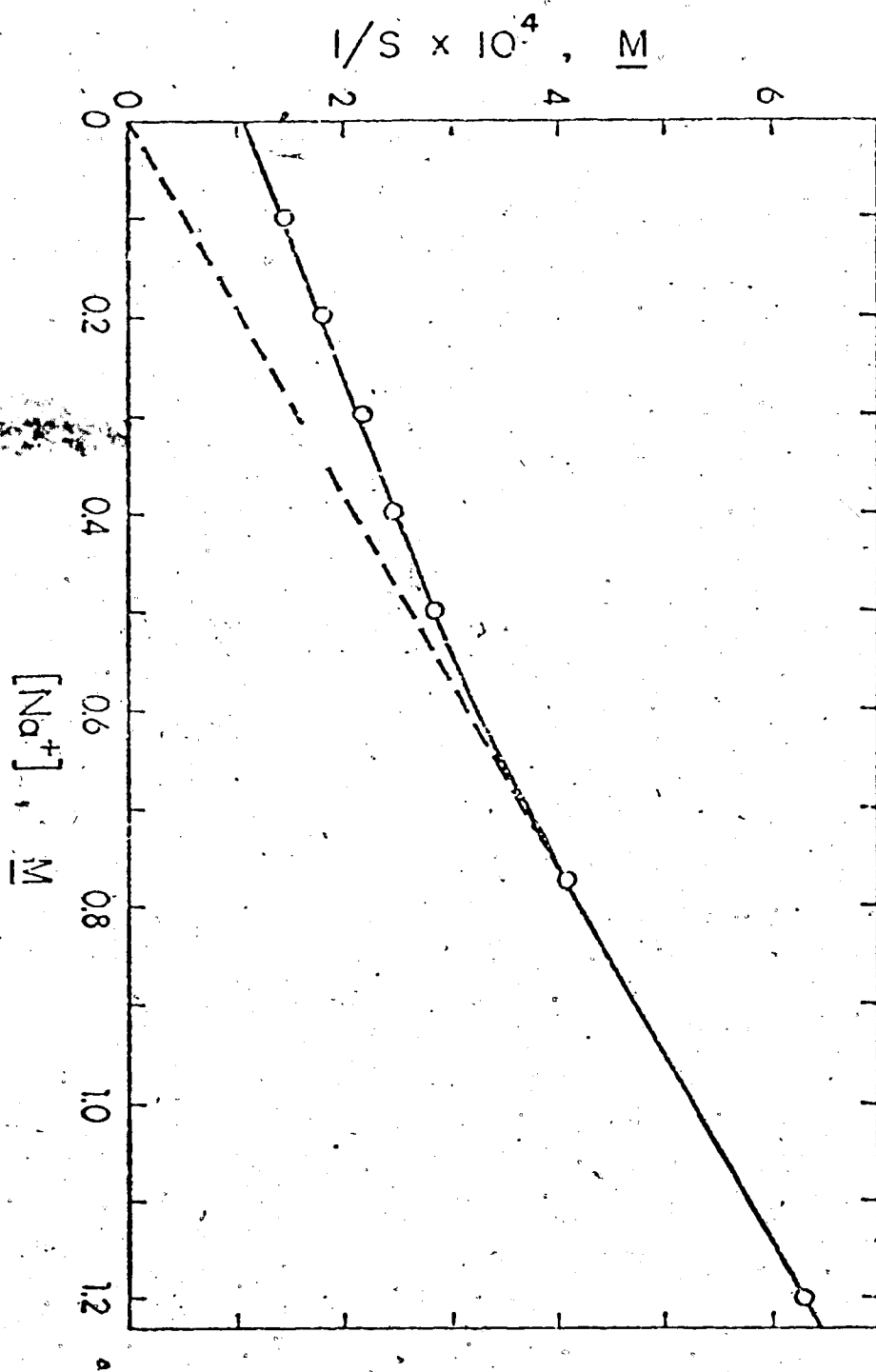


Figure 8. Plot of the ratio of the intercept to slope from Table 7 against  $Na^+$  concentration in external solution

## Comments on the Two Models

### Quasi-heterogeneous model

Comparing the value of  $\bar{a}$ , the effective capacity, with that for  $\text{Na}_D^+$  measured previously in a single electrolyte NaCl solution, it is seen that  $\bar{a}$  is larger. This means that not all sorbed  $\text{Na}^+$  is replaced by  $\text{H}^+$ . If  $\bar{a}$  is plotted against  $\text{Na}_D^+$  on a log-log scale (Figure 8a), a linear relation is observed.

The values of  $k_2/k_1$  and  $k_4/k_1$  indicate that the tendency for HCl to replace NaCl is  $10^4$  times greater than the reverse process. This large difference is unexpected for a simple replacement mechanism not involving specific interaction. In that process, the sorption tendency depends chiefly on the hydration radii, and so the sorption constant  $k_4/k_1$  should hardly exceed 10 or so. From the value of  $k_4/k_1$  measured, the presence of specific interaction of  $\text{H}^+$  with the resin is suspected. In order to confirm such interaction, the reverse experiment should be run at the other end of the concentration range, with the resin in the  $\text{H}^+$  form and trace NaCl in HCl solution. This is done in the next chapter.

### Homogeneous model

The ion association concept is valuable in treating the homogeneous model. Association has already been confirmed by NMR experiments and thermo-

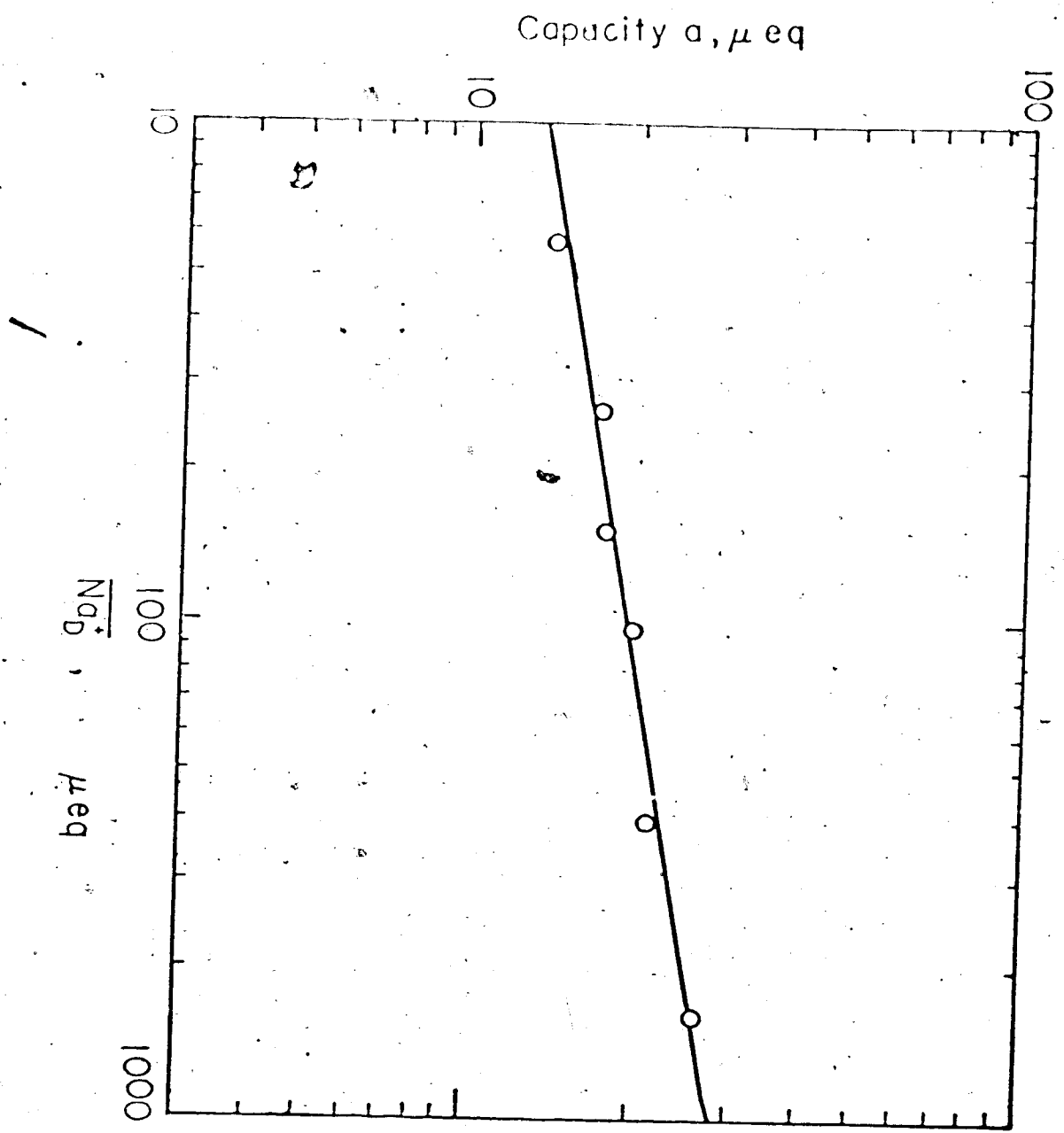


Figure 8a. Plots of  $\text{Na}^+$  sorption due to cationic inversion against the effective capacity  $a$

dynamics. The internal hydration number  $\bar{n}$  has been measured by NMR using a temperature variation technique<sup>82, 83</sup>. The value of  $\bar{n}$  for  $H^+$  is 2.3; this compares with a value of 3.4 in aqueous solution. Little difference is seen for  $Na^+$  and  $K^+$ . The smaller  $\bar{n}$  indicates a "partial bonding" between  $H^+$  and  $-SO_3^-$  groups, even though it is much weaker than a covalent bond. This supports fairly well the idea that association of  $H^+$  with the resin is  $10^2$ – $10^3$  times stronger than  $Na^+$ , as observed experimentally ( $K_O$   $14.4$ – $5.3 \times 10^{-4}$ ). The system  $HCl-H_2O-LiCl$ -sulfonated polystyrene 0.5 to 24% DVB resin has been studied<sup>128</sup>, and the ion exchange constant  $K_{Li/H}$  measured for resins in both  $Li^+$  and  $H^+$  forms. The ratio of  $K_{Li/H}$  at various percentages of DVB corresponding to internal molality  $\bar{m}$  (capacity  $c$ /internal water  $g$ ), to  $K_{Li/H}$  at 0.5% DVB ( $\bar{m} = 0.7$ ) in  $H^+$  form and  $Li^+$  form were plotted against  $\bar{m}$ . It was found that the ratio for resins in the  $H^+$  form did not vary with  $\bar{m}$ , whereas that in the  $Li^+$  form did. This was explained by the authors as being due to a greater degree of localization of  $H^+$  in the resin compared with  $Li^+$ ; the decrease in internal water content in the resin will not affect interaction between the localized ions until with increased crosslinking the ions begin to overlap.



Association also exists between sodium ions and sulfonate sites, though to a much smaller extent, as Creech<sup>126</sup> and Dinius<sup>84</sup> proved by  $\text{Na}^{23}$  NMR quadrupole relaxation measurements. A broad line width leads to the conclusion that some sodium ions are loosely bound and thus restricted in motion.

It should be emphasized that since the activity of counter ions in the resin depends solely on  $\bar{V}_s$ , the state of resin swelling is extremely important in the homogeneous model. First, as is shown in Figure 8a,  $\bar{a}$  is not a constant, but varies from 11 to 25 meq/16.9 meq sulfonate group as  $[\text{Na}^+]$  varies from 0.1 to 1.2 M. This is a consequence of resin shrinkage. An increase in  $[\text{Na}^+]$  causes the resin to contract and thus  $\bar{m}$  to increase. A higher ionic strength in the resin phase will promote the number of sulfonate groups able to be bound by ions  $\text{H}^+$  and  $\text{Na}^+$ . Also, Equation (AII9) predicts a straight line passing through the origin in a plot of intercept  $I$  over slope  $S$  vs.  $[\text{Na}^+]$ ; the deviation from a straight line passing through zero in Figure 8 at low sodium ion concentrations is caused by the presence of internal water in the resin. The rate of change in water content with  $[\text{Na}^+]$  is largest at low external  $\text{Na}^+$  concentration (0.1 M to 0.5 M), so  $K_0$  changes appreciably with  $[\text{Na}^+]$  in that concentration range. Resin shrinkage almost ceases once the external

concentration reaches 0.1 N; after this point it should pass through the origin as represented in the figure by the dotted line. Changes in the internal activity coefficient may also cause deviation from 1.0 and a change in  $\alpha$ .

The fact that  $\alpha$  is much smaller than  $\epsilon$ , the exchange capacity, may be a result of not all the sulfonate groups being capable of undergoing  $H^+$  ion exchange, or that the sulfonate groups capable of undergoing ion exchange are fundamentally different from the exchangeable ones. This might occur if, for example, two sulfonate groups are present on the same benzene ring, the second group being introduced incidentally by a disulfonation reaction in the manufacturing process even though carried out under well-controlled monosulfonation conditions.

It is possible that the resin may contain in addition to sulfonic acid groups a small number of weak acid exchange groups, i.e.,  $-COOH$  carboxylic acid groups as an impurity. These are believed to be introduced during the sulfonation step in the manufacturing process, for hot concentrated sulfuric acid can oxidize some of the carbon-carbon linkages between benzene rings to carboxylic acid groups in amounts ranging up to 5% of the total exchange capacity<sup>129,130</sup>. These groups are normally present in small quantity, so that they are not

noticeable when the resin is in the  $H^+$  form. They may, however, play a significant role once the acid concentration in the external solution becomes low, as is the case where the resin is predominantly in the  $Na^+$  form. Under these conditions the resin may show an abnormal uptake of  $H^+$ . Though the presence of carboxylic acid groups in a sulfonic acid resin cannot be confirmed directly by instrumental techniques, their level can be measured by photometric and potentiometric titrations of 2-methylpyridine ( $pK_b = 8$ ) in the presence of Dowex 50W  $\times$  8 resin in the  $Li^+$  forms as proposed by Cantwell and Pietrzyk<sup>131,132</sup>. The total level of impurity in the resin studied amounted to 5 meq/g of resin, and the  $pK_b$  of the basic impurity was found to be 8, which corresponds to the carboxylate group.

The homogeneous model proposed above is still valid except that the association is now considered to be between  $H^+$  and carboxylic groups rather than sulfonate groups. The homogeneous treatment can then serve as a method of determining the quantity as well as the  $H^+/Na^+$  exchange constant of the carboxylic sites.  $a$  calculated from (AII8), (AII9) gives the total milliequivalents of carboxylic groups in the column of resin, while  $(\frac{V_s + k_{Na}c}{k_H cK})$  is the exchange constant of  $Na^+$  for  $H^+$ . Both show dependence upon the NaCl concentration and the degree of swelling of the resin. The

amount of  $\text{-CO}_2\text{H}$  found in Cantwell's work was approximately  $5 \times 16.9 / 5.2 = 15$   $\mu\text{g}$  per 16.9 meq. of resin, which is within the range of 11 to 25  $\mu\text{g}$  per 16.9 meq. of resin measured in this work. Even though the uptake of  $\text{H}^+$  by  $\text{-COO}^-$  may be a major factor in explaining the abnormal behavior of  $\text{H}^+$  sorption at trace levels, association of  $\text{H}^+$  and  $\text{-SO}_3^-$  (which is confirmed by NMR experiments) cannot be excluded. Thus both  $\text{-COO}^-$  and to a less extent  $\text{SO}_3^-$  likely contribute to the extra-sorption of  $\text{H}^+$ .

#### Chromatography

Elution chromatography can also be applied to measure ion exchange constants, providing the constant is independent of the amount of solute used. By inserting known values of  $\underline{V}_m$  and  $[\text{Na}^+]$  into Equation (11),  $\underline{V}_R$  can be calculated.

$$\underline{V}_R = \underline{V}_m + \frac{0.87 \times 16.9}{[\text{Na}^+]}$$

In practice, chromatograms obtained at several NaCl concentrations show skewed elution peaks, which indicates a nonlinear isotherm. This nonlinearity is even more obvious in a plot of  $\underline{V}_R$  against sample size. The shape of the curves obtained in such a plot is similar to those shown in Figure 5;  $\underline{V}_R$  rises slowly with decreasing sample size, and can no longer be

related to the partition coefficient in a simple way. Although  $K$  or  $\overline{H}_t^+/[H^+]$  cannot be found directly from  $\underline{V}_R$ , the value for  $\underline{V}_R$  still reflects the distribution of solute between the resin and external solution phases. However, the limiting value of  $(\overline{H}_t^+/[H^+])_0$  at infinite dilution of solute can be calculated from the limiting value for  $\underline{V}_R^0$  obtained by extrapolation.

$$\underline{V}_R^0 = \underline{V}_m + \left( \frac{\overline{H}_t^+}{[H^+]} \right)_0 \left( \frac{\overline{H}_t^+}{[H^+]} \right)_0$$

Good agreement was found between values of  $(\overline{H}_t^+/[H^+])_0$  obtained in this way and the extrapolated value found from Figure 5. Values of  $(\overline{H}_t^+/[H])_0$  obtained from the intercepts of Figure 6 are tabulated in Table 7. Three sets of values for  $(\overline{H}_t^+, [H^+])_0$  have been plotted against  $[Na^+]^{-1}$  in Figure 9 to provide a comparison among them.

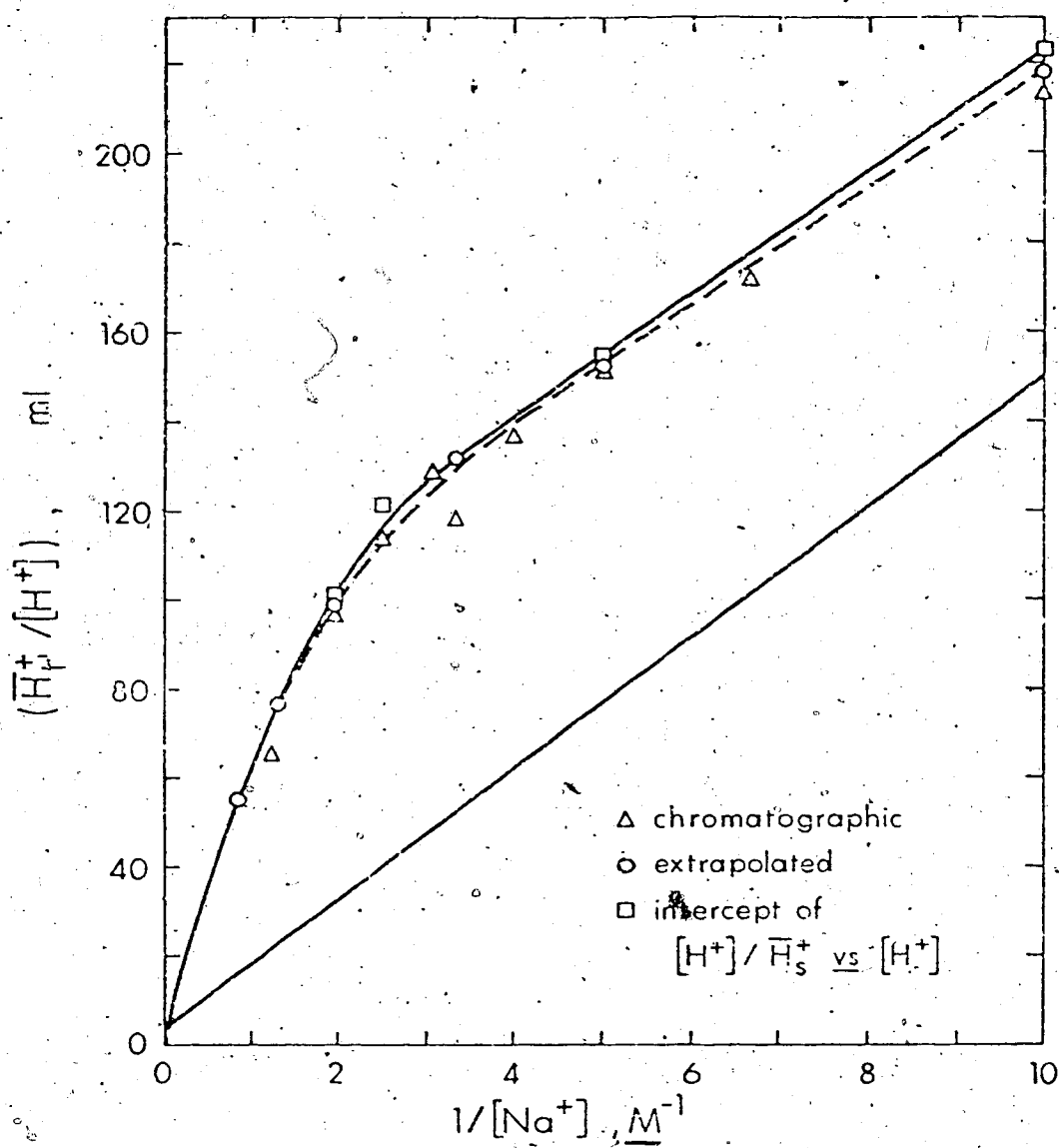


Figure 9. Comparison of three methods for determining the ratio of total  $H^+$  in resin phase over  $H^+$  concentration at different  $Na^+$  concentrations in external solution.

## CHAPTER IV

### FURTHER STUDIES OF THE HOMOGENEOUS MODEL

#### Sorption of Trace NaCl from Solutions of HCl on Dowex

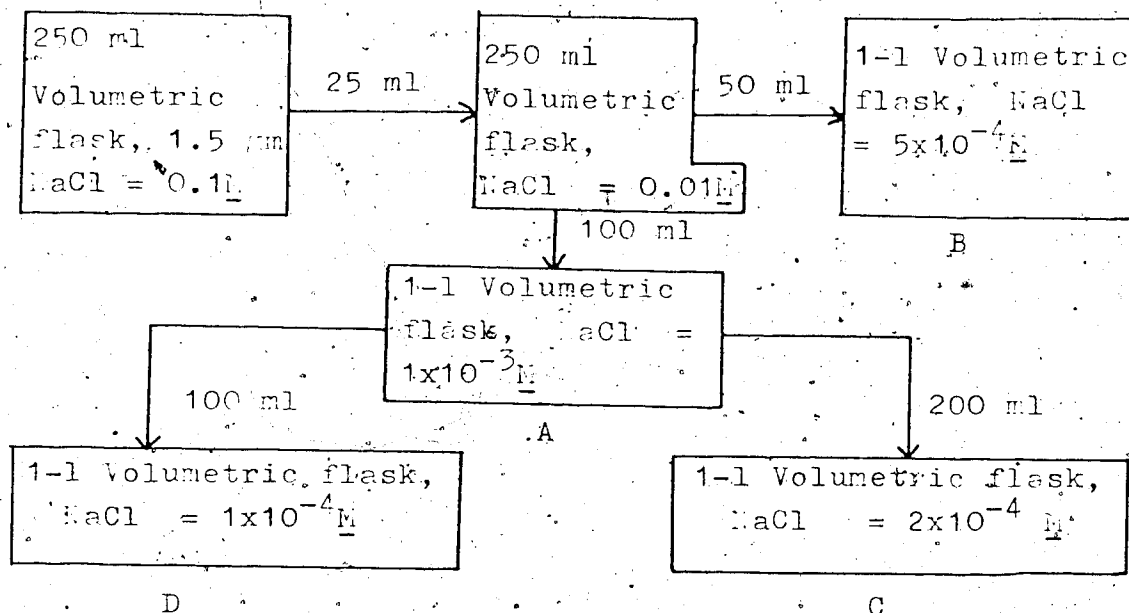
50W x 8

#### Experimental Procedure

This work was carried out using the same procedure as that of Chapter III, except that  $H^+$  and  $Na^+$  were reversed, and the concentration of  $Na^+$  was determined by flame photometry.

#### Measurement of $Na_t^+$

The concentrations of HCl studied were 0.1, 0.15, 0.4, 0.5, 0.75, and 1.2 M. The solutions were prepared immediately before use in a 5-litre plastic bottle, and were transferred to oven-dried volumetric flasks as required in the preparation of the equilibrating solutions. Four equilibrating solutions were used at each HCl concentration, each containing a different concentration of sodium ion ranging from  $10^{-3}$  to  $10^{-4}$  M. They were prepared according to the following scheme:



The concentration of acid present in each individual series of equilibrating solutions was measured by titration with 0.15 M NaOH, using phenolphthalein as indicator, while the concentration of NaCl was calculated directly from the weight taken in the first 250-ml volumetric flask. The experimental steps were as described in Chapter III, except that 1 M HCl was used to wash the sorbed NaCl from the column. A 500-ml volumetric flask was used to collect the washings for HCl concentrations of 0.1, 0.15 and 0.2 M; a 200-ml flask for 0.4 and 0.5 M; a 100-ml flask for 0.75 M; and a 50-ml flask for 1.2 M. About 50 ml of washings were collected, and then



diluted to volume with 1 M HCl.

#### Flame Photometric Determination of Na<sup>+</sup>

A Heath unit consisting of a monochromator, photomultiplier tube, and recorder was used to measure the concentration of sodium in the column effluents. The settings were as follows: oxidant: O<sub>2</sub>, dial setting of 13 on flow meter, 20 psi on tank regulator; fuel: H<sub>2</sub>, dial setting of 1 on flow meter, 10 psi on tank regulator; slit width: 28  $\mu$ m; wavelength setting, 588.9 nm; and sensitivity dial setting,  $0.5 \times 10^{-9}$  to  $5 \times 10^{-8}$ .

The detailed operating procedure used was that provided in the handout of Chemistry Course 615, Analytical Spectroscopy, University of Alberta. The intensity was recorded on a Heath recorder and was measured until a steady signal was obtained, about 4 minutes. A matrix-matching technique was employed for calibration, that is, five standard solutions containing NaCl concentrations of  $0.26 \times 10^{-4}$ , 0.53, 1.06, 2.65 and  $5.30 \times 10^{-4}$  M were prepared and all made 1 M in HCl. Where the concentration of the samples measured was so high that the signal was out of the range of the standard solutions, further dilution was used as required to bring the readings into range. After correcting the background measured by closing

the detector shutter (since the same reading was given by 1 M HCl alone), the intensity of the signals of the standard solutions, multiplied by the sensitivity factor, was plotted against  $[\text{Na}^+]$  on full log graph paper and the concentration of the samples read from the plot. Then  $\overline{\text{Na}}_t^+$  could be obtained by multiplying the concentration by the volume of the container.

#### Measurement of $K_{\text{Na/H}}$

$K_{\text{Na/H}}$  was measured by the column method described in Chapter III, but with the resin in the  $\text{H}^+$ -enriched form. Since in this experiment  $\text{Na}^+$  was a minor component, it had to be determined directly to avoid subtraction errors. This was done by the above procedure. The ionic strengths studied were 0.1, 0.2, 0.5 and 1 M, with concentration ratios for  $[\text{HCl}]$  to  $[\text{NaCl}]$  of 17.7, 7.4, 1.95 and 0.79 at each ionic strength. The ratio under unity was measured by an acid-base titration, as outlined in Chapter III, because it was  $\text{Na}^+$  rich. The solutions were prepared from a 4.5 M HCl stock solution standardized by 0.15 M NaOH after tenfold dilution. Then 215, 200, 150 and 100-ml portions of stock HCl solution were added to a series of 1- $\ell$  volumetric flasks and the ionic strength brought to 1 M by addition of exactly weighed portions of NaCl. The solutions at ionic strengths of 0.1, 0.2 and 0.5 M were made by successive dilution of the 1 M solution.

### Results and Discussion

The data were handled in a similar way to that described in Chapter III. Values for  $K_{Na/H}$  ( $\bar{X}_H = 1$ ) were determined at the various ionic strengths by extrapolation (Table 8, Figure 10), and found to be 1.31 for 0.1 M, 1.33 for 0.2 M, 1.31 for 0.5 M, and 1.29 for 1 M ionic strengths. The values of  $K_{Na/H}$  ( $\bar{X}_H = 1$ ) at any other HCl concentration can then be obtained by interpolation. Since the variation in  $K_{Na/H}$  ( $\bar{X}_H = 1$ ) with ionic strength is slight, the use of a graph is not necessary, and interpolated numbers are listed in column 5, Table 9. From these data  $\overline{Na_e^+}/[Na^+]$  can be calculated as outlined in Chapter III by

$$\frac{\overline{Na_e^+}}{[Na^+]} = K_{Na/H}(\bar{X}_H=1) \frac{C}{[H^+]}$$

From the previous experiment  $\underline{v}_m$  is estimated to be around 3.5 ml. The sum of  $\overline{Na_e^+}/[Na^+]$  and  $\underline{v}_m$ , then, which represents the uptake of  $Na^+$  due to exchange and dead volume, is shown in column 6 of Table 9.

Values for  $\overline{Na_e^+}/[Na^+]$  obtained by the column equilibration method are plotted against  $[Na^+]$  at various HCl concentrations in Figure 11. The series of horizontal straight lines observed indicates the independence of total  $Na^+$  sorption (exchange and

Table 8

Variation of  $K_{Na/H}^*$  with ionic strength and concentration ratio for Dowex 50W x 8 at 21°C.

$\frac{[H^+]}{[Na^+]}$	Ionic strength	$\bar{X}_H$	$K_{Na/H}^*$
17.65	1	0.928	1.358
	0.5	0.926	1.401
	0.2	0.924	1.444
	0.1	0.930	1.324
7.375	1		1.438
	0.5	0.834	1.460
	0.2	0.826	1.551
	0.1	0.831	1.495
1.945	1	0.573	1.445
	0.5	0.569	1.470
	0.2	0.555	1.560
	0.1	0.558	1.536
0.7865 <sup>a</sup>	1	0.376	1.303
	0.5	0.360	1.393
	0.2	0.351	1.453
	0.1	0.352	1.445

<sup>a</sup> Measured by NaOH titration, as described in Chapter III.

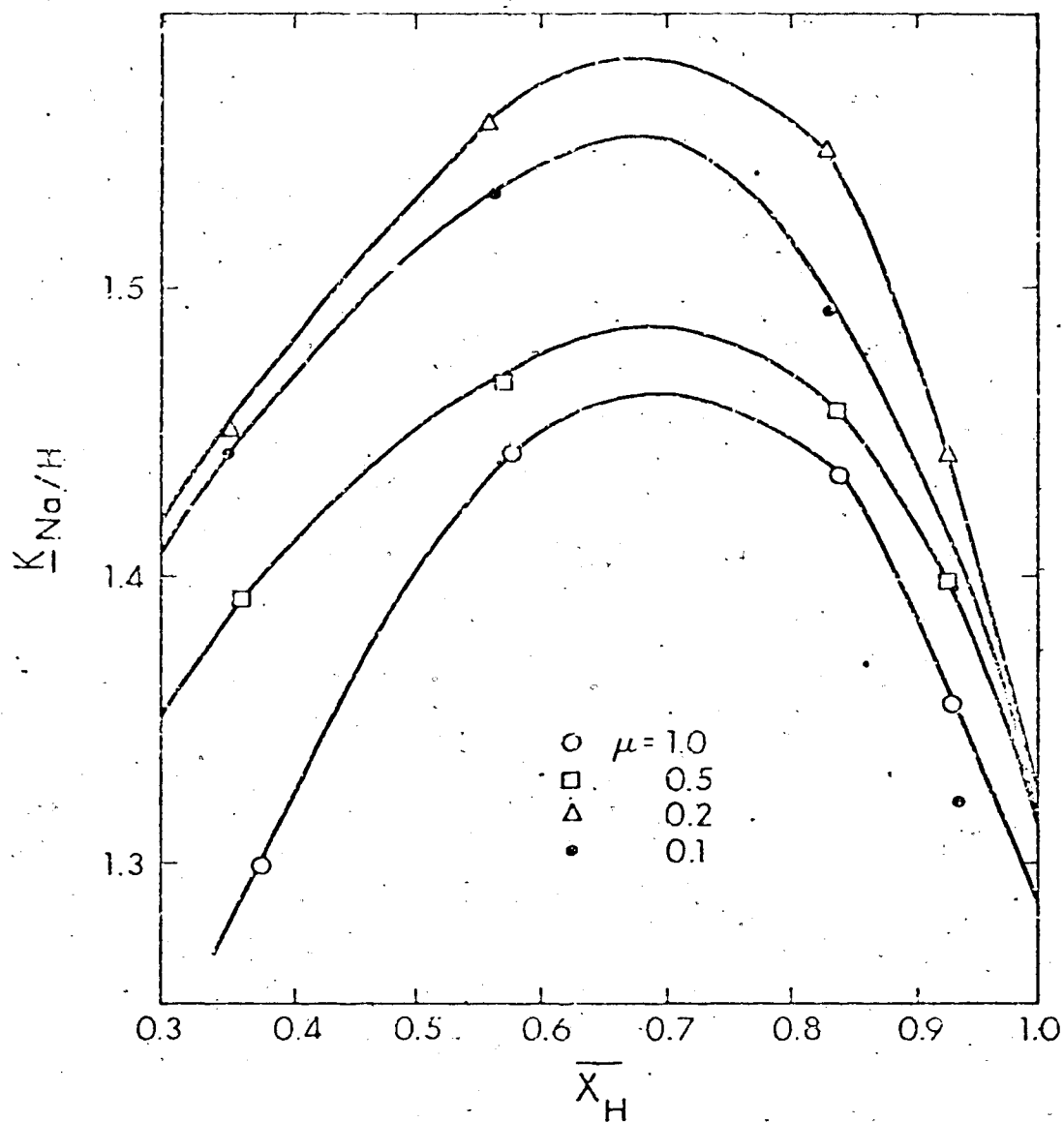


Figure 10. Plots of ion exchange constant  $\bar{K}$  for  $Na^+ - H^+$  exchange on Dowex 50W  $\times$  8 as function of the mole fraction of resin in the  $H^+$  form at ionic strengths of 0.1, 0.2, 0.5 and 1.

Table 9

Total sorption of  $\text{Na}^+$  as a function of  $[\text{HCl}]$  and  $[\text{NaCl}]$  on Dowex 50W-8 at  $21^\circ\text{C}$ .

$[\text{H}^+]$ M	$[\text{Na}^+]$ $10^{-4}$ M	$\text{Na}_\text{C}$ μeq	$\frac{\text{Na}_\text{C}}{[\text{Na}^+]}$ ml	$K_{\text{Na/R}} (X_{\text{H}} - 1)$ (interpolated value)	$\frac{\text{Na}_\text{C}}{[\text{Na}^+]} + v_m$
1.177	10.27	22.5	21.9	1.29	22.0
	5.134	11.1	21.5		
	2.054	4.5	21.9		
	1.027	2.27	22.1		
0.7555	10.27	31.1	30.3	1.30	32.6
	5.134	17.3	33.7		
	2.054	7.09	34.5		
	1.027	3.63	35.3		
0.5073	10.27	46.7	45.5	1.31	46.5
	5.134	23.3	45.3		
	2.054	9.08	44.2		
	1.027	4.79	46.6		
0.4097	10.27	53.8	52.4	1.32	57.5
	5.134	26.7	51.9		
	2.054	11.2	54.5		
	1.027	5.70	55.5		
0.2160	10.27	108	105	1.33	110
	5.134	57	111		
	2.054	23	112		
	1.027	11.5	112		
0.1480	10.27	164	160	1.31	156
	5.134	80.1	156		
	2.054	33.3	162		
	1.027	15.8	154		
0.09744	10.27	229	223	1.30	229
	5.134	116	226		
	2.054	46.2	225		
	1.027	23.5	229		

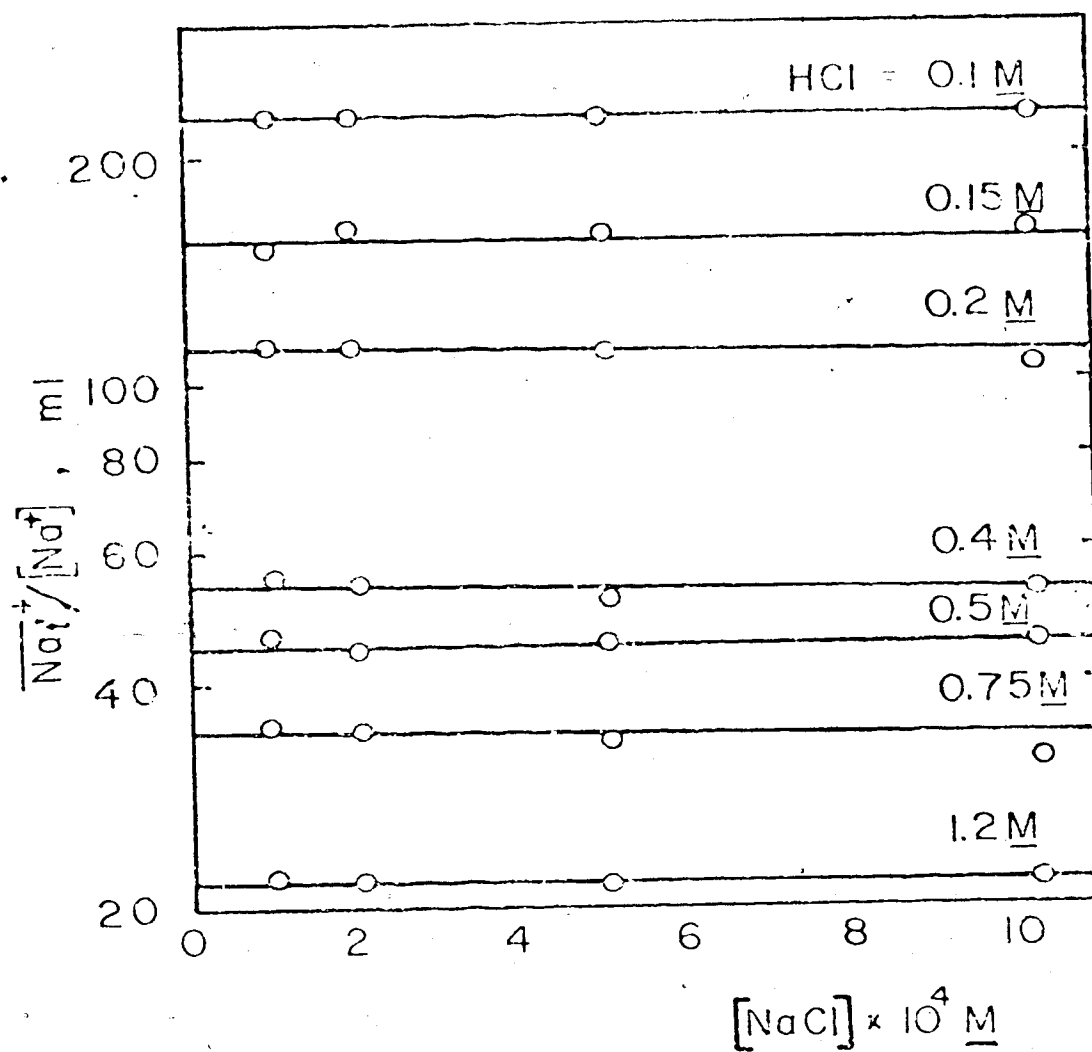


Figure 11. Plots of ratio of total  $Na^+$  in resin phase over  $Na^+$  concentration against  $Na^+$  concentration at varying concentrations of  $H^+$  in the external solution

corrected on the  $\text{Na}^+$  concentration. This differs significantly from the  $\text{H}^+$  experiment in the preceding chapter (figure 10). It is even more apparent if the average values of  $\text{Na}_0^+ / [\text{Na}^+]$  from Figure 11 are plotted against  $1/[\text{H}^+]$ , i.e., the points fall exactly on the hypothetical curve for pure exchange, i.e.,  $\text{Na}_0^+ / [\text{Na}^+] = \frac{1}{[\text{H}^+]}$  from column 6, Table 2 (Figure 12).

Figure 11 and 12 both reveal that there is no additional hold-up of  $\text{Na}^+$  in the HCl solution other than exchange. A special situation therefore appears to exist with the trace  $\text{H}^+$  case. The homogeneous model, especially the sorption by  $-\text{COO}^-$ , appears to be better than the heterogeneous one in dealing with sorption phenomena since a special affinity for  $\text{H}^+$  cannot be explained by the latter.

### Sorption of NaCl in HCl on Dowex 50W-8

#### Experimental Procedure

The procedure used was as described in section 1 of this chapter. All solutions were prepared by direct weighing of HCl (Fisher, Analytical grade) dried at  $110^\circ$ , and diluting of a  $0.01\text{M}$  NaCl stock solution, prepared by dissolving 1.1707 g NaCl and diluting to 2 litres in a volumetric flask. The preparation scheme was:



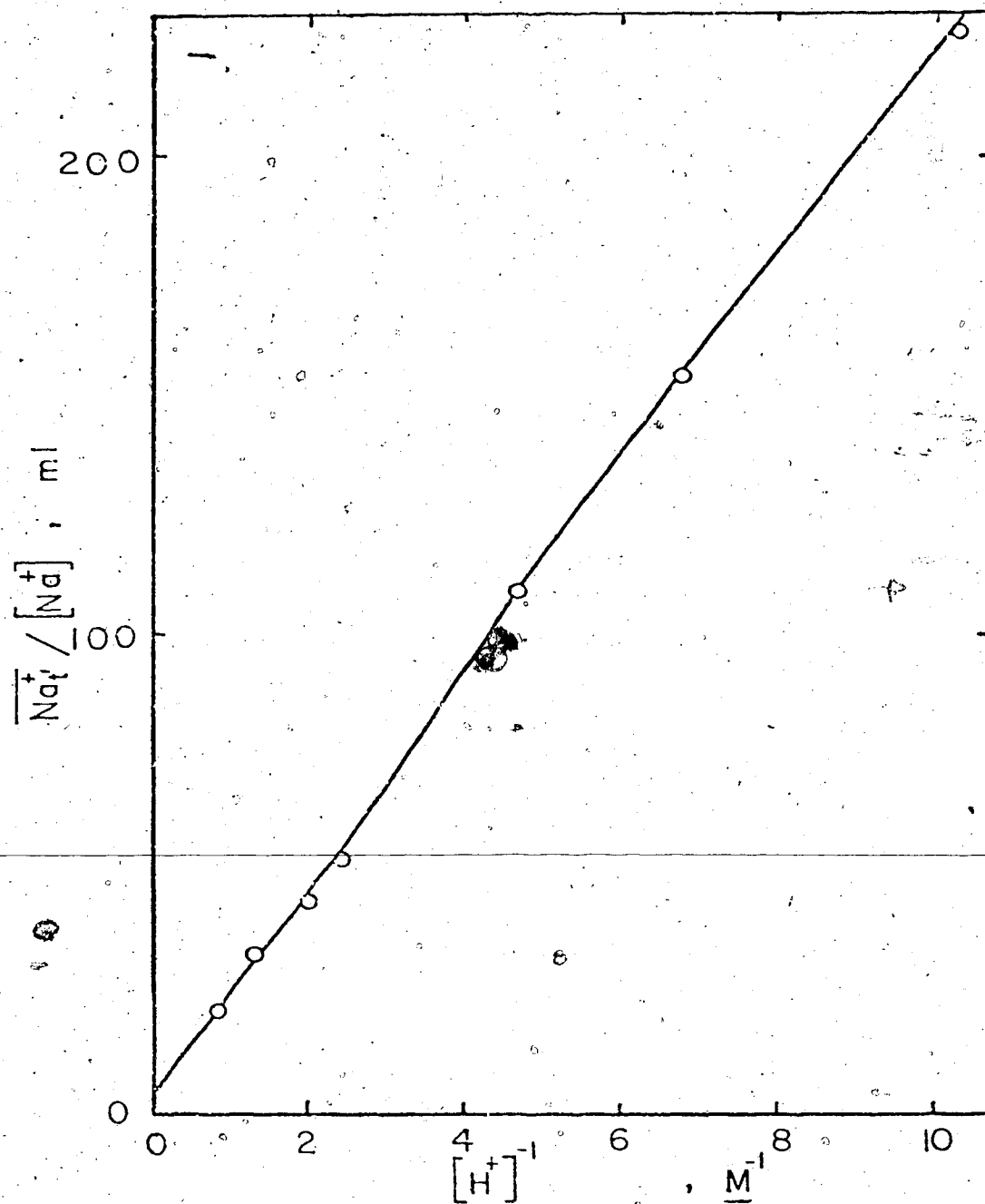
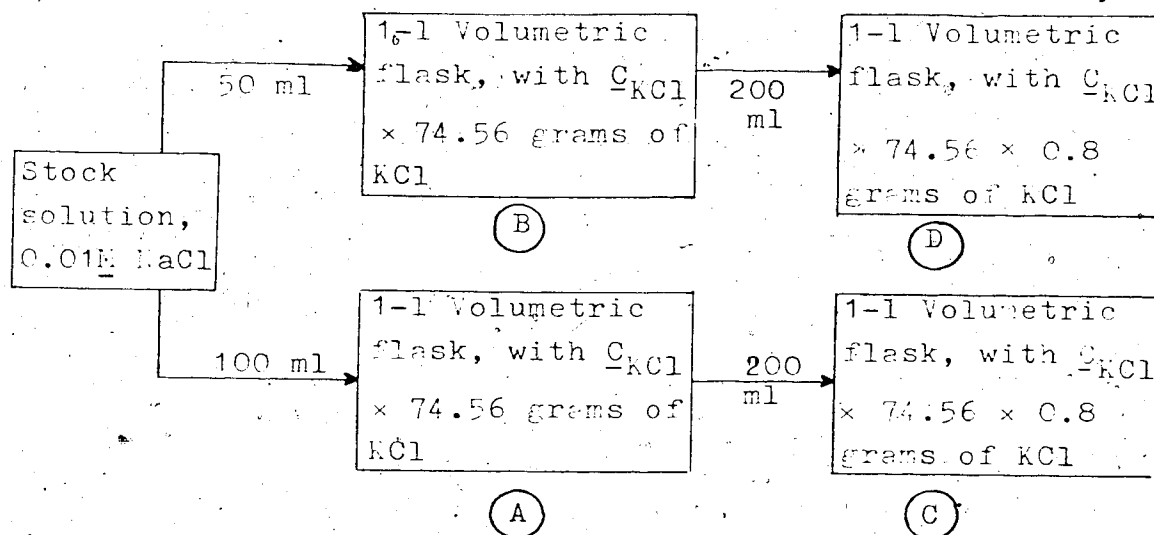


Figure 12: Plots of ratio of total  $Na^+$  in resin phase over  $Na^+$  concentration against reciprocal of  $H^+$  concentration at zero concentrations of  $Na^+$  in the external solution



$C_{KCl}$  was the concentration of KCl desired in molarity.

The solutions under study contained 0.1, 0.2, 0.3, or 0.5 M KCl, each with  $[NaCl] = 1 \times 10^{-4}$ ,  $2 \times 10^{-4}$ ,  $5 \times 10^{-4}$ , or

$10 \times 10^{-4}$  M. Since a suitable on-line monitor unit for sodium ion was not available (a sodium ion electrode not being satisfactory at the  $K^+$  concentrations present), the column was brought to equilibrium by passing a large volume of equilibrating solution, about 500 ml, through the column at a flow rate of 120 ml/hr without monitoring. 1 M HCl was used as washing solution.

The photometric determination of  $Na^+$  was done as described previously. The standard solutions used for calibration contained  $2.004 \times 10^{-5}$ ,  $5.01 \times 10^{-5}$ ,  $1.002 \times 10^{-4}$ ,  $2.004 \times 10^{-4}$  and  $5.01 \times 10^{-4}$  M NaCl solution,

together with 1 M HCl and 8 meq KCl/50 ml as background matrix. The data obtained were handled as outlined before in Chapters III and IV.

### Results and discussion

The value for  $\bar{K}_{Na/K}$  reported at  $\bar{X}_{Na} = 0$  (by extrapolation) by Reichenberg and McCauley<sup>133</sup> is 0.8. Plots of  $\log \bar{Na}_t^+ / [Na^+]$  against  $[Na^+]$  at constant KCl concentration are shown in Figure 13. A set of straight lines can be drawn within experimental error (8%) at different concentrations of KCl<sup>97</sup>, indicating that sorption of NaCl is negligible. The values of  $\bar{Na}_t^+ / [Na^+]$ , calculated from  $\bar{K}_{Na/K}$  ( $\bar{X}_{Na} = 0$ ) and corrected for  $V_m$ , are shown in column 5 of Table 10, and plotted in Figure 14 as a function of  $[KCl]^{-1}$  (solid line). The values of  $\bar{Na}_t^+ / [Na^+]$  at NaCl concentrations of  $1 \times 10^{-4}$  M and  $1 \times 10^{-3}$  M are also included in the same graph for comparison. The  $1 \times 10^{-3}$  M points fall on the hypothetical curve (solid line), while the  $1 \times 10^{-4}$  M points scatter around the line at low KCl concentrations. This indicates clearly that there is no detectable association of  $Na^+$  in dilute KCl solution. Because the association of  $Na^+$  with either carboxylic or sulfonic groups of the resin is comparable to that of  $K^+$ , even though both are negligible relative to  $H^+$ , slight association of  $Na^+$  might occur in the presence of KCl,

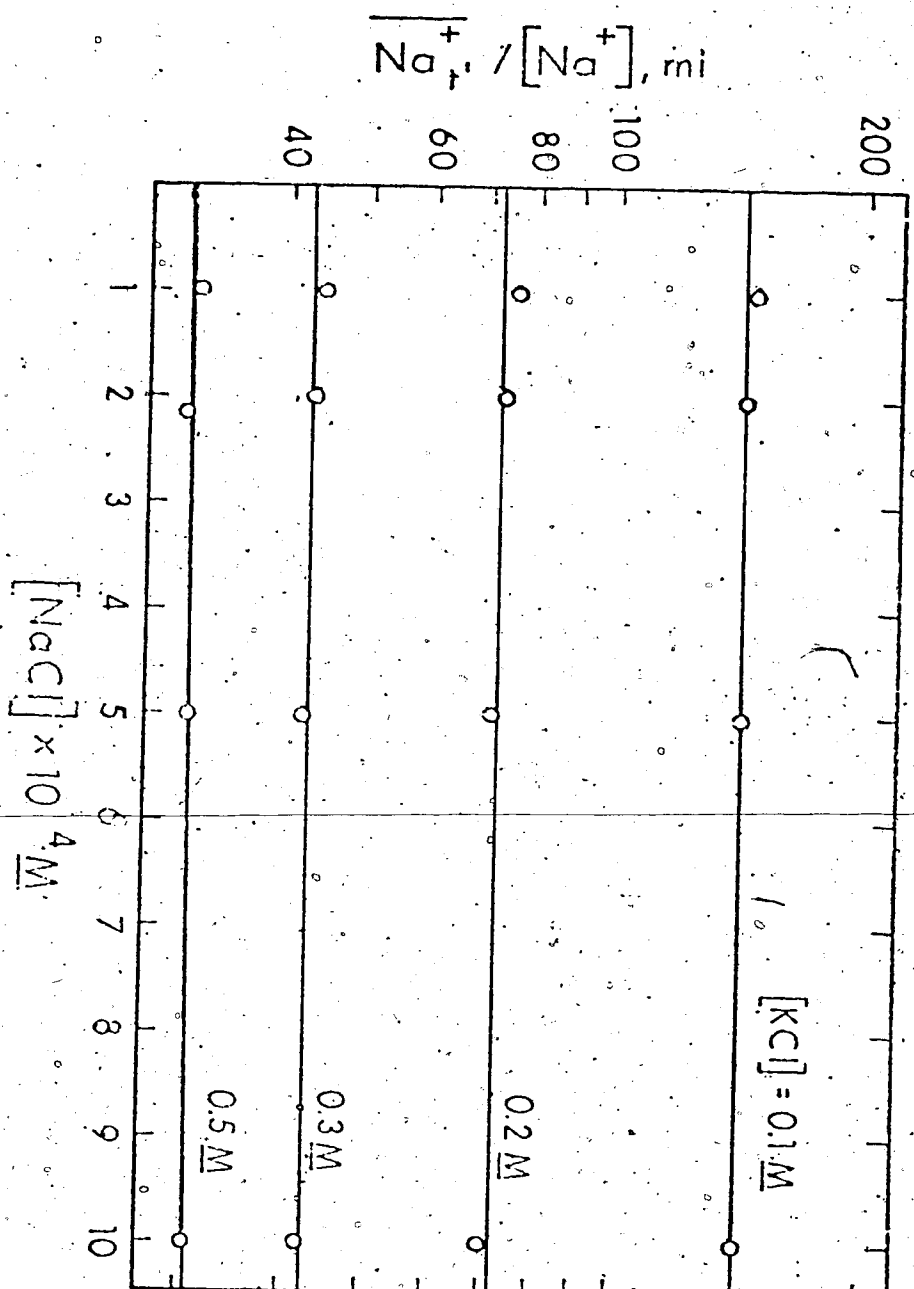


Figure 13. Plots of ratio of total  $\text{Na}^+$  in resin phase over  $\text{Na}^+$  concentrations against  $\text{Na}^+$  concentrations at varying concentrations of  $\text{K}^+$  in external solution.

Table 10

Total sorption of NaCl at various concentrations  
of KCl and NaCl on Dowex 50W x 8.

$[K^+]$ M	$[Na^+]$ $10^{-4}$ M	$\overline{Na_t^+}$ μeq	$\overline{Na_t^+}$ [Na <sup>+</sup> ] ml	$\overline{Na_e^+}$ [Na <sup>+</sup> ] ml	$+ \frac{v}{m}$
0.1	10.02	141	141	140	
	5.01	70.6	141		
	2.004	28.7	143		
	1.002	14.7	147		
0.2	10.02	70	70	71	
	5.01	35.6	71		
	2.004	14.6	73		
	1.002	7.5	75		
0.3	10.02	42	42	48	
	5.01	21	42		
	2.004	8.6	43		
	1.002	4.4	44		
0.5	10.02	30.7	30.5	30.5	
	5.01	15.3	30.5		
	2.004	6.0	30		
	1.002	3.1	31		

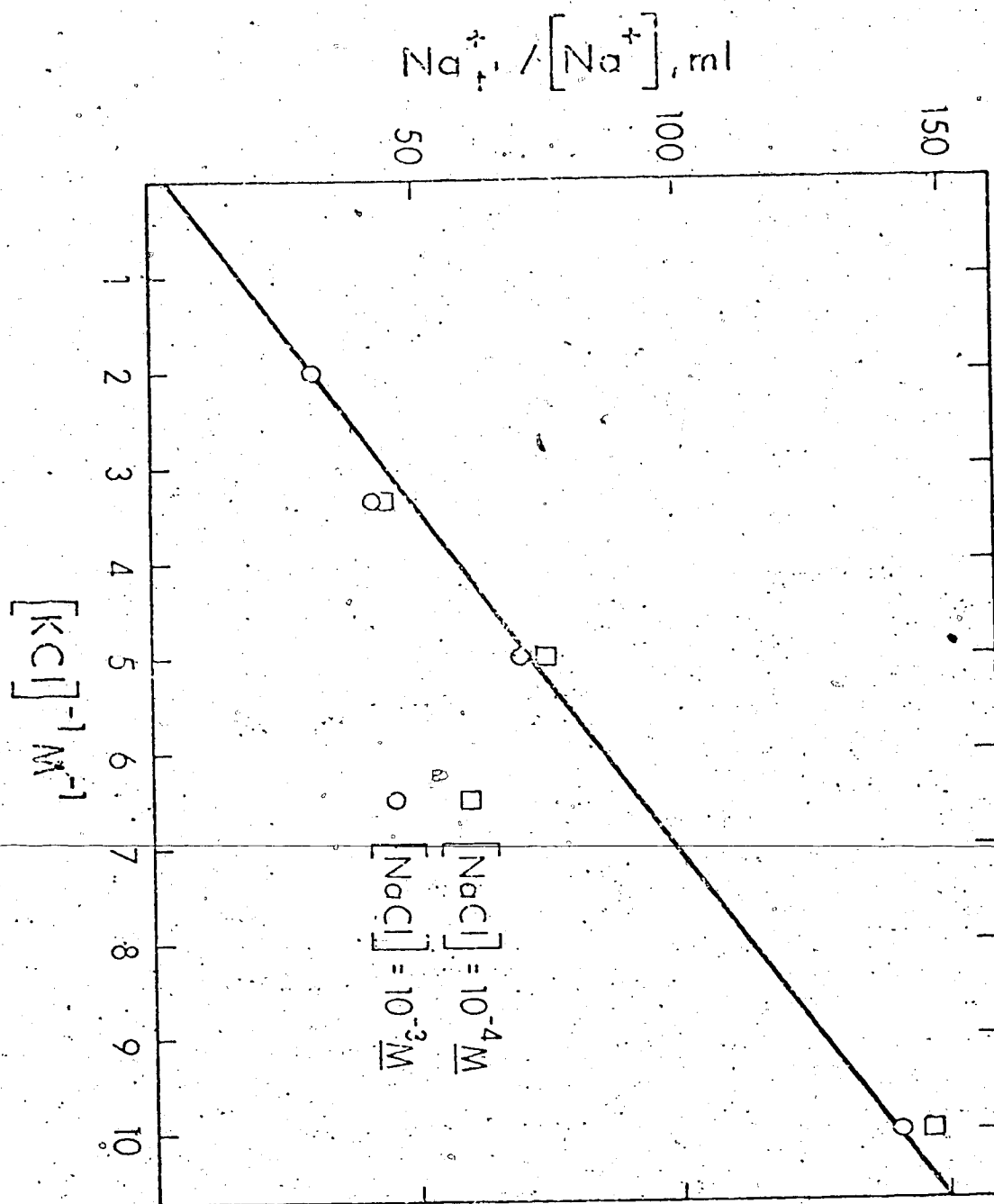


Figure 14. Plots of ratio of total  $\text{Na}^+$  in resin phase over  $\text{Na}^+$  concentration against the reciprocal of  $\text{K}^+$  concentration at varying concentrations of  $\text{NaCl}$  in external solution

whereas it is not likely in HCl solution (Chapter IV, section 1). The possibility of  $\text{Na}^+$  association was mentioned in the Results and Discussion sections of Chapter III. In any event, the degree of association is too small to cause observable deviation from linearity in  $\log \overline{\text{Na}^+}_t / [\text{Na}^+]$  vs  $[\text{Na}^+]$  plots (Figure 13) as has been shown in Figure 5, Chapter III:

#### Sorption of HCl in NaCl on Dowex 50W x 2

This experiment was designed to provide further information on the sorption of  $\text{H}^+$  on cation exchange resins. As was shown in the previous experiments, the additional uptake of electrolyte is observed only for  $\text{H}^+$ , and so association theory can be used to explain the specificity. The homogeneous model is then more appropriate in describing  $\text{H}^+$  sorption. An experiment using Dowex 50W x 2, with only 2% crosslinking, was thought to be potentially useful in giving more support to the above statement. It is known that sorption of electrolyte by Donnan invasion will increase with internal water content if the heterogeneous model holds. It should then be possible to predict increased sorption of  $\text{H}^+$  by performing the experiment on resins with a low degree of crosslinking, since a larger amount of  $\text{Na}^+$  is available to be replaced. On the other hand, sorption should remain nearly unchanged if association

is the case, because association depends chiefly on the nature and number of exchange groups on the resin, and only to a small extent on the extent of swelling.

### Experimental Procedure

The procedure was the same as that described in Chapter III. The resin used was Dowex 50W  $\times$  2 (Dow Chemical Co.) with the following specifications: particle size, 50-100 mesh; capacity, 5.2 meq/dry gram; 0.6 meq/ml bed; wet mesh, 25-50; moisture content, 74-82% by weight. About 10 ml of fully swollen resin, or about 6.5 meq in  $H^+$  form, was required to fill the column, compared with 16.9 meq for Dowex 50W  $\times$  8 resin. The exact capacity of the resin in the column was determined by titrating the  $H^+$  displaced by NaCl with 0.1034  $M$  NaOH, and was found to be 6.557 meq. Values of  $K_{H/Na}$  were measured at ionic strengths of 0.1, 0.5 and 1 and at concentration ratios  $[NaCl]/[HCl]$  of 1.208, 3.417, 7.833 and 16.66 at each ionic strength. The dead volume  $v_m$  was estimated by titrating the  $H_2O$  washings from the column with 0.1034  $M$  NaOH, or coulometrically as outlined in Chapter III immediately after the ion step. Values of  $\overline{H_t^+}$  were obtained as before at NaCl concentrations of 0.1, 0.2 and at HCl concentrations of  $9.714 \times 10^{-4}$ ,  $7 \times 10^{-4}$ ,  $1.943 \times 10^{-4}$  and  $0.9714 \times 10^{-4} M$ . When



equilibrating solutions containing  $9.714 \times 10^{-4}$  and  $4.857 \times 10^{-4}$  M HCl, one modification was added; before the column was washed with 0.8 M NaCl, it was washed first with distilled water, and the hydrogen ion in the washings titrated coulometrically.  $\overline{H}_t^+$  should be equal to the sum of the  $H^+$  content in the water and NaCl washings. The water washings were measured separately to check if there was any sorbed  $H^+$  removed from the column by water.

### Results and Discussion

The same procedure as that outlined in Chapter III was followed. Values of  $\underline{K}_{H/Na}$  ( $\overline{X}_H = 0$ ) at integral levels of [NaCl] were measured from Figure 15 (Table 11), where  $\underline{K}_{H/Na}$  is plotted against  $\overline{X}_{Na}$  at different ionic strengths, and at [NaCl] concentrations of 0.1, 0.2 and 0.4 M were found to be 0.95, 0.97 and 0.99 (Table 12, column 5), Figure 16. The values of  $\overline{H}_t^+$  and  $\underline{v}_m$  are reported on the basis of a column containing 16.9 meq rather than 6.557 meq, the column capacity in the work with Dowex 50W x 8. This was done so that results could be compared on the same basis with those in Chapter III. The data show a larger degree of scattering than in Chapter III.  $\underline{v}_m$  is estimated to be approximately 10 ml.

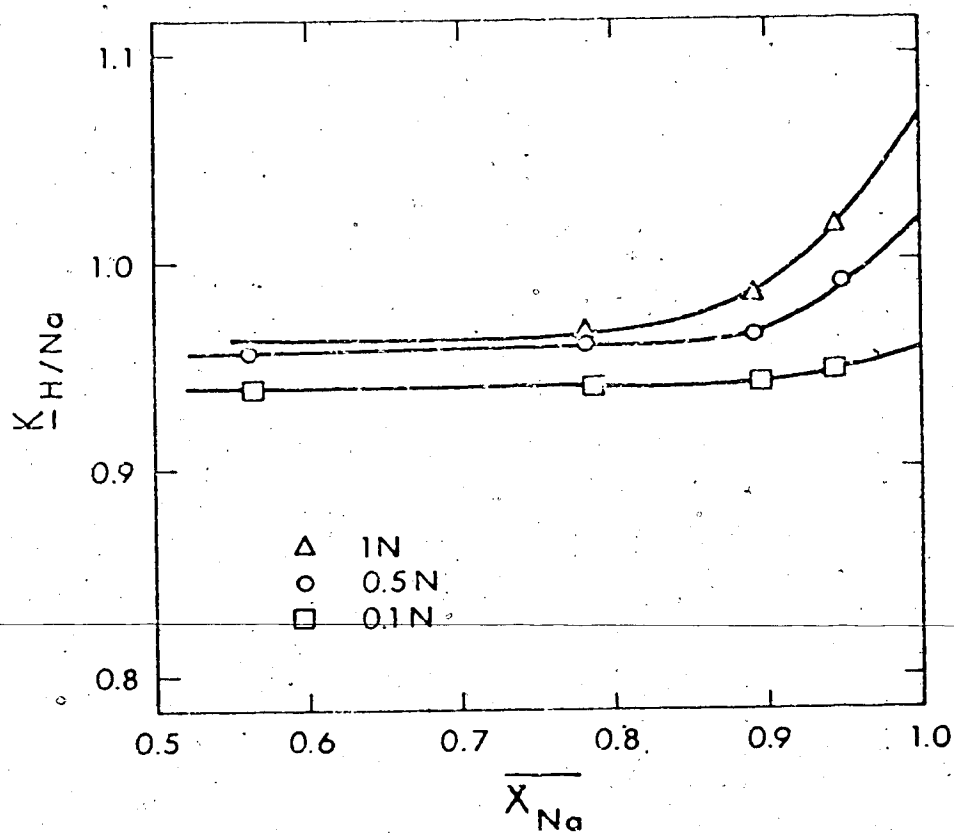


Figure 15. Plots of ion exchange constant  $K$  for  $H^+-Na^+$  exchange on Dowex 50W X 2 as a function of the mole fraction of resin in the  $Na^+$  form at ionic strengths of 1, 0.5 and 0.1

Table 11

Variation of  $K_{H/Na}$  with ionic strength and concentration ratio (Dowex 50W  $\times$  2 21°C).

$\frac{[Na^+]}{[H^+]}$	Ionic strength $\underline{M}$	$\overline{X}_{Na}$	$K_{H/Na}$
1.208	1	-	-
	0.5	0.558	0.957
	0.1	0.562	0.939
3.417	1	0.78	0.965
	0.5	0.781	0.960
	0.1	0.786	0.939
7.833	1	0.889	0.982
	0.5	0.891	0.964
	0.1	0.895	0.941
16.66	1*	0.943	1.017
	0.5*	0.944	0.990
	0.1*	0.946	0.946

\* By coulometry.

Table 12

Total sorption of  $H^+$  as a function of  $[HCl]$  and  $[NaCl]$  on Dowex 50W  $\times 2$ .

$[NaCl]$ $\underline{M}$	$[HCl]$ $10^{-4} \underline{M}$	$\overline{H}_t^+$ $\mu eq$	$\frac{\overline{H}_t^+}{[H^+]}$ $ml$	$K_{H/Na} (\overline{X}_H = 0)$	$\frac{\overline{H}_e^+}{[H^+]} + v_m$ $ml$	$\frac{\overline{H}_s^+}{[H^+]}$ $ml$
0.1	9.714	168	173	0.95	171	2
	4.857	86	177			6
	1.943	36	185			14
	0.9714	19	196			25
0.2	9.714	92.6	95.3	0.97	92	3.3
	4.857	51.5	106			14
	1.943	22.7	117			25
	0.9714	11.4	117 (124)			32
0.4	9.714	65	67	0.99	52	15
	4.857	33.7	69.3			17
	1.943	15.4	81.6			29.6
	0.9714	10.4	107 (93)			41

Table 13

Intercept and slope of lines in Figure 18.

$[NaCl]$ $\underline{M}$	$I$ $ml^{-1}$	$S$ $meq^{-1}$	$a$ $\mu eq$	$I/S$ $\underline{M} \times 10^{-6}$
0.1	0.008	323	3	24
0.2	0.02	106	9	180
0.4	0.018	86	12	216

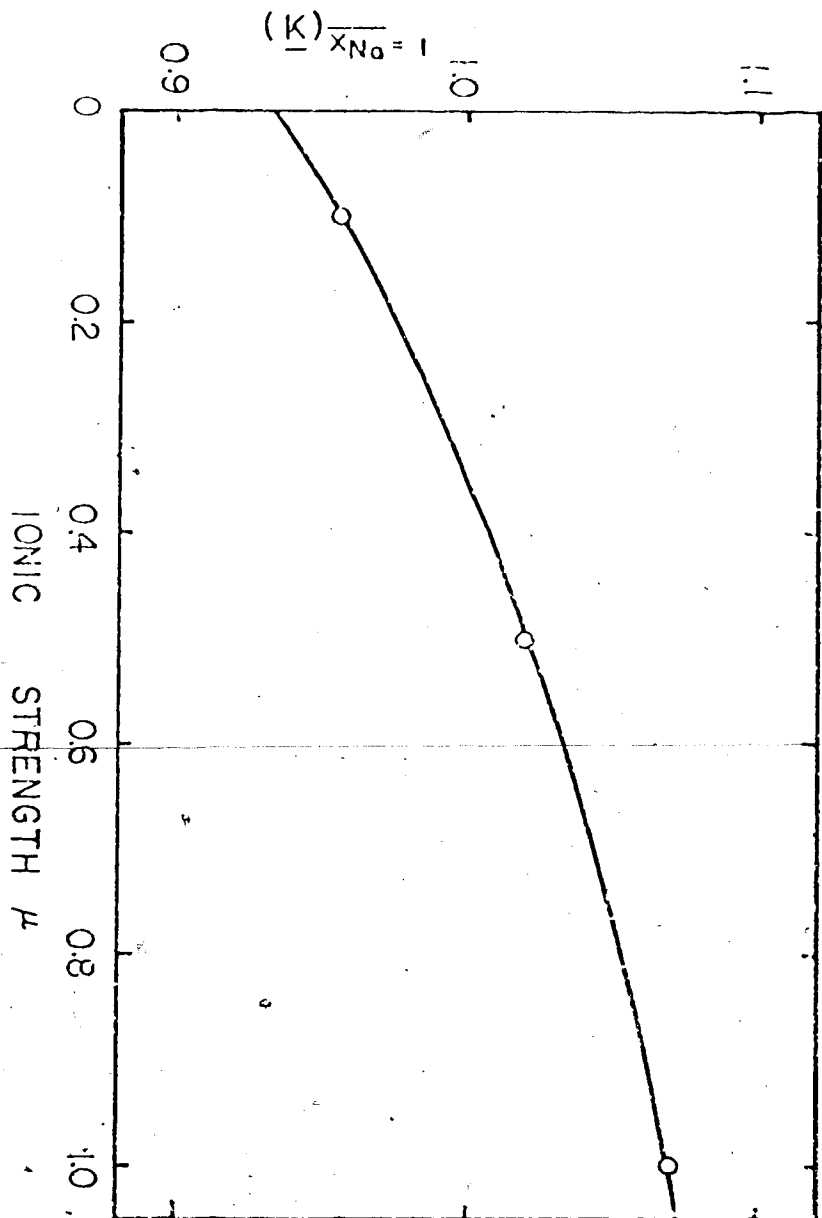


Figure 16. Variation of ion exchange constant  $K$  for  $H^+$ - $Na^+$  exchange on Dowex 50W  $\times 2$  in  $Na^+$  form with ionic strength

The relation between  $H_t^+$ ,  $[H^+]$  and  $[H^+]$  at various NaCl concentrations is shown in Figure 17 and in Table 12, column 4. Extensive curvature is seen here also, as it was for  $H^+$  in Chapter III. This confirms  $H^+$  retention by the resin. In Figure 18 are shown plots of  $[H_t^+]/[H_s^+]$  (column 7, Table 12) against  $[H^+]$ . Straight line relationships are obtained in each case. The inverse of the slopes of these lines gives  $\underline{a}$ , the quantity of fixed ionic groups capable of ion binding. The values obtained, 3, 9, and 12 eq., are considerably lower than those found for Dowex 50W x 8 at corresponding  $Na^+$  concentrations. This again shows the importance of the degree of swelling in the resin. As was mentioned in Chapter III,  $\underline{a}$  depends on the external salt concentration, which is related directly to water uptake and thus to the internal ionic strength. Being able to take up more water than Dowex 50W x 8, Dowex 50W x 2 has a lower internal ionic strength ( $\underline{c}/\underline{V}_s$ ) at a given NaCl concentration. This results in a correspondingly smaller value for  $\underline{a}$ .

The sorption of  $H^+$ , ( $\overline{H_t^+}/[H^+]$ ), for Dowex 50W x 8 is greater than for Dowex 50W x 2 at the same NaCl concentration. This is also a consequence of larger water uptake in the 2% crosslinked resin; when the ratio of intercept to slope I/S of the lines in Figure 18 (Table 13) is plotted against  $[Na^+]$  (Figure 19), the

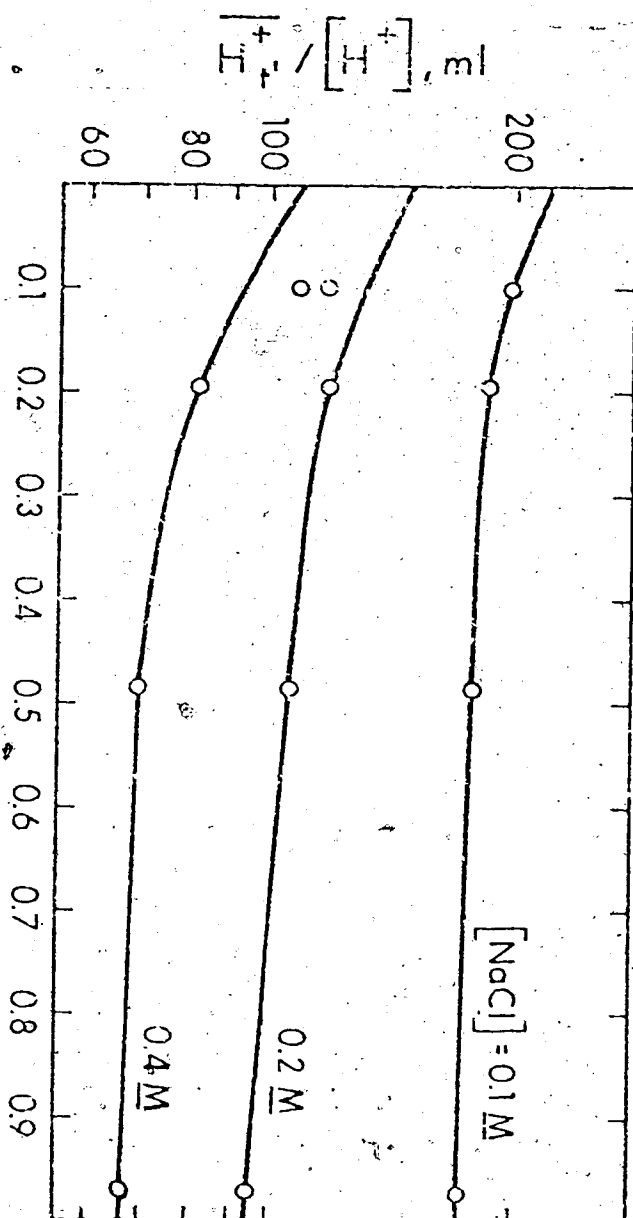


Figure 17. Plots of ratio of total  $H^+$  in the resin phase of 16.9 meq Dowex 50W  $\times 2$  over  $H^+$  concentration against  $H^+$  concentration at varying concentrations of  $H^+$  in the external solution

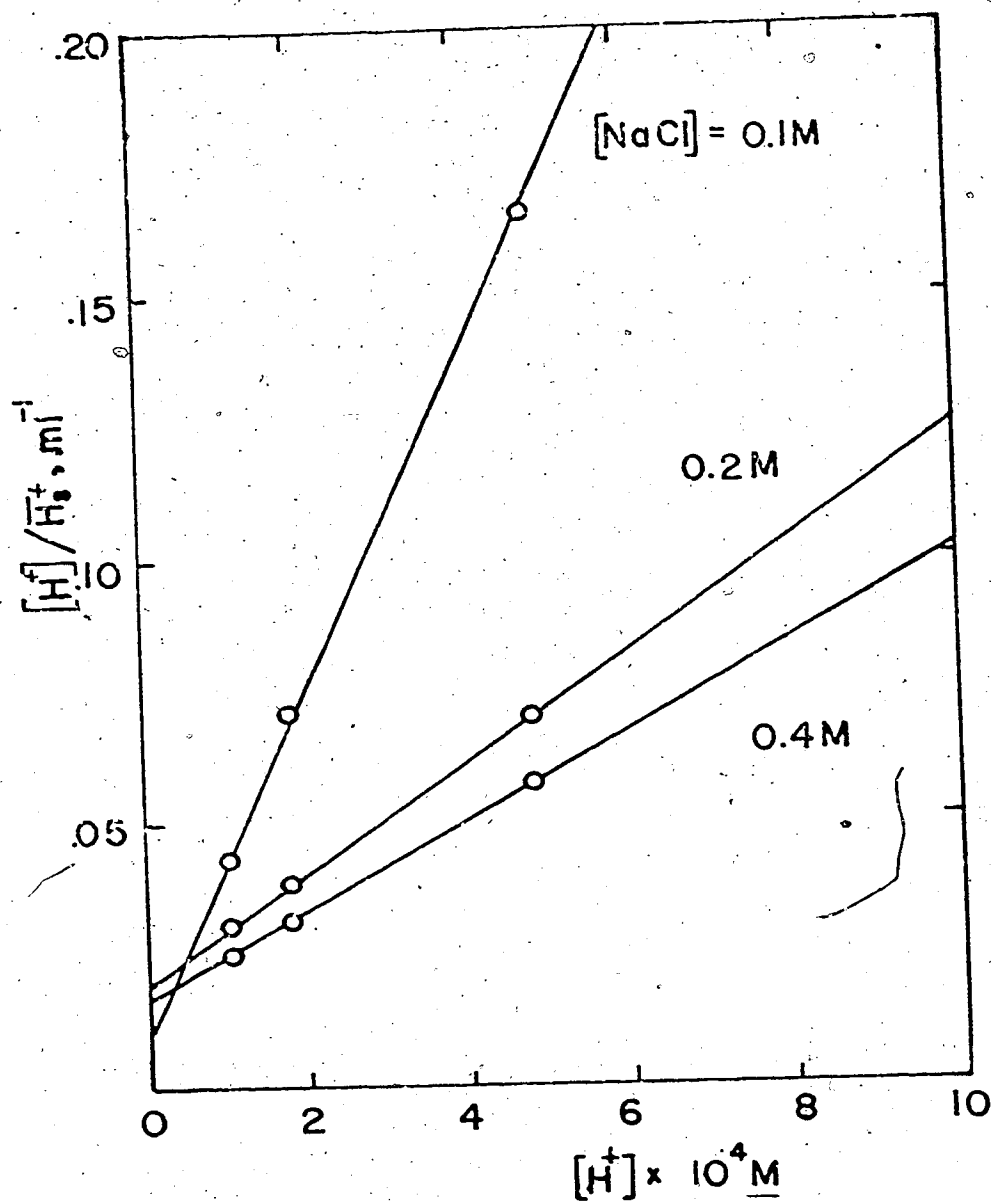


Figure 18. Plots of  $H^+$  concentration in external solution over sorbed  $H^+$  on Dowex 50W x 2 against  $H^+$  concentration in external solution at several concentrations of  $Na^+$  in the external solution.



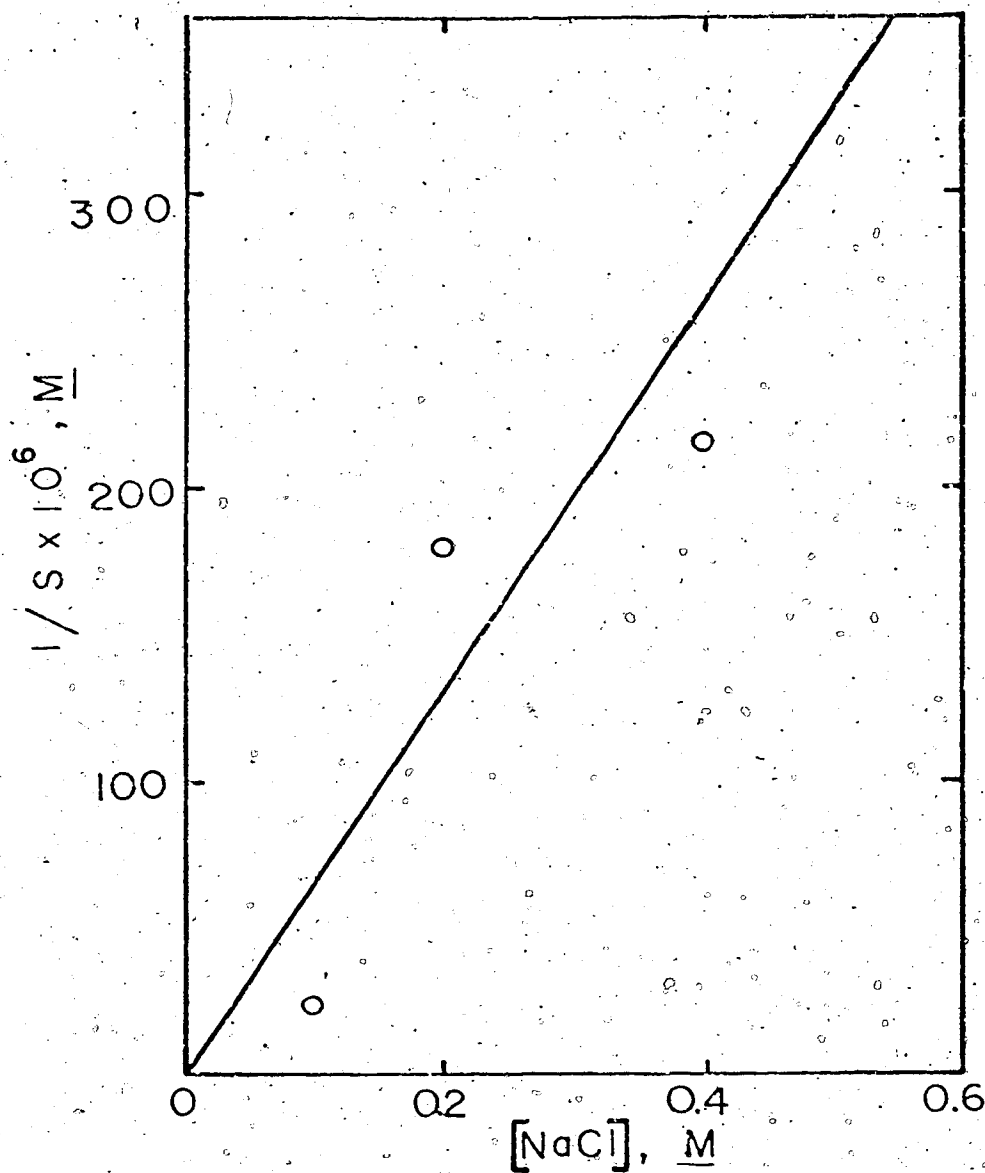


Figure 19. Plots of the ratio of the intercept to slope from Table 13 against  $Na^+$  concentration in the external solution

increase in  $I/S$  with  $[Na^+]$  is apparent. A least squares line drawn through these points passes through the origin as described by Equation (AII9). The slope thus found is  $6.6 \times 10^{-4}$ , which agrees well with that obtained on Dowex 50W $\times$ 8 ( $14.4 \times 10^{-4}$  to  $5.2 \times 10^{-4}$ ).

The measurements of the acid content of the water washings show large scatter due to the difficulty inherent in measuring low levels. However, the average value for the total moles divided by the concentration of HCl is around 10 ml, or close to the column dead volume. That sorbed  $H^+$  cannot be flushed out by distilled water proves the validity of the homogeneous model. Unlike adsorption in internal water (heterogeneous model), the association of  $H^+$  with fixed ionic groups will hold the  $H^+$  in the resin, unaffected by distilled water washing.

#### Sorption of HCl in NaCl on Amberlyst 15 Macroreticular Resin

Macroreticular resins are rigid, porous, heterogeneous resin materials. They are described as consisting of two phases<sup>8,9,134</sup>, one a quasi-homogeneous gel-phase as in conventional gel-type resins, and the other a phase composed of large pores or voids which are occupied by water in a hydrated state. In the terminology of adsorbents exhibiting catalytic properties,

three types of pores can be distinguished: open pores, which are open to the flow of fluid; semi open pores; and closed pores. An NMR study of macroreticular resins showed the chemical shift difference between peaks for internal water and external water to be smaller than for conventional resins<sup>134</sup> of similar structure. This is attributed to a smaller gel-phase in the macroreticular resin. The effect of the gel-phase on the sorption of trace  $H^+$  from solutions of NaCl is a factor that has not previously been investigated. For this reason an equilibrium study of this system was undertaken.

#### Experimental Procedure

The resin studied was Amberlyst 15 (Rohm and Haas Company, Philadelphia). The specifications by the manufacturer were: size, 20-30 mesh; bulk density, 595 g/l; percentage swelling, 66%; exchange capacity, 49 meq/g dry and 2.9 meq/ml bed; surface area, 40~50 m<sup>2</sup>/g; porosity, 0.3~0.35 ml pore/ml bead; average pore diameter, 200~600 Å. The experimental procedure was as described in Chapters III and IV, section 3. About 20 meq of resin was used, and the capacity determined in the column by titrating the displaced  $H^+$  with 0.1791 M NaOH (17.42 meq). Values of  $K_{H/Na}$  were measured at

ionic strengths of 1, 0.5, and 0.1 M, and at concentration ratios of [NaCl] to [HCl] of 1.208, 3.417, 7.833, and 16.66. The quantity  $\overline{H}_t^+$  was obtained as described before at NaCl concentrations of 0.1, 0.2, 0.4, and 0.9 M, and at HCl concentrations of  $9.714 \times 10^{-4}$ ,  $4.857 \times 10^{-4}$ ,  $1.943 \times 10^{-4}$  and  $0.9714 \times 10^{-4}$  M.

### Results and Discussion

The constants of  $K_{H/Na}$  ( $\overline{X}_H = 0$ ) were measured from Figure 20, in which  $K_{H/Na}$  is plotted against  $\overline{X}_{Na}$  at different ionic strengths (Table 14). Values for  $K_{H/Na}$  ( $\overline{X}_{Na} = 1$ ) at [NaCl] = 0.1, 0.2, 0.4, and 0.9 M were found to be 1.95, 1.97, 2.05, and 2.52 by interpolation (Table 15, column 5), Figure 21. The values of  $\overline{H}_t^+$  and  $\overline{v}_m$  have been converted to a basis of 16.9 meq from 17.42 meq. The average  $\overline{v}_m$  was estimated to be 6 ml. Figure 22 shows a plot of  $\log \overline{H}_t^+ / [H^+]$  against  $[H^+]$ . The points thus obtained reflect a basic difference between the two types of resins. No sign of extra  $H^+$  hold-up is observed. The hypothetical values for pure exchange (Table 15, column 6) are represented by dotted lines on the same graph. The close proximity of those points to the plot expected for pure exchange leads also to the conclusion that  $H^+$  hold-up is absent. It should be mentioned that the values of  $K_{H/Na}$  for this macroreticular resin vary strongly with  $\overline{X}_{Na}$  and

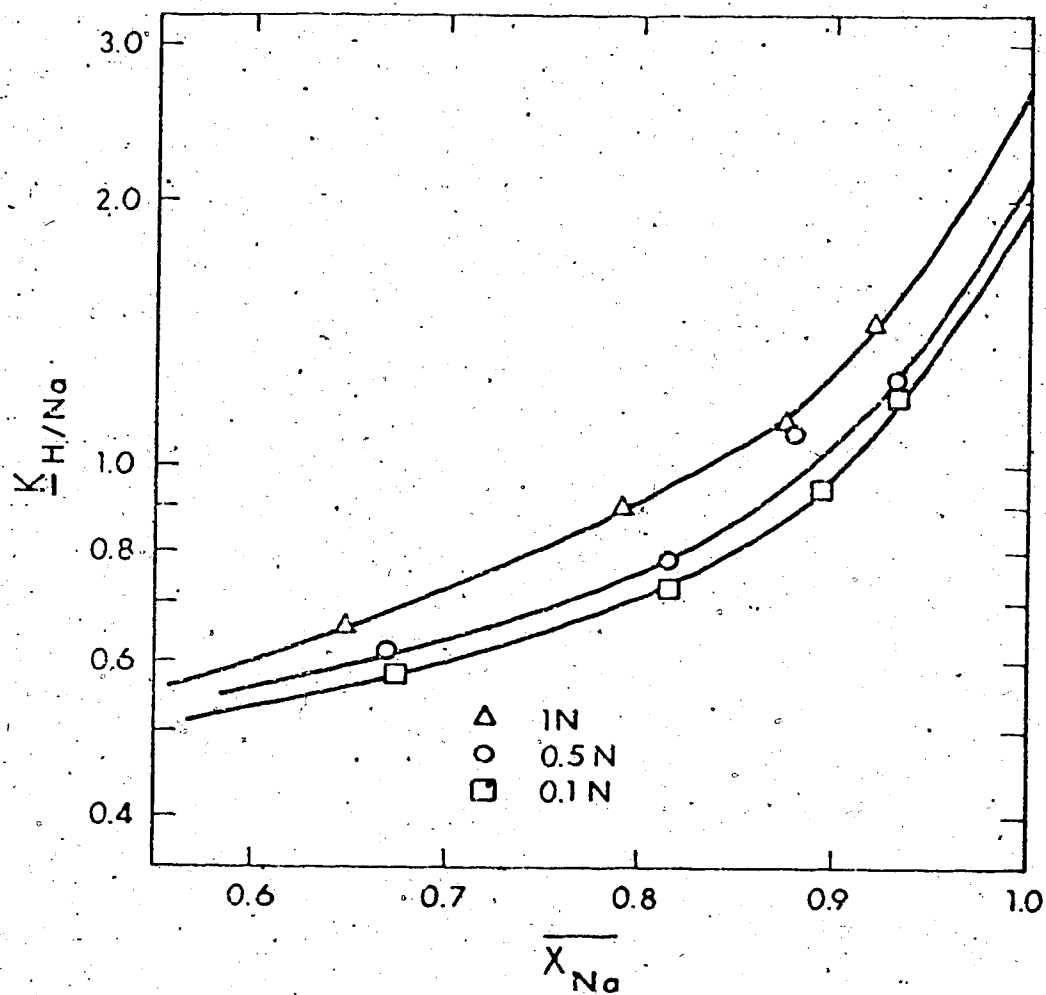


Figure 20. Plots of ion exchange constant  $K$  for  $H^+ - Na^+$  exchange on Amberlyst 15 as function of the mole fraction of resin in the  $Na^+$  form at ionic strengths of 1, 0.5 and 0.1

Table 14

Variation in  $K_{H/Na}$  with ionic strength and concentration ratio for the macroreticular resin Amberlyst 15 at 21°C.

$\frac{[Na^+]}{[H^+]}$	Ionic strength	$\bar{X}_{Na}$	$K_{H/Na}$
1.2085	1	0.647	0.657
	0.5	0.670	0.614
	0.1	0.675	0.582
3.4170	1	0.794	0.885
	0.5	0.814	0.780
	0.1	0.818	0.731
7.8339	1	0.874	1.123
	0.5	0.877	1.091
	0.1	0.893	0.938
16.6678	1	0.920	1.447
	0.5	0.931	1.260
	0.1	0.932	1.221

Table 15

Total sorption of  $H^+$  as a function of  $[HCl]$  and  $[NaCl]$  on Amberlyst 15 at 21°C.

$[NaCl]$	$[HCl]$	$\overline{H_t^+}$	$\frac{\overline{H_t^+}}{[H^+]}$	$K_{H/Na} (\overline{X}_H=0)$	$\frac{\overline{H_e^+}}{[H^+]} + v_m$
$\underline{M}$	$10^{-4} \underline{M}$	$\mu eq$	$ml$		$ml$
0.1	9.714	133	343	1.95	336
	4.857	165	339		
	1.943	65.9	339		
	0.9714	38.6	397		
0.2	9.714	153	158	1.97	172
	4.857	89.9	185		
	1.943	35.9	185		
	0.9714	15.1	155		
0.4	9.714	102	105	2.05	93
	4.857	52.9	109		
	1.943	19.8	102		
	0.9714	8.94	92		
0.9	9.714	54.4	56	2.52	53
	4.857	28.7	59		
	1.943	10.1	52		
	0.9714	4.66	48		

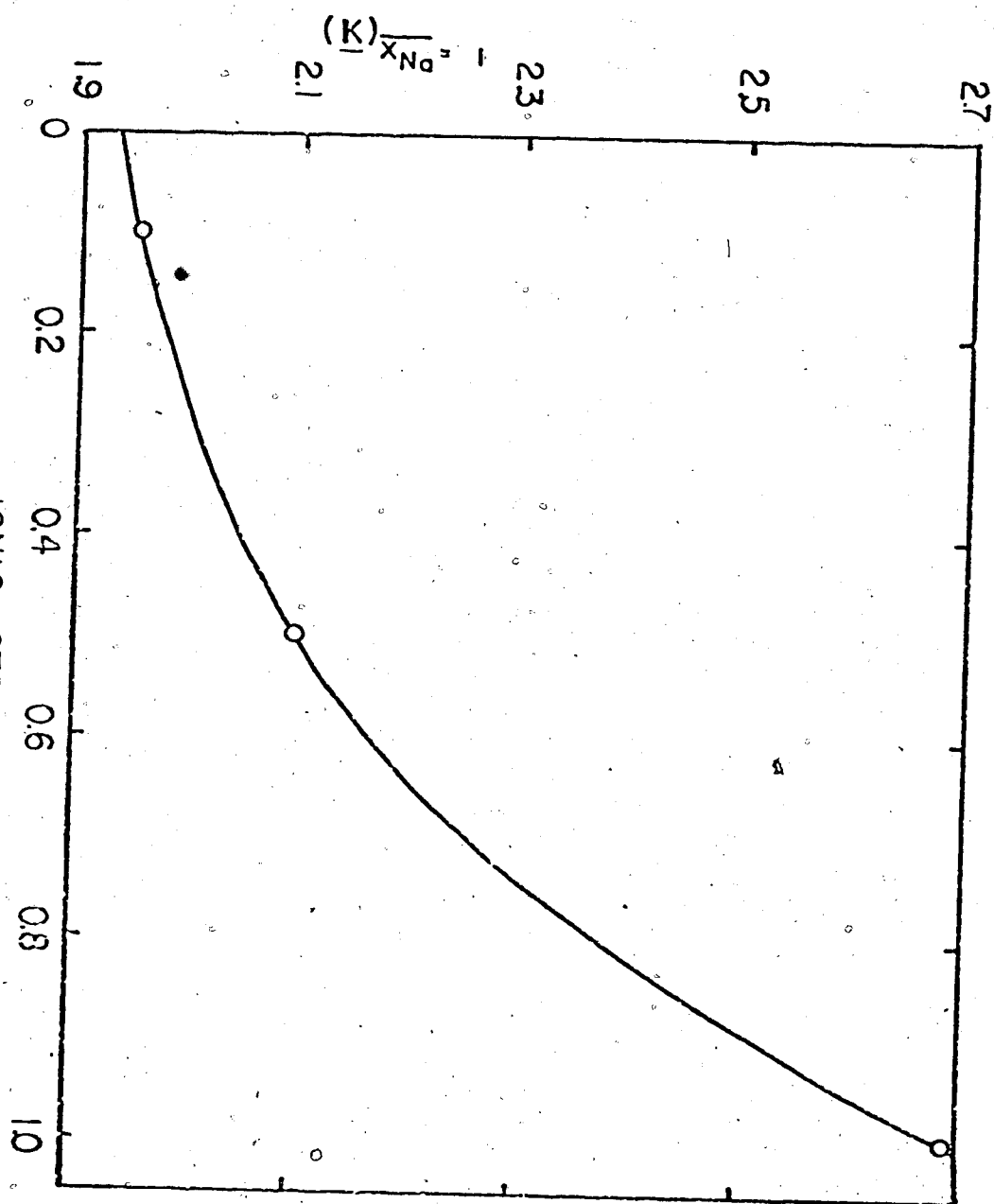


Figure 21. The variation of ionic exchange constant  $K$  for  $H^+ - Na^+$  exchange on Amberlyst 15 in  $Na^+$  form with ionic strength



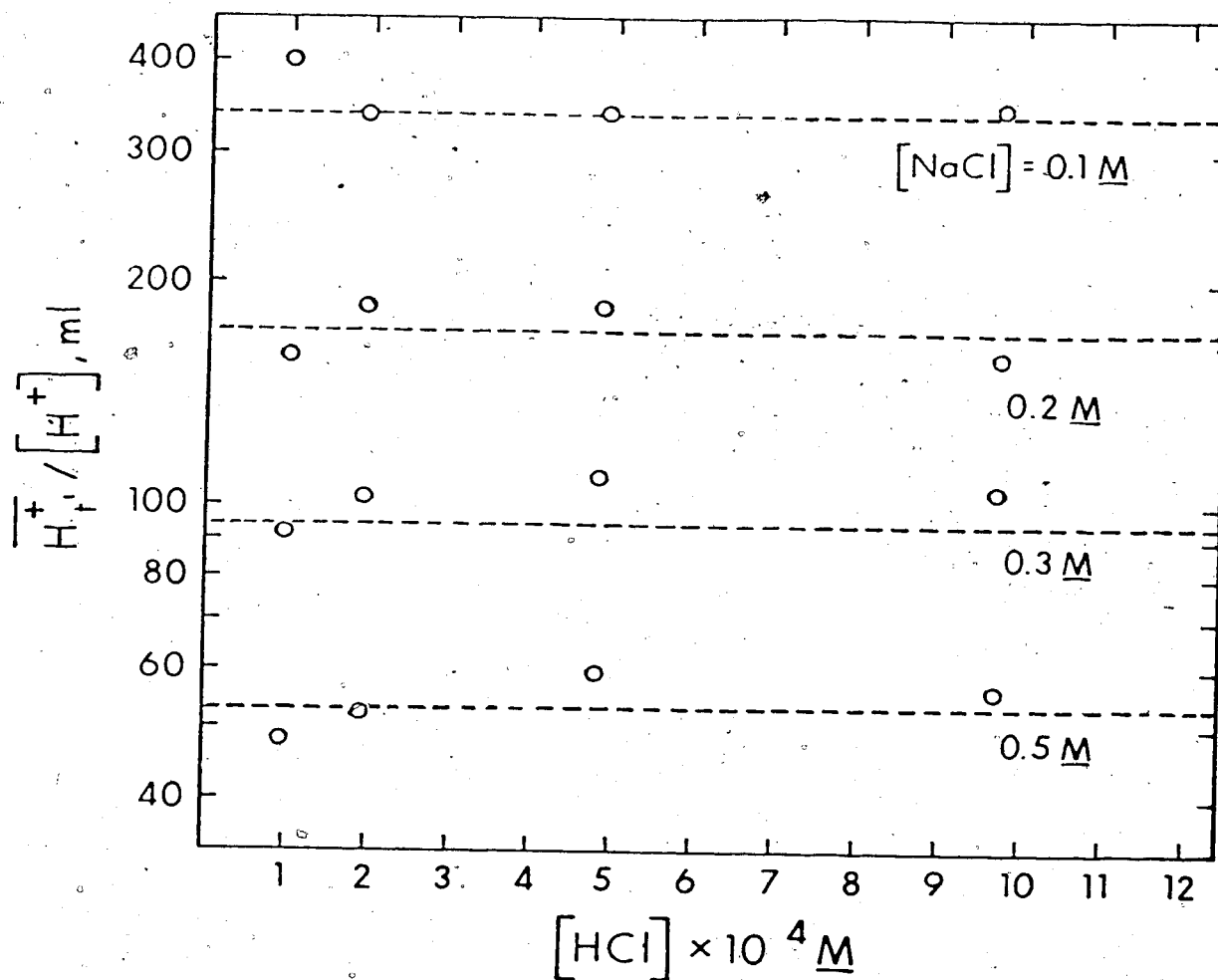


Figure 22. Plots of ratio of total  $H^+$  in the resin phase of Amberlyst 15 over  $H^+$  concentration against  $H^+$  concentration at varying concentrations of  $Na^+$  in the external solution. Dotted lines are the hypothetical values for pure exchange calculated by  $K_{H/Na}(\bar{X}_{Na}=1)$  on Figure 21.

with ionic strength, especially near saturation in the  $\text{Na}^+$  form. This behavior resembles that of conventional resins of high crosslinking (25% DVB), where the resin itself is rigid and sorption is small. The high sensitivity to  $\bar{X}_{\text{Na}}$  is due to a large osmotic pressure  $\pi$  so that even a slight change in volume caused by varying the resin composition results in an appreciable PV term and a significant change in  $K_{\text{H}/\text{Na}}$ .

Considering the pores in a macroreticular resin as belonging to the resin phase, then sorption of electrolyte due to Donnan invasion should be larger than for a gel-type resin<sup>7</sup> because the Donnan potential is ineffective in the pores. The pore water has the same properties as external water, and so is better considered to be in the external phase. In terms of the heterogeneous model, the amount of electrolyte in the gel-phase determines the extent of the hold-up of  $\text{H}^+$  other than exchange. Since the gel-phase volume of a macroreticular resin is extremely small, the amount of  $\text{H}^+$  sorbed would be expected to be lower than that of a gel-type resin.

Even though the homogeneous model is satisfactory for gel-type resins, it is not suitable for macroreticular ones, which contain only a minute amount of gel-phase. If the quantity of gel water is not sufficient to spread uniformly over the resin phase, it may

form a number of small, localized "water pockets" or domains whereby ions are hindered from moving from one pocket to another. This may be responsible at least in part for the early curvature seen for macroreticular resins in Figure 20 relative to the late curvature seen for Dowex 50W x 8 in Figure 10. The observed association reflects greater selectivity for  $H^+$  at  $\bar{X}_{Na}$  levels of 0.85 and higher in the Amberlyst resin.

Since the overall affinity for hydrogen ions by the macroreticular resin is much less than for the conventional resins, the presence of carboxyl groups in any appreciable amount is unlikely. This may be the result of milder sulfonating conditions in the production of the resin.

In general, if the quantity of gel water in a macroreticular resin is low,  $H^+$  sorption is not predicted by either the homogeneous or heterogeneous model.

#### Sorption of HCl in the Presence of Large Quantities of NaCl on an Empty Column

The experiments for measuring  $H^+$  sorption cannot be considered complete until the extent of sorption on an empty column has been measured. Silicate glass

is known to possess exchange properties<sup>136,137</sup> and to be able to take electrolyte in dilute solution. The exchange capacity and specificity of glass depends strongly on the composition and surface treatment of the glass.<sup>0</sup> The concentration of the ionic sites in borosilicate glass (Pyrex)<sup>0</sup> is reported to be on the order of  $3 \times 10^{-3}$  mole/cm<sup>3</sup>,<sup>138</sup> This is even higher than that found in sulfonated polystyrene resins, though most are inactive, highly specific and do not take part in exchange. Nevertheless, some of the sorption of H<sup>+</sup> found in the previous experiments may come from the glass surface, as well as from the resin itself. Therefore measurements on an empty column were made to clarify this point.

#### Experimental Procedure

The same Pyrex column used in the previous experiments was studied, with the glass wood plug retained at the bottom. A reference mark was etched near the top of the column. The volume of the column was determined by weighing the water held by the column when filled to the mark and dividing by the density of water at 22°C (0.99777). Equilibrating solutions containing NaCl concentrations of 0.1, 0.2, and 0.4 M, and HCl concentrations of 9.714, 4.857, 1.943, and  $0.9714 \times 10^{-4}$  M, were passed through the column at a flow rate of

150 ml/hr for 2 hrs, and then the liquid level was brought to the mark on the top of the column. The solution remaining in the column was collected in an 80-ml beaker, together with 50 ml of 0.8 M NaCl washings from the column, and the acid present was titrated coulometrically to obtain the value of  $\overline{H^+}$ . The ratios  $\overline{H^+}/[H^+]$  were compared with the volume of the column that had been measured previously to indicate whether any sorption was taking place on the glass surface.

#### Results and Discussion

The volume of the column was found to be 10.33 ml. Results of the values of  $\overline{H^+}/[H^+]$  at different HCl and NaCl concentrations are listed in column 4, Table 16, and compared with 10.33 ml. The measurement of  $\overline{H^+}$  was not very accurate owing to the small sample size, but an average value of  $\overline{H^+}/[H^+]$  of around 10.1 ml was obtained. Therefore the sorption of  $H^+$  on glass wall can be considered negligible, and the hold-up of  $H^+$  is entirely due to the resin itself.

Table 16H<sup>+</sup> sorption on empty Pyrex column (10.33 ml volume)

at 20°C.

[Na <sup>+</sup> ] <u>M</u>	[H <sup>+</sup> ] 10 <sup>-4</sup> <u>M</u>	H <sup>+</sup> μeq	$\frac{\overline{H^+}}{[H^+]}$ ml
0.1	9.714	8.95	9.2
	4.857	4.98	10.3
	1.943	1.75	9.0
	0.9714	0.87	9.0
0.2	9.714	9.41	9.7
	4.857	4.41	9.1
	1.943	1.65	8.5
	0.9714	-	-
0.4	9.714	9.65	9.9
	4.857	7.62	15.7
	1.943	2.03	10.5
	0.9714	-	-
			10.1 Average

## CHAPTER V

### SORPTION OF WEAKLY DISSOCIATED ELECTROLYTES ON THE SULFONIC ACID ION EXCHANGE RESIN

DOWEX 50W x 8

#### Sorption of Nonelectrolytes

Ion exchangers in a fully hydrated state are known to sorb a great variety of nonpolar substances, such as phenols<sup>139,140</sup>, ethylacetate<sup>141</sup>, and alcohols<sup>142</sup> in both aqueous and nonaqueous systems. The interaction between neutral sorbed molecules and the resin is believed to come from several sources<sup>143</sup>, as discussed below.

Simple true dissolution of neutral solutes in the interior solvent of the resin phase. The amount of solute sorbed can be related to the external concentration by the following equation<sup>144</sup>:

$$\ln \frac{\bar{a}_N}{a_N} = \ln \frac{\bar{a}_N}{a_N} - \frac{\pi \bar{V}_N}{RT} \quad (15)$$

where  $\bar{a}_N$  is the activity of solute in the resin phase

$a_N$  is the activity of solute in the external solution

$\pi$  is the osmotic pressure

$\bar{V}_N$  is the partial molal volume of the solute.

The activity of the solute in the resin is always less than that in the solution owing to the fact that the

osmotic pressure  $\pi$  in the resin tends to squeeze the solute out into the solution in order to relieve the strain. Having a higher osmotic pressure (hard spring analogy<sup>145</sup>), a highly crosslinked resin will sorb less solute. Furthermore, increased crosslinking will also decrease solvent uptake in the resin, which will in turn reduce the sorption of highly solvated solutes such as, for instance, alcohol in water as solvent. The size of the solute molecule also plays a significant part in sorption; a large solute is more susceptible to the squeezing effect of osmotic pressure, and sorption thus is reduced correspondingly. In the extreme case, in which both osmotic pressure and the size of the solute molecules are small (low degree of crosslinking), solute molecules in the internal phase will not experience any additional force from the resin, and will behave as if they were in the external solvent. Under these conditions the distribution of solute in both phases will even out. Assuming the same activity coefficients in both phases ( $\overline{\gamma}_N = \gamma_N$ ), the concentration of solute in the resin has to be equal to that in the solution. On the other hand, large molecules will interact extensively with the resin hydrocarbon skeleton due to increasing polarizability; this type of interaction will promote sorption in the resin. These are two



opposing effects; the larger will determine the overall sorption tendency.

London dispersion interactions between the hydrocarbon part of the organic solute and the benzene nuclei of the resin.

London dispersion forces are short range forces that are directly proportional to the polarizability of two molecules undergoing interaction, and inversely proportional to the sixth power of the distance between them. Dispersion interactions of solutes with benzene nuclei are significant only for those solute molecules near the skeleton; others further in the interior of the solution are practically unaffected. These dispersion forces chiefly account for surface adsorption phenomenon or so-called chemisorption, where only a monolayer of molecules is built up on the surface. Thus the dispersion interactions between a solute and the hydrocarbon matrix of a resin are heterogeneous in nature and are referred to as adsorption, while the dissolution described above is homogeneous and referred to as simple absorption. In contrast to true dissolution, where the molality ratio of solute in the resin to the solution,  $\overline{m}_N/m_N$ , is less than 1, the ratio may exceed 1 in cases of strong dispersion interactions. Sorption of this type can usually be represented by the Langmuir isotherm<sup>146,147</sup>.

$$\bar{X} = \frac{ka'[X]}{1 + k[X]} \quad (16)$$

where  $a'$  is the maximum amount of solute the resin can hold per unit weight of resin, in m mole/g

$k$  is the adsorption constant

$X$  is the external concentration of solute  $M$

$\bar{X}$  is the amount of solute adsorbed per g of resin m mole/g.

Equation (15) for true dissolution can be put into the form

$$\bar{a}_N / a_N = k_6 \quad (17)$$

Neglecting activity effects, this can be written as

$$\frac{[\bar{X}_N]}{[X_N]} = k_7 \quad (17a)$$

where  $k_7 \leq 1$ .

Equation (16) has two limiting forms:

$$\lim_{[X] \rightarrow \infty} \bar{X} = a', \text{ and } \lim_{[X] \rightarrow 0} \bar{X} = ka'[X]$$

and can be rewritten as

$$[\bar{X}_N] = k_8 \quad \text{at high concentrations} \quad (18a)$$

and as

$$\frac{[\bar{X}_N]}{[X_N]} = k_9 \quad \text{at low concentrations} \quad (18b)$$

The magnitude of  $k_9$  may be greater or smaller than 1, depending on the strength of the London dispersion

forces and the internal activity coefficients. Usually it has a value larger than 1 for moderately large molecules. From Equations (17a) and (18b), it can be shown that dispersion interactions and dissolution both have the same form of sorption isotherms at low external concentrations, and differ only in the magnitude of the sorption coefficients  $k_7$  and  $k_9$ .

An unresolved problem in Reichenberg's work<sup>143</sup> is that the order of the molality ratios  $\overline{m}_N/m_N$  of acetic acid, propionic acid and *n*-butyric acid is inverted, *n*-butyric acid being sorbed the least at high external concentration. A plausible answer to this difficulty is considered here in terms of osmotic pressure.

It has been pointed out previously<sup>143</sup> that resin sorption at moderate concentrations is a true and uniform absorption not confined to the surface of the resin particles. Therefore an increase in external geometrical surface area of the resin bead by fine grinding should not increase the sorption of a non-electrolyte such as acetic acid in a moderate concentration range ( $\sim 2M$ ). The independence of sorption on particle surface area rules out the possibility of adsorption. But on the basis of the amount of acetic acid sorbed on resin particles of 200  $\mu m$  diameter, a multilayer 230 molecules deep is calculated on an adsorption basis. This is highly unlikely. Only the several

outmost layers which are close to the hydrocarbon backbone will interact with the skeleton by London dispersion forces; the rest of the 230 layers, constituting the major portion of the sorbed solute, are unaffected.

The uptake of solute as a whole can be regarded either as absorption, or as a simple dissolution step, described by Equation (15). Osmotic pressure will then favor the sorption of small molecules. The predicted extent of sorption in descending order then is acetic acid, propionic acid and *n*-butyric acid; this is as observed by Reichenberg and Wall at concentrations of 2 M. At relatively low external concentrations the solute sorbed forms at most several layers which are all capable of interacting with the hydrocarbon skeleton; hence adsorption on the surface will be significant.

The normal order expected on the basis of London dispersion forces is then obtained, with the larger solute sorbed more strongly. The normal order is the reverse of the trend shown above, acetic acid being adsorbed the least owing to smallest interaction with the matrix.

Moreover, the transition of the molality ratio  $\overline{m}_N/m_N$  from more than 1 to less than 1 at increasing concentration is further evidence of a switching of the driving force from London dispersion interactions to pure dissolution.

Adsorption of neutral molecules at low concentrations has been confirmed experimentally by Davies and Thomas<sup>148</sup>. Adsorption usually will be the dominant mechanism when the solute molecules are too large to penetrate easily the molecular pores of the crosslinked resin where dissolution in the interior of the resin becomes unfeasible. It has also been reported<sup>149</sup> that macroporous anion exchange resins sorb a variety of polar compounds and dyes such as humic acids, methylene blue, eosin and bromophenol blue. The sorptions are described satisfactorily by the Langmuir isotherm. Also, at high concentrations hydrochloric acid and eosin are sorbed to an increased extent; this indicates multi-layer adsorption, which is consistent with that observed by Reichenberg. An attempt was made to correlate solute structure with sorbability and to select optimal temperature conditions for sorption processes.

"Salting-out" effects by polar groups on the resin.

Resin materials may be regarded as having a "salting out" effect on solutes. The simplest interpretation of this effect is that ions of the salt added tie to a number of solvent molecules in such a way that the solvent molecules are prevented from functioning normally. In other words, the solvation of ions leaves less "free water" molecules to dissolve the solute.

Even though the "true" internal molality, defined as number of moles of solute sorbed per kg of free solvent, is not influenced by salting out effects, the observed apparent internal molality, defined on the basis of total internal solvent, will greatly diminish as the amount of salt, and the salting out effect, increases. If the true dissolution and osmotic pressure can be assumed to be negligible, the salting out effect will still render the molality ratio less than 1. Equation (15) for true dissolution can account for the salting out effect by inclusion of a term for the internal activity coefficient; a large salting out effect is reflected in a large internal activity coefficient. Reichenberg<sup>143</sup> was able to estimate the hydration number of the fixed sulfonate groups on the resin to be 4, by use of the equation

$$\frac{E}{\underline{G} - \underline{G}_O} = \underline{k}_w \underline{m}$$

where E is the quantity of solute sorbed in meq

$\underline{G}$  g of water sorbed

$\underline{m}$  molality

$\underline{G}_O$  is the hydrated water in grams

$\underline{k}_w$  partition coefficient between 2 phases.

$\underline{k}_w$  is found to be very close to 1, which confirms true dissolution and negligible osmotic pressure.

Even though modern NMR studies have proven that solvation of the counter ions is greater than that of the fixed charge groups (Chapter I), the "salting out" concept implied by the Reichenberg idea is still a valuable concept.

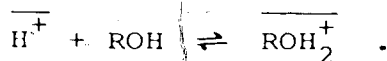
#### Polar interactions

Attraction between the dipoles of nonelectrolyte solutes and the ionic sites of a resin also contributes to sorption. The dependence of sorption on the nature of the resin and of the exchangeable ion reflects this type of interaction.

#### Specific interactions with counter ions in the resin: the "salting in" effect.

Solutes which can form complexes with counter ions are sorbed strongly. The extent of sorption depends on the stability constants of the complexes formed. These sorptions are all stoichiometric, and the sorption isotherm levels off above that concentration where the counter ions have been used up in forming complexes. For example, cation exchangers with transition metals as counter ions sorb ammonia or amines strongly<sup>150,151</sup>, while anion exchangers in the bromide or chloride form can take up bromine and iodine through formation of  $\text{Br}_7^-$  and  $\text{I}_7^-$ .<sup>152,153</sup> Sometimes the stability constants of the complexes formed are so small that

complex formation is only appreciable at high solute concentrations; complexes thus formed are labile, and never stoichiometric. Under these conditions, the sorption of solute is normal at low concentration, but goes up at higher concentrations. Sorption of alcohols on cation exchange resins in the hydrogen form is one such example. The reaction<sup>143</sup> responsible for greater sorption of alcohol on a resin in the hydrogen form than in the sodium form is



Owing to the high concentration of counter ions present in the resin ( $\sim 6\text{M}$ ), the extent of formation of the labile complex  $\overline{\text{ROH}_2^+}$  is appreciable. The alcohol is said to be "salted in" by the  $\text{H}^+$  in the cation exchanger.

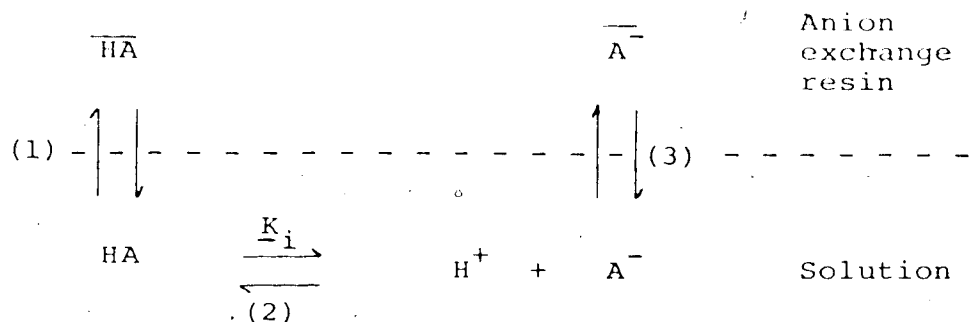
The properties of ion exchange resins in sorbing neutral molecules have been fully utilized in chromatography<sup>154</sup> for the separating of nonelectrolytes such as alcohols, sugars, hydantoin, caffeine and phenacetin. In all these cases the ability to sorb may be attributed to interaction with hydrogen ions on the sulfonate groups.

#### Simultaneous Sorption and Exchange of Weakly Dissociated Electrolytes: Organic Ions as Counter Ions

For any weakly dissociated electrolyte, there will be simultaneous sorption of undissociated molecules



and exchange of ionized organic ions with counter ions in the resin. For instance, weak acids in aqueous solution can both be sorbed and exchanged on anion exchangers. The reactions can be expressed schematically as



Step (1) represents sorption of the neutral molecule HA, (2) dissociation, and (3) exchange of the  $\text{A}^-$  anion. The relative magnitudes of steps (1) and (3) depend on the dissociation constant of the weak acid  $K_i$ , the selectivity of the resin for the ion  $\text{A}^-$  and the concentration of HA. For relatively weak acids ( $K_i \approx 10^{-5}$ ), molecular sorption is always greater than ion exchange sorption, according to Tsitorich and Semenova<sup>155</sup>.

Molecular sorption of benzoic acid on the anion exchange resin AN-2F in the  $\text{Cl}^-$  form was found by them to be 1.5 to 7 times larger than that sorbed by exchanging benzoate with  $\text{Cl}^-$  in the resin. The same holds for 2-chlorobenzoic acid and 2,4-dichlorobenzoic acid.

Owing to the presence of molecular sorption, the apparent capacity of the anion exchanger was found to be abnormally high<sup>156</sup>.

The factors governing molecular sorption have been discussed previously. In addition to these general factors, for the exchange sorption of organic ions the resin selectivity toward various organic ions is involved. The interaction of large organic ions with a resin has been discussed at length at the microscopic level by Feitelson<sup>157</sup> in terms of water structure, entropy change, and rotational motion of the organic ion. Macroscopically, this is similar to the sorption of nonelectrolytes, where two counteracting forces determine the selectivity. Thermodynamics (Gregor's model, Chapter I) favors the uptake of smaller ions due to osmotic pressure (Chapter I). Since the volume of most organic ions is much larger than that of simple solvated inorganic ions, the resin will prefer the inorganic species. Selectivity is even less for organic ions so large that they are physically excluded from entering through the small pores into the interior of the resin. Moskvichev and Samsonov<sup>156</sup> also attributed the low selectivity of organic ions to weak Coulombic forces between the ions and the fixed charge groups in terms of the Harris and Rice model (Chapter III). The decreasing selectivity with increasing loading of

the resin by organic ions was interpreted to be the result of dehydration of the resin.

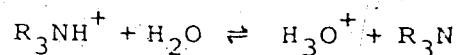
On the other hand, London dispersion forces are greater for larger organic counter ions, especially those with organic groups resembling the matrix component such as styrene-type compounds on polystyrene resins. Osmotic pressure is often the deciding factor. London dispersion interactions must be considered only when the relative selectivity of a resin for several organic ions is compared.

Simultaneous Sorption and Exchange of Weakly Dissociated Electrolytes: Organic Ions as Coions and Hydrogen Ion as Counter Ion

It is of interest to know how sorption of a weak acid is affected by the presence of other electrolytes as well as by dissociation of the acid. A related unresolved problem is whether molecular sorption of a weak acid HA and electrolyte sorption of the organic ion  $A^-$  on a sulfonated cation exchange resin are independent of each other.

The experiment described here falls into two parts. The first part is a study of the simplest system, where the weak acid HA is in equilibrium with sulfonated polystyrene resin in the  $H^+$  form. From this work the behavior in the resin of a weak acid  $\overline{HA}$  and

its coion  $\bar{A}^-$  can be obtained. The second part is an investigation of the system HA-NaCl-H<sub>2</sub>O-sulfonated polystyrene resin. This system was chosen because the exchange sorption of protons with  $\text{Na}^+$  is well known and can easily be measured independently by using a strong acid, such as HCl, under conditions where no molecular sorption takes place (Chapter III). In the case where organic ions are present as counter ions, for example  $\text{R}_3\text{NH}^+\text{Cl}^-$ -NaCl-H<sub>2</sub>O-sulfonated polystyrene resin, the exchange sorption of organic ions cannot be determined without interference from other species that form simultaneously through reactions such as hydrolysis.

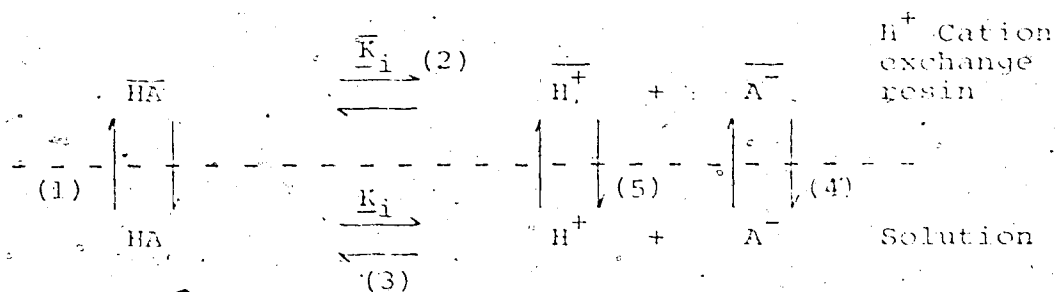


The data required for the first part were obtained from Reichenberg's work<sup>143</sup>. For the second part the systems phenylacetic acid (HPAA)-NaCl-H<sub>2</sub>O-Dowex 50W × 8, benzene sulfonic acid (HBSA)-NaCl-H<sub>2</sub>O-Dowex 50W × 8, and chloroacetic acid (HCAA)-NaCl-H<sub>2</sub>O-Dowex 50W × 8 were studied.

#### Thermodynamic Model

Most weak acids in aqueous solution undergo dissociation to a known extent, but their behavior in a resin phase is usually not known. In the homogeneous model, where the resin is regarded as a concentrated solution

phase containing  $\overline{H^+}$ ,  $\overline{HA}$  and  $\overline{A^-}$ , it is reasonable to postulate that the equilibrium between  $\overline{HA}$  and  $\overline{A^-}$  in the resin,  $\overline{K}_i$ , will possess a dissociation constant of the same order of magnitude as that in aqueous solution. The counter ion concentration being as high as 6 M in the resin, dissociation in the resin phase is subject to a strong salt effect under conditions where the activity coefficients in the resin  $\overline{\gamma}_{\pm}$  differ somewhat from the external solution; a slight deviation of  $\overline{K}_i$  from  $K_i$  is expected. The whole process can be represented by several equilibria, schematically shown as follows:



### Scheme 1

Step (1) represents molecular sorption, (2) internal dissociation, (3) dissociation in aqueous solution, and (4) and (5) Donnan invasion sorption. A similar mechanism has been proposed by Savitskaya<sup>158</sup> for different systems. The equilibrium between sulfonated polystyrene cation exchange resins of 5 $\frac{1}{2}$ , 10, and 15% DVB with acetic acid, propionic acid, *n*-butyric acid, and benzoic acid was studied by Reichenberg and Wall<sup>143</sup>. Only the results for 10% DVB resin, shown in Table 17, were used to test the hypothesis proposed above.

The value of  $\bar{K}_1$  is immediately obtainable if values for  $\bar{H}^+$ ,  $\bar{A}^-$  and  $\bar{HA}$  are known. The data provide only  $\bar{H}^+$  and  $\bar{HA}$ , and therefore  $\bar{A}^-$  has to be determined before  $\bar{K}_1$  can be calculated. Since HA is a rather weak acid and the internal proton concentration is high the coion concentration  $\bar{A}^-$  has to be very small if the assumption that  $\bar{K}_1 \approx K_1$  is to be valid. The large amount of HA sorbed makes the accurate measurement of  $\bar{A}^-$  impossible. However, because it is known that sorption of the coion of a strong electrolyte is governed by Donnan invasion theory (Chapter III), so that the internal molality of coion is proportional to the square of the concentration of dissociated electrolyte in solution,  $\bar{A}^-$  can be estimated.

This system can further be checked by thermodynamics. If Equilibrium (2), described by  $\bar{K}_1$ , exists, then the following relationships also should exist:

$$\frac{[\overline{H^+}][\overline{A^-}]}{[\overline{HA}]} = \bar{K}_1$$

$$[\overline{A^-}] = \underline{K}_4 [A^-]^2 \quad \text{step (4), Donnan invasion}$$

$$\therefore \bar{K}_1 \frac{[\overline{HA}]}{[\overline{H^+}]} = \underline{K}_4 [A^-]^2$$

$$\text{and} \quad [\overline{H^+}] \approx \frac{C}{V_s}$$

$$\therefore [\overline{HA}] = \frac{\underline{K}_4}{\bar{K}_1} \frac{C}{V_s} [A^-]^2$$

$[A^-]$  can be related to  $C_0$  by making the assumption that  $[\overline{HA}] = C_0$ , the total acid concentration in solution.

$$[A^-]^2 = \frac{C_0 \bar{K}_1}{\underline{K}_4}$$

Then

$$\overline{HA} = \frac{\underline{K}_4 \bar{K}_1 C}{\bar{K}_1 V_s} C_0 \quad (19)$$

For the case of true dissolution,  $[\overline{HA}]$  is proportional to  $C_0$ , with a proportionality constant  $\underline{k}_7$  (Equation (17a)). Comparing Equation (17a) with (19),  $\underline{k}_7$  ( $K_1$ ) is found to be identical with  $\underline{K}_4 \bar{K}_1 C / \bar{K}_1 V_s$ . From Scheme 1, the total number of unknowns in the system can be seen to be 6 ( $\overline{HA}$ ,  $\overline{H^+}$ ,  $\overline{A^-}$ ,  $HA$ ,  $H^+$ , and  $A^-$ ). The number of

equilibrium equations available is 5, and there are also 2 equations in charge balance and 1 equation in material balance:

$$[H^+] = [A^-] \quad \text{charge balance in solution}$$

$$[H^+] = [A^-] + \frac{C}{V_s} \quad \text{charge balance in resin}$$

$$C_o = [HA] + [A^-] \quad \text{material balance in solution.}$$

Thus there are altogether eight equations for six unknowns. However, Equilibria (4) and (5) are identical, since  $H^+$  and  $A^-$  cannot be separated, and Equilibrium (1) is also dependent because  $K_1$  or  $k_7$  can be calculated from Equilibria (2), (3) and (4) (Equation (19)). Thus only 3 independent equilibria are available, but are sufficient to completely define the system.

It is possible that the sorption of a non-electrolyte is not true dissolution, but rather surface adsorption as described by the Langmuir isotherm (Equations (16), (18a), (18b)), and so is not compatible with Equation (19) as derived. Scheme 1 would then have oversimplified the real situation. It can be further postulated that in surface adsorption,  $H^+$  and  $A^-$  are not in direct equilibrium with  $HA$  as measured. Thermodynamics makes use of an activity coefficient  $\bar{\gamma}_N$  to reconcile these two factors as well as to correct



for "non-ideal" interactions from surface adsorption. Scheme 1 is still valid, for the activity coefficient  $\overline{\gamma}_N$  is incorporated into Equilibrium (2) such that Equation (19) becomes

$$\overline{\gamma}_N [\overline{HA}] = \frac{K_4 K_i}{K_i V_s} \subseteq C_o.$$

Comparing this expression with the Langmuir isotherm Equation (16):

$$[\overline{HA}] = \frac{a' k C_o}{1 + k C_o}$$

it can be shown that

$$\overline{\gamma}_N = \frac{K_4 K_i}{K_i V_s} \subseteq \left( \frac{1 + k C_o}{a' k} \right) = \frac{k_{10}}{k_{11}} + C_o.$$

The magnitude of  $\overline{\gamma}_N$  varies linearly with the external concentration  $C_o$ , and ranges from 0 to 1 as the sorption varies from surface adsorption only to true dissolution only. The physical significance of  $\overline{\gamma}_N$  is that those molecules sorbed by London dispersion interactions are not entirely in the internal solution where the equilibrium occurs; even though the interaction is so mild that the molecule is practically in the internal solution with a limited degree of freedom; the molecules still experience an attraction to the polymer skeleton to some degree so that they are not completely "free". Thus



as expressed by Equilibria (6) and (1). Using the same analysis procedure as in Scheme 1, there are seven unknown species and nine equations (two charge balance, one material balance and six equilibria), with  $\underline{K}_1$  ( $\underline{k}_7$  in Equation (17a)) equal to  $\underline{K}_4 \underline{K}_1 \underline{c} / \underline{K}_1 \underline{v}_s$  and

$$\overline{HA}^* = \frac{\underline{k}_a' [\overline{HA}]}{1 + \underline{k} [\overline{HA}]}$$

Of the six equilibria only four, 6, 2, 3, and 5, are mutually independent.

The quantity of sorbed acid measured,  $\overline{HA}_t$ , is thus the sum of two forms:

$$\overline{HA}_t = \overline{HA} + \overline{HA}^*$$

Since  $\overline{HA}^*$  is only a hypothetical species, there is no way to measure  $\overline{HA}$  and  $\overline{HA}^*$  separately. However, they can be estimated by making several bold but valid assumptions. Equilibrium (1) is a true dissolution step, where  $\overline{HA}$  is not subjected to any non-ideal interactions. Being a neutral molecule,  $\overline{HA}$  is also not affected by the high charge density and high dielectric constant present in the internal solution; the distribution coefficient  $\underline{K}_1$  ( $\underline{k}_7$ ) is determined by the osmotic pressure and the size of the solute molecules (Chapter III, Equation (12)).

$$\underline{K}_1 = \exp\left[-\frac{\pi \overline{V}_N}{RT}\right] \quad (20)$$

It is not easy to obtain good experimental values of  $\bar{V}_N$ , the partial molal volume of the solute, which is defined as  $(\partial V / \partial n_N)_{T, P, n_1, n_2}$ , the volume increase upon the addition of one mole of solute to the resin under specific internal conditions (same water content and solute as that at the sorption condition). It is related but not directly proportional to the molecular weight of the solute, and also somewhat different from the partial molal volume in water owing to the presence of a resin matrix that will squeeze the solution into a smaller volume. As calculated by the addition rule,  $\bar{V}_N$  should also be smaller than the molecular volume at the boiling point, where the molecules acquire greater translational freedom. The value of  $\bar{V}_N$  is assumed to be around 50-100 cm<sup>3</sup>/mol, while  $\pi$  varies from 0 to 500 atm, and is about 120 atm for 8% DVB, and 200 atm for 10% DVB<sup>159,87</sup>. So  $K_1$  lies somewhere between 0.8 and 0.5. If the resin is not highly crosslinked and the volume of the solute is not exceedingly large,  $K_1$  can be approximated to be 1. A similar argument holds for Donnan invasion sorption of the A<sup>-</sup> organic anion, which depends on the osmotic pressure term in a similar fashion (Chapter III). The values of  $K_5$  and  $K_4$  can be approximated by sorption of the strong electrolyte HCl on the resin in H<sup>+</sup> form (Chapter III, Equation (13a)).



### Interpretation of Previous Work

The thermodynamic models proposed above can be tested with the data from Reichenberg and Wall's<sup>143</sup> experiment, where the sorption of benzoic acid, *n*-butyric acid, propionic acid and acetic acid  $\overline{HA}_t$  were measured for sulfonated polystyrene resin in the hydrogen form at 2.5%, 10% and 15% DVB. Only the data for 10% DVB resin, shown in Table 17, was used. Figure 23 shows a plot of  $\log \overline{HA}_t$  against  $\log C_o$ . Acetic acid, benzoic acid and propionic acid all form straight lines with slopes of 0.90, 1.0 and 0.74. *n*-Butyric acid shows a concave curve that tends to flatten at high concentrations.

As was mentioned before, true dissolution can be assigned only when the molality ratio is less than unity, and the slope of a plot of  $\log \overline{HA}_t$  against  $\log[HA]$  is equal to one. Apparently, acetic acid does meet the requirement except that the slope (0.9) is a little less than one, which indicates the presence of slight interaction. Thus acetic acid can be regarded to be sorbed primarily by true dissolution. Propionic acid and *n*-butyric acid, especially the latter, have larger London dispersion interactions and a larger molality ratio. They are sorbed by surface adsorption. Benzoic acid has a slope of one, yet a molality ratio of five. This large molality ratio indicates an

Table 17

Internal dissociation constant  $K_i$  of organic acids in 1 g of dried (5.3 meq) 10% DVB sulfonated polystyrene resin in the hydrogen form at 25°C.<sup>a</sup>

Solute	Molality	Solute sorbed $\frac{HA_T}{m}$ moles	H <sub>2</sub> O sorbed g	$[A^-]$ $10^{-4} M$	$\bar{A}^-$ $\mu eq$ $10^{-5}$	$(\bar{K}_i)_1$	$(\bar{K}_i)_2$	$K_i$
$\underbrace{\hspace{10em}}_{10^{-5}}$								
Benzoic acid	0.0100	0.045	0.84	8.04	4.5	0.63	5.6	6.46
	0.0200	0.089	0.84	11.4	9.0	0.64	5.5	
Acetic acid	0.0100	0.008	0.84	4.19	1.2	1		1.76
	0.0200	0.015	0.84	5.95	2.5	1.1		
	0.0503	0.030	0.84	9.41	6.2	1.3		
	0.101	0.059	0.84	13.3	12.4	1.3		
	0.202	0.116	0.84	18.9	24.8	1.4		
	0.514	0.27	0.83	30.1	63.0	1.5		
	1.056	0.53	0.82	43.0	129	1.6		
	2.234	0.97	0.80	62.7	274	1.8		
Prop-ionic acid	0.456	0.31	0.83	24.7	42.5	0.88	1.1	1.34
	0.941	0.54	0.82	35.5	88	1.05	1.1	
	2.013	0.93	0.80	51.9	188	1.3	1.1	
n butyric acid	0.541	0.43	0.83	29.1	58	0.86	1.3	1.54
	1.134	0.74	0.82	41.8	122	1.06	1.3	
	2.517	0.87	0.79	62.3	270	2.08	1.4	

<sup>a</sup>Data calculated on basis of one gram (5.3 meq) of dry resin.

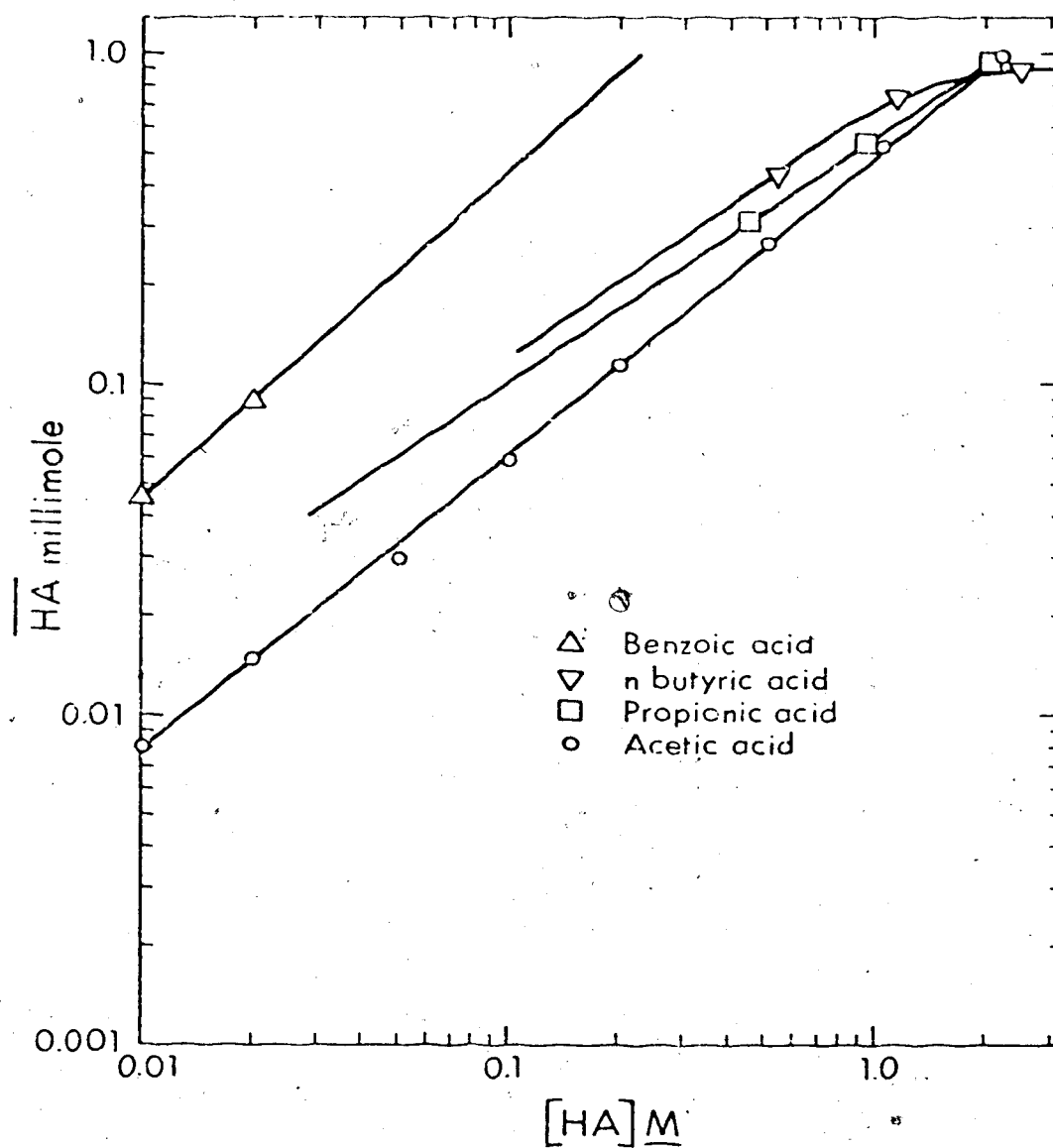


Figure 23. The sorption of organic weak acids on 5.3 meq Dowex 50 x 8 in H<sup>+</sup> form at various organic acid concentrations in external solution



adsorption mechanism is involved, because the Langmuir isotherm expression has the same form as the expression for true dissolution at low concentration.

The sorption of the organic anion (conjugated base) of each of the acids can be approximated by the sorption of  $\text{Cl}^-$  in  $\text{HCl}$  solution with the resin in the  $\text{H}^+$  form. Sorption of  $\text{Cl}^-$  had been measured in an earlier part of this work (Chapter III, p. 71, Equation (13a)) and found to obey the empirical equation

$$\bar{A}^- = 222[A^-]^2$$

on the basis of 16.9 meq of resin. Referring to one gram of dry resin in the hydrogen form (5.3 meq/g), the equation can be rewritten as

$$\bar{A}^- = 69.6[A^-]^2 \quad (21)$$

where  $\bar{A}^-$  is expressed in  $\mu\text{eq}$  and  $[A^-]$  in  $\text{M}$ . Then  $[A^-]$  in the aqueous solution can be found from the following formula:

$$[A^-]^2 = \frac{\bar{A}^-}{69.6} = \frac{K_i C_0}{69.6}$$

The quantity of cation sorbed per gram of dry  $\text{H}^+$  resin,  $\bar{A}^-$ , can be calculated readily and is shown in column 6 of Table 17;  $\bar{H}^+$  is equal to 5.3 meq, the capacity of one gram of dry resin. The internal

dissociation constant can then be readily calculated.

$$(\overline{K}_i)_1 = \frac{\overline{A^-} \times 10^{-3} \times 5.3}{\overline{HA_t} \times \underline{V}_s}$$

The bracket and subscript 1 refer to the case of true dissolution. The values of  $(\overline{K}_i)_1$  are shown in column 7 of Table 17.

It was found that  $(\overline{K}_i)_1$  for acetic acid is nearly constant, except for a slight increase from  $1 \times 10^{-5}$  to  $1.8 \times 10^{-5}$  with increasing concentration. This variation may be caused by the presence of slight London dispersion forces. The value of  $(\overline{K}_i)_1$  reaches  $1.8 \times 10^{-5}$ , equal to that in the external solution ( $K_i = 1.76 \times 10^{-5}$ ) at high concentrations where the interaction becomes insignificant compared with true dissolution. Propionic acid shows a greater variation in  $(\overline{K}_i)_1$ , and reaches  $1.3 \times 10^{-5}$  at high concentrations ( $K_i = 1.34 \times 10^{-5}$ ). The value of  $(\overline{K}_i)_1$  for *n*-butyric acid shows the largest variation. Being the biggest of the three acids, *n*-butyric acid interacts most strongly with the matrix. The final value of  $(\overline{K}_i)_1$  is  $2.08 \times 10^{-5}$ , which is larger than  $K_i$  ( $1.54 \times 10^{-5}$ ).  $(\overline{K}_i)_1$  for benzoic acid is 10 times less than  $K_i$  ( $6.46 \times 10^{-5}$ ) due to the interaction being strongest.

It appears clear that propionic acid, *n*-butyric acid and benzoic acid all undergo surface adsorption.

According to Scheme 2  $\overline{HA}$ , but not  $\overline{HA}_t$ , is in equilibrium with  $H^+$  and  $A^-$ . Since the partial molal volumes  $\overline{V}_N$  of these acids are not known,  $K_1$  and thus  $\overline{HA}$  can be estimated only with an accuracy of an order of magnitude as follows (see Equation (20)). The osmotic pressure for 10% DVB resin is 210 atm<sup>159,87</sup>. The molar volume of acetic acid, calculated from its density of 1.1 g/cc, is equal to 54 ml/mole. On the basis of strong interaction of acetic acid with water, and the squeezing effect of the resin, it is reasonable to assume that the volume is reduced by about a factor of 2. This gives a value of  $\overline{V}_N$  for acetic acid of around 30 ml/mole. Using a value for  $R$  of 0.08205 atm l/°K mole and a temperature of 300°K,  $K_1$  can be estimated for acetic acid to be

$$K_1 \approx e^{-\pi \overline{V}_N / RT} \approx 0.8.$$

Estimating the size of benzoic acid to be about double that of acetic acid, or 60 ml/mole, then from Equation (20)  $K_1$  for benzoic acid is 0.6. For propionic acid and *n*-butyric acid  $K_1$  should lie between these two values, and is estimated to be 0.75 for propionic and 0.7 for *n*-butyric acid. Using these values,  $(\overline{K}_i)_2$ , the internal dissociation constant with surface adsorption, can be calculated for propionic acid, *n*-butyric acid and benzoic acid by

$$(\overline{K}_i)_2 = \frac{[\overline{H}^+][\overline{A}^-]}{[\overline{HA}]} = \frac{[\overline{H}^+][\overline{A}^-]}{\underline{K}_1[\overline{HA}]}$$

The values of  $(\overline{K}_i)_2$  obtained are listed in column 8 of Table 17, and can be compared with  $\underline{K}_i$  in column 9 of Table 17.  $(\overline{K}_i)_2$  for benzoic acid is  $5.6 \times 10^{-5}$  ( $\underline{K}_i = 6.4 \times 10^{-5}$ ), for propionic acid  $1.1 \times 10^{-5}$  ( $1.34 \times 10^{-5} = \underline{K}_i$ ), and for *n*-butyric acid  $1.4 \times 10^{-5}$  ( $\underline{K}_i = 1.54 \times 10^{-5}$ ).

By introduction of Equilibrium (6) into Scheme 2,  $(\overline{K}_i)_2$  can be rewritten as:

$$(\overline{K}_i)_2 = \frac{[\overline{H}^+][\overline{A}^-]}{[\overline{HA}]} = \frac{c\underline{K}_4[\overline{A}^-]^2}{\underline{V}_s \underline{K}_1 \underline{K}_i [\overline{A}^-]^2} = \frac{c\underline{K}_4}{\underline{V}_s \underline{K}_1 \underline{K}_i}$$

and constant values of  $(\overline{K}_i)_2$  can be obtained. In any event, the magnitude of  $(\overline{K}_i)_2$  can be used to confirm the existence of Equilibrium (1) in Scheme 2, as well as the internal dissociation Equilibrium (2). The close proximity of  $(\overline{K}_i)_2$  to  $\underline{K}_i$  validates Scheme 2, whereas for acetic acid  $(\overline{K}_i)_1$  is close to  $\underline{K}_i$ , which indicates Scheme 1 is valid for this acid.

Neither  $(\overline{K}_i)_1$  nor  $(\overline{K}_i)_2$  appear to be seriously affected by the high charge density in the resin phase.

A last question to be considered is whether  $\bar{K}_1$  can be measured directly without making the approximations introduced above. Measurement of  $\bar{K}_1$  requires a knowledge of  $\overline{HA}$  and  $\overline{A^-}$ . The portion of sorbed HA present through true dissociation,  $\overline{HA}$ , must be free of interaction with the matrix.  $\overline{HA}$  is equal to  $\overline{HA}_t$  if it does not interact with the matrix at all, which is rare.  $\overline{A^-}$  also cannot be measured due to masking by  $\overline{HA}$  and  $\overline{HA}^*$ . If a physical method were available which could distinguish among  $HA^*$ ,  $\overline{HA}$  and  $\overline{A^-}$ , then  $\bar{K}_1$  could be measured directly.

#### Simultaneous Sorption and Exchange: HA-NaCl-H<sub>2</sub>O-Dowex

50W x 8

#### Experiment

##### Reagents

All reagents used were of analytical grade as described in Chapters II and III, except for benzene sulfonic acid, chloroacetic acid, and phenylacetic acid (Terochem Laboratories Ltd., Alberta) which were technical grade and were used as received.

##### Preparation of solutions

The same scheme as in section 2 of Chapter IV was used, except that HA and NaCl were employed in place of NaCl and KCl.

### Procedure

Three acids, benzene sulfonic acid (HBSA), phenylacetic acid (HPAA), and chloroacetic acid (HCAA), were studied in this experiment. The detailed procedure used was as described in Chapter III. The equilibrating solutions contained  $[\text{NaCl}]$  equal to 0.1, 0.2, 0.3 and 0.5  $\text{M}$ , and  $[\text{HA}]$  equal to  $10^{-4}$ ,  $2 \times 10^{-4}$ ,  $5 \times 10^{-4}$ , and  $10 \times 10^{-4}$   $\text{M}$ . The exact concentration of the specific acid was found in each case by titrating the 0.1  $\text{M}$  HA stock solution with 0.1034  $\text{M}$  NaOH, using phenolphthalein as indicator, and was found to be 0.1026  $\text{M}$  for HCAA, 0.09714 for HPAA, and 0.104 for HBSA. The concentration of HBSA in the equilibrating solutions for the first part of the experiment was  $1.004 \times 10^{-4}$ ,  $2.008 \times 10^{-4}$ ,  $5.02 \times 10^{-4}$ , and  $10.04 \times 10^{-4}$   $\text{M}$ ; [HPAA] for the second part of the experiment was  $0.924 \times 10^{-4}$ ,  $1.848 \times 10^{-4}$ ,  $4.62 \times 10^{-4}$ , and  $9.24 \times 10^{-4}$   $\text{M}$ ; and [HCAA] for the last part of the experiment was  $1.026 \times 10^{-4}$ ,  $2.054 \times 10^{-4}$ ,  $5.135 \times 10^{-4}$ , and  $10.26 \times 10^{-4}$   $\text{M}$ .

The equilibrating solutions were passed through the column at a flow rate of 120 ml/hr. A glass electrode was used as monitor, and the flow was stopped when the pH of the effluent had decreased to a constant value equal to that of the equilibrating solution. The column then was washed with 0.8  $\text{M}$  NaCl for the HCAA and HBSA cases, and with 0.8  $\text{M}$  NaOH solution for HPAA.

The washings were collected in 50-ml volumetric flasks, diluted to the filling mark, and then analyzed for acid content (or  $A^-$  content, in the case of HPAA) by UV spectrophotometry. The same equilibrating procedure was carried out twice for each equilibrating solution; the second time 50 ml of 0.8 M NaCl solution was used to wash the effluent from the column for all three acids, and the acid content was determined by coulometry.

#### Determination of $HA^-$ and $A^-$ by UV Spectrophotometry

A double beam UV spectrophotometer, Unicam SP 1700, with absorbance scale expansion ( $A = 1, 2$ ) was used for the UV measurements. The measurements were taken in 4-cm quartz cells with a deuterium source lamp and an A setting of 1. The cells were not identical, and so could not be exchanged during this work.

#### HBSA

This compound has a strong absorption at 240 to 280 nm, which corresponds to the benzene B band<sup>162</sup>. The background ~~caused by~~ presence of 0.8 M NaCl and HCl was corrected for by using 0.8 M NaCl and  $2 \times 10^{-3}$  M HCl as reference solutions. The measurement was made at a fixed wavelength of 262 nm, which corresponds to the highest peak in the fine structures of the band. An adjustment of the wavelength was made until the largest reading in A was obtained. The absorbance was

then recorded from the digital screen display with the wavelength unchanged for the rest of the measurements.

A calibration plot was run on five standard solutions of known HBSA concentration:  $4.016 \times 10^{-4}$ ,  $2.008 \times 10^{-4}$ ,  $1.004 \times 10^{-4}$ ,  $0.4016 \times 10^{-4}$ , and  $0.2008 \times 10^{-4}$  M. Each contained a matching matrix, i.e. 0.8 M NaCl and  $2 \times 10^{-3}$  M HCl. The calibration plot was linear, and showed no curvature at the concentrations used. The concentration of HBSA in the 50-ml volumetric flask could be obtained from the calibration graph once the absorbance of the sample had been measured. The value for  $\overline{\text{HBSA}}_t$  was then obtained by multiplying the concentration by the volume collected. Because HBSA is completely ionized at the concentrations employed, error due to partial ionization is not present.

#### HPAA

The procedure used here was the same as described in the previous section except that 0.8 M NaOH was used as the reference solution. The absorption peak used was also that of the benzene B band, as reported in the literature<sup>163</sup>. The measurement was done by scanning from 200 to 280 nm at a speed of 100 nm per min. Each sample was measured twice and the absorbance reading taken at the wavelength of highest absorbance, 258 nm. The standard solutions for the calibration plot



contained  $7.165 \times 10^{-4}$ ,  $2.583 \times 10^{-4}$ ,  $1.791 \times 10^{-4}$ ,  $0.8956 \times 10^{-4}$ ,  $0.4478 \times 10^{-4}$ , and  $0.2239 \times 10^{-4}$  M HPAA in 0.8 M NaOH solution. Values of  $\overline{\text{HPAA}}_t$  were obtained by multiplying the concentration of HPAA read from the calibration curve by the volume collected, 50 ml.

#### HCAA

The carbonyl chromophore of chloroacetic acid absorbs at 204 nm with a molar absorptivity of 4.1. This absorption is caused by a  $n \rightarrow \pi^*$  transition (R band)<sup>162</sup>. Since 204 nm is near the edge of the spectrophotometer range, care must be taken if reliable results are to be gotten. The background solution of 0.8 M NaCl showed a strong absorption at 204 nm that blocked use of this wavelength. However, chloroacetic acid solution also showed a broad band at 220 to 240 nm without fine structure. To eliminate most of the NaCl interference, a wavelength of 238 nm was used for all readings of absorbance, with a solution 0.8 M in NaCl and  $2 \times 10^{-3}$  M in HCl as reference. An internal addition method was used. The absorbance of the sample  $A_0$  was taken with H<sub>2</sub>O as reference; then a precision syringe (Hamilton) of 0.1 ml capacity was used to add 0.08 ml of  $1.026 \times 10^{-2}$  M chloroacetic acid into the sample cell, the volume of the sample cell having previously been determined to be 12.85 ml by weighing

before and after filling with  $H_2O$ . The absorbance  $A_1$  was recorded again assuming that the volume had not changed by the addition of 0.08 ml acid. Finally the absorbance of the background solution, 0.8 M NaCl plus  $2 \times 10^{-3}$  M HCl, ( $B'$ ) was measured.

Letting  $c$  be the concentration of the sample HCAA, in moles/l, and  $a_1$  be the molar absorptivity, then

$$A_0 = a_1 c + B'$$

$$A_1 = a_1 \left[ c + \frac{1.026 \times 10^{-2} \times 0.08}{12.85} \right] + B'$$

and

$$\begin{aligned} c &= \left( \frac{A_1 - A_0}{A_0 - B'} \right) \frac{1.026 \times 10^{-2} \times 0.08}{12.85} \text{ M} \\ &= \left( \frac{A_1 - A_0}{A_0 - B'} \right) (6.388 \times 10^{-5}) \end{aligned}$$

### Results and Discussion

The experiments were run at trace concentrations of acids, which simulates the condition of a trace solute in ion exchange chromatography. In the concentration range of  $10^{-3}$  M or less, weak acids may undergo appreciable dissociation, so that simultaneous sorption and exchange have to be considered. The results of this experiment can also be used to prove the association theory in Chapter III indirectly. This is discussed later.

# HBSA-NaCl-H<sub>2</sub>O-Dowex 50W x 8 System

All data were calculated on the basis of 16.9 meq of resin. The results of the measurements are given in Tables 18 and 19. Since HBSA is a strong acid ( $K_1 = 0.2$ ), it can be considered completely dissociated at the concentrations concerned. The amount of HBSA sorbed,  $\overline{\text{HBSA}}_t$ , uncorrected for dead volume  $\underline{v}_m$ , was measured from the calibration curve, then multiplied by the volume collected (column 6, Table 18). The value of  $\overline{\text{HBSA}}_t$ , divided by  $\underline{C}_0$ , the total concentration of HBSA in solution (column 7, Table 18), was found to be approximately 3.5 ml, or equal to  $\underline{v}_m$  within experimental error. It is concluded that a strong acid like HBSA is not sorbed by sulfonic acid ion exchange resins to any significant extent, even though HBSA has a structure so similar to the resin matrix that a large interaction is expected. The solution contains appreciable quantities of  $\text{BSA}^-$  coions, but only the molecular form of HBSA is responsible for the molecular sorption. Thus Equilibria (6) and (1) are verified. Furthermore, the observation that sorption of coion  $\text{BSA}^-$  is also negligible shows that Donnan invasion is still the dominant factor in coion sorption.

The total  $\text{H}^+$  sorbed,  $\overline{\text{H}^+}_t$ , (Table 19, column 3), uncorrected for dead volume of the column, was divided by  $\underline{C}_0$  (column 5, Table 19) and compared with the

Table 18

• Spectrophotometric determination of benzene-sulfonic acid HBSA on Dowex 50W  $\times 8$ .<sup>a</sup>

[NaCl] M	$\frac{C_o}{M} \times 10^{-4}$	Absorbance of the washing	[HBSA] from calibra- tion curve $M \times 10^{-4}$	Vol. collec- ted ml	HBSA <sub>t</sub> meq	$\frac{HBSA_t}{C_o}$ ml
0.1	10.04	0.121	0.65	51.863	3.37	3.36
	5.020	0.060	0.325	51.538	1.68	3.34
	2.008	0.030	0.165	51.917	0.857	4.27
	1.004	0.016	0.085	51.92	0.441	4.39
0.2	10.04	0.120	0.65	51.917	3.37	3.36
	5.020	0.083	0.45	51.863	2.33	4.64
	2.008	0.026	0.14	51.838	0.722	3.60
	1.004	0.008	0.045	51.917	0.234	2.33
0.3	10.04	0.126	0.675	51.917	3.50	3.49
	5.020	0.063	0.34	51.917	1.76	3.50
	2.008	0.018	0.10	51.917	0.519	2.59
	1.004	0.012	0.065	51.863	0.337	3.36
0.5	10.04	0.138	0.730	51.538	3.76	3.75
	5.020	0.067	0.345	51.863	1.79	3.56
	2.008	0.019	0.105	51.863	0.545	2.72
	1.004	0.008	0.045	51.917	0.232	2.33

<sup>a</sup>Based on 16.25 meq of resin.

Table 19  
Coulometric determination of  $H^+$  sorbed on  
(16.25 meq) Dowex 50W  $\times 8$   $H^+$  in HBSA/NaCl mixture.

[NaCl] M	$C_0$ $M \times 10^{-4}$	$H_t^+$ meq	$\frac{H_t^+}{C_0}$ ml	$H_t^+$ $C_0$ corrected to 16.9 meq
0.1	10.04	156.3	156	162
	5.020	80.36	160	166
	2.008	36.90	184	191
	1.004	18.31	183	190
0.2	10.04	87.77	87.4	90.9
	5.020	48.46	96.5	100
	2.008	23.48	117	122
	1.004	12.36	123	128
0.3	10.04	63.94	63.7	66.2
	5.020	36.33	72.4	75.3
	2.008	18.61	92.7	96.4
	1.004	10.14	101	105
0.5	10.04	46.27	46.1	48.0
	5.020	25.48	50.8	52.8
	2.008	12.66	63.0	65.6
	1.004	8.243	82.1	85.4

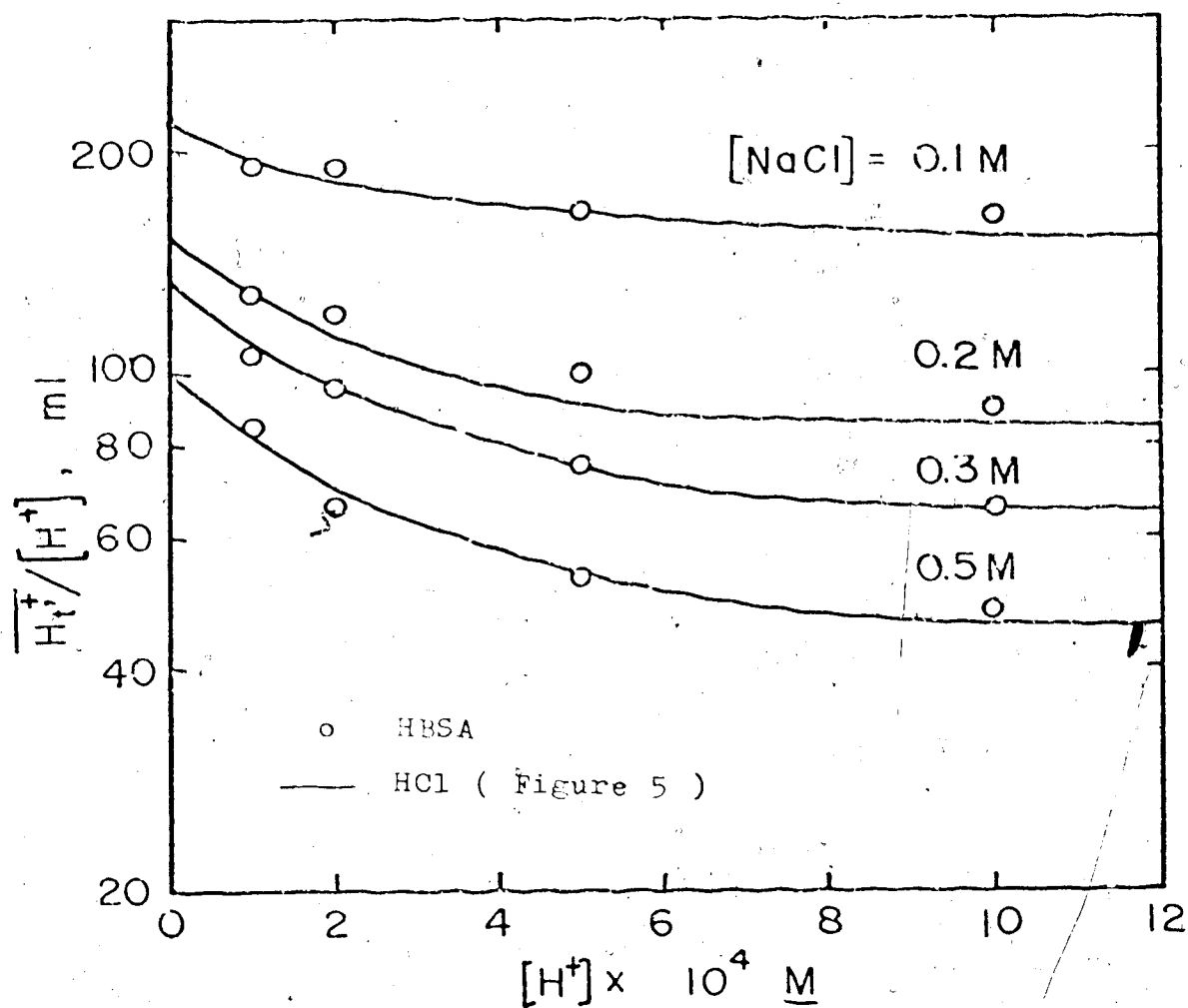
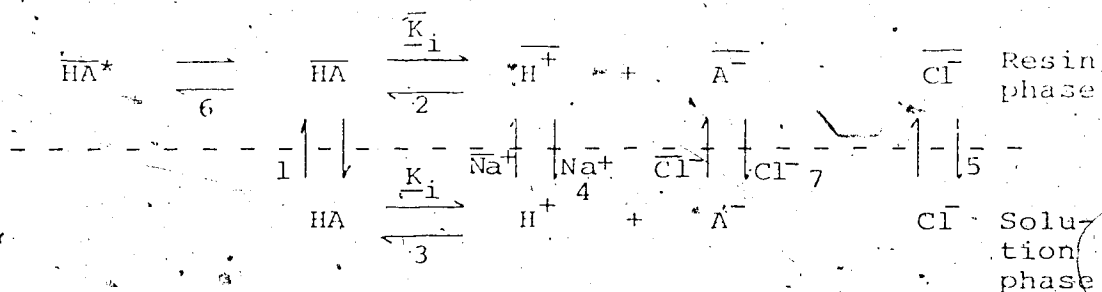


Figure 24. Comparison of the ratio of total sorbed HBSA on Dowex 50W x 8 over  $H^+$  concentration in equilibrium with HBSA in external solution at various  $H^+$  and NaCl concentrations and with that of HCl in Figure 5.

results obtained for the system NaCl-HCl-Dowex 50W × 8 in Chapter III by a plot of  $\log \frac{H_t^+}{C_0}$  against  $\frac{C_0}{C_0}$  (Figure 24). The value of  $\frac{H_t^+}{C_0}$  for HBSA falls closely on the lines obtained for NaCl/HCl exchange after correction to the same capacity of 16.9 meq. This indicates that the organic coions have little effect on the exchange sorption of counter ions, and that the abnormal high  $H^+$  sorption at low  $H^+$  concentration is still observed.

#### HPAA-NaCl-H<sub>2</sub>O-Dowex 50W × 8 System

The effect of incomplete dissociation of an electrolyte on its ion exchange behavior has been reported<sup>160</sup>. The systems studied were 0.1 to 0.01 M sodium chloroacetate on Zeo-Karb 225, a sulfonated polystyrene resin in the hydrogen form, and sodium acetate on the same resin. The effects of neutral molecule sorption were neglected, although this is usually not justified for weak electrolytes. The system as a whole is complicated, and involves many equilibrium steps due to incomplete dissociation of the weak electrolytes. Utilizing the same treatment as in Scheme 2, a third scheme can be written:



### Scheme 3

There are 11 unknowns,  $\overline{HA^*}$ ,  $\overline{H^+}$ ,  $\overline{A^-}$ ,  $\overline{H}$ ,  $\overline{Na^+}$ ,  $\overline{Cl^-}$ ,  $\overline{HA}$ ,  $\overline{H^+}$ ,  $\overline{A^-}$ ,  $\overline{Na^+}$ ,  $\overline{Cl^-}$  for the solution of which 7 equilibrium and 4 material or charge-balance expressions are required.

$$\underline{C}_O = [A^-] + [HA]$$

$$[A^-] = [H^+]$$

$$[Cl^-] = [Na^+]$$

$$\overline{H^+} + \overline{Na^+} = \overline{A^-} + \overline{Cl^-} + \underline{C}$$

All the equilibria are mutually independent.

The strength of the London dispersion interactions determines the existence of species  $\overline{HA^*}$  through

Equilibrium (6). Equilibria (1), (2), (3), (5) and

(6) are essentially the same as described in Scheme 2,



but Equilibria (4) and (7) are entirely different in that (4) is an exchange reaction with  $H^+$  replacing  $Na^+$ ,

$$K_4 = K_{H/Na} = \frac{[H^+]}{[H^+]} \frac{[Na^+]}{[Na^+]}$$

and (7) is a similar equilibrium involving the  $A^-$  and  $Cl^-$  coions.  $K_4$  can be obtained independently from the exchange of the strong acid HCl and NaCl. Equilibrium (7) is also an exchange reaction in which  $A^-$  exchanges with the major coion  $Cl^-$  in the resin as if the resin were an anion exchanger. Similar to the exchange of cation, the equilibrium between  $A^-$  and  $Cl^-$  will be established at a level that depends on the partial molar volume difference between  $A^-$  and  $Cl^-$ . The derivation is given in Appendix III.

$$K_5 = K_{A/Cl} = \frac{[A^-]}{[A^-]} \frac{[Cl^-]}{[Cl^-]}$$

As was revealed in the experiment on HBSA sorption (section 1, Chapter V), there is no significant sorption of BSA<sup>-</sup> coion. Thus  $PAA^-$  should be very small compared with  $HPAA_t$ , and the absorbance measured should come from the molecular species HPAA only. The amount of HPAA sorbed on the resin,  $HPAA_t$ , as obtained from the absorbance data, is shown in column 8 of Table 20. The value for  $HPAA_t$  has been corrected for the contribution from the column dead volume. The concentration

Table 20

Coulometric and spectrophotometric determination  
of HPAA sorbed on 16.25 meq of Dowex 50W x 8,  $\overline{\text{HPAA}}_t$  in  
HPAA/NaCl mixture at 25°C.

[NaCl]	$C_0$	[HPAA]	$[H^+]$ ( $= [PAA^-]$ )	$\overline{H}_t^+$	$(\overline{H}_t^+)$ HCl/NaCl	$\overline{\text{HPAA}}_t$	
M	$10^{-4}$ M	$10^{-4}$ M	$10^{-4}$ M	meq	meq	meq	Spect. meq
0.1	9.24	7.29	1.95	62.5	33.9	28.6	29.2
	4.62	3.31	1.31	34.5	23.7	10.8	11.9
	1.848	1.10	0.75	17.6	14.1	3.52	3.3
	0.924	0.44	0.48	10.8	9.3	1.5	1.7
0.2	9.24	7.29	1.95	50.0	20.8	29.2	28.7
	4.62	3.31	1.31	26.5	15.2	11.3	12.8
	1.848	1.10	0.75	13.7	9.52	4.2	4.8
	0.924	0.44	0.48	8.56	6.32	2.2	2.1
0.3	9.24	7.29	1.95	46.2	17.8	28.4	29.1
	4.62	3.31	1.31	23.5	13.1	10.4	12.7
	1.848	1.10	0.75	9.98	8.22	1.8	2.8
	0.924	0.44	0.48	7.44	5.49	1.9	1.9
0.5	9.24	7.29	1.95	28.9	13.1	15.8	26.4
	4.62	3.31	1.31	14.0	9.70	4.31	9.5
	1.848	1.10	0.75	6.85	6.06	0.794	3.0
	0.924	0.44	0.48	4.35	4.06	0.294	0.96

of neutral species HPAA present in the external solution in equilibrium with  $\overline{\text{HPAA}}$  can be estimated from  $K_1$ , assuming negligible activity effects.

$$[\text{H}^+] = [\text{PAA}^-] = \frac{-K_1 + \sqrt{K_1^2 + 4K_1C_0}}{2} \quad (22)$$

and

$$[\text{HPAA}] = C_0 - [\text{PAA}^-]$$

The values of  $[\text{HPAA}]$  and  $[\text{H}^+]$  (or  $[\text{PAA}^-]$ ) are shown in columns 3 and 4 of Table 20. The internal water content of 8% DVB  $\text{Na}^+$  sulfonated polystyrene resin has been reported as 9 moles/per equivalent of resin<sup>87</sup>, which is equivalent to 2.6 g of water per 16.25 meq of resin. The molality ratio, calculated by  $\overline{\text{HPAA}}_t / V_s [\text{HPAA}]$ , is on the order of 15 (column 4, Table 21), which is larger than the sorption of benzoic acid on the resin in the  $\text{H}^+$  form (5.5). Plots of  $\log \overline{\text{HPAA}}_t$  against  $\log [\text{HPAA}]$  at four NaCl concentrations, 0.1, 0.2, 0.3 and 0.5 M, all yield straight lines (Figure 25), with slopes of 1, 0.90, 0.96, and 1.17 (average of 1). High molality ratios and slopes of unity together indicate strong London dispersion interactions at low concentrations. The extent of molecular sorption,  $\overline{\text{HPAA}}_t$ , is not influenced by  $[\text{NaCl}]$  up to 0.3 M. The slightly lower value for  $\overline{\text{HPAA}}$  observed at  $[\text{NaCl}] = 0.5 \text{ M}$  may be due to activity effects and to shrinkage of the resin at high electrolyte concentrations.

Table 21

Calculation of internal dissociation constant  $\bar{K}_i$  for phenylacetic acid, HPAA, in

Dowex 50W x 8.

$\bar{M}$	$10^{-4} \bar{M}$	$[HPAA]$	$[H^+]$ ( $= [PAA^-]$ )	$\frac{[HPAA]}{[HPAA]}$	$Cl^-$ $\mu eq$	$\frac{PAA}{10^{-3}}$ $\mu eq$	$\frac{V_{CO}}{m_{CO}}$ $\mu eq$	$\frac{H^+}{(H^+)} HCl/NaCl$ $\mu eq$	$H^+$ $\mu eq$	$\bar{K}_i$ eqt. (23)	$\bar{K}_i$ eqt. (24)
0.1	7.29	1.95	15.4	4.0	7.8	5.83	3.2	30.7	27.6	6.1	5.5
	3.31	1.31	13.8		5.2	2.65	1.6	22.1	18.5	6.5	
	1.10	0.75	11.5		3.1	0.60	0.6	13.5	10.6	10.1	
	0.44	0.48	13.6		1.9	0.38	0.3	8.3	6.8	6.2	
0.2	7.29	1.95	15.2	16.1	15.6	5.83	3.2	17.6	13.8	7.0	5.5
	3.31	1.31	14.9		10.4	2.65	1.6	13.6	9.3	7.9	
	1.10	0.75	12.2		6.0	0.60	0.6	8.9	5.3	13.1	
	0.44	0.48	16.8		3.7	0.38	0.3	6.0	3.4	8.7	
0.3	7.29	1.95	15.4	36.2	23.6	5.83	3.2	14.6	9.2	8.7	5.5
	3.31	1.31	14.8		15.7	2.65	1.6	11.5	6.2	10.1	
	1.10	0.75	9.8		8.7	0.60	0.6	7.6	3.5	16.3	
	0.44	0.48	16.6		5.7	0.38	0.3	4.8	2.3	10.5	
0.5	7.29	1.95	13.9	101	39.5	5.83	3.2	9.9	5.5	9.8	5.5
	3.31	1.31	11.0		26.3	2.65	1.6	8.1	3.7	11.8	
	1.10	0.75	10.5		14.9	0.60	0.6	5.5	2.1	20.1	
	0.44	0.48	8.4		9.7	0.38	0.3	3.5	1.4	13.1	

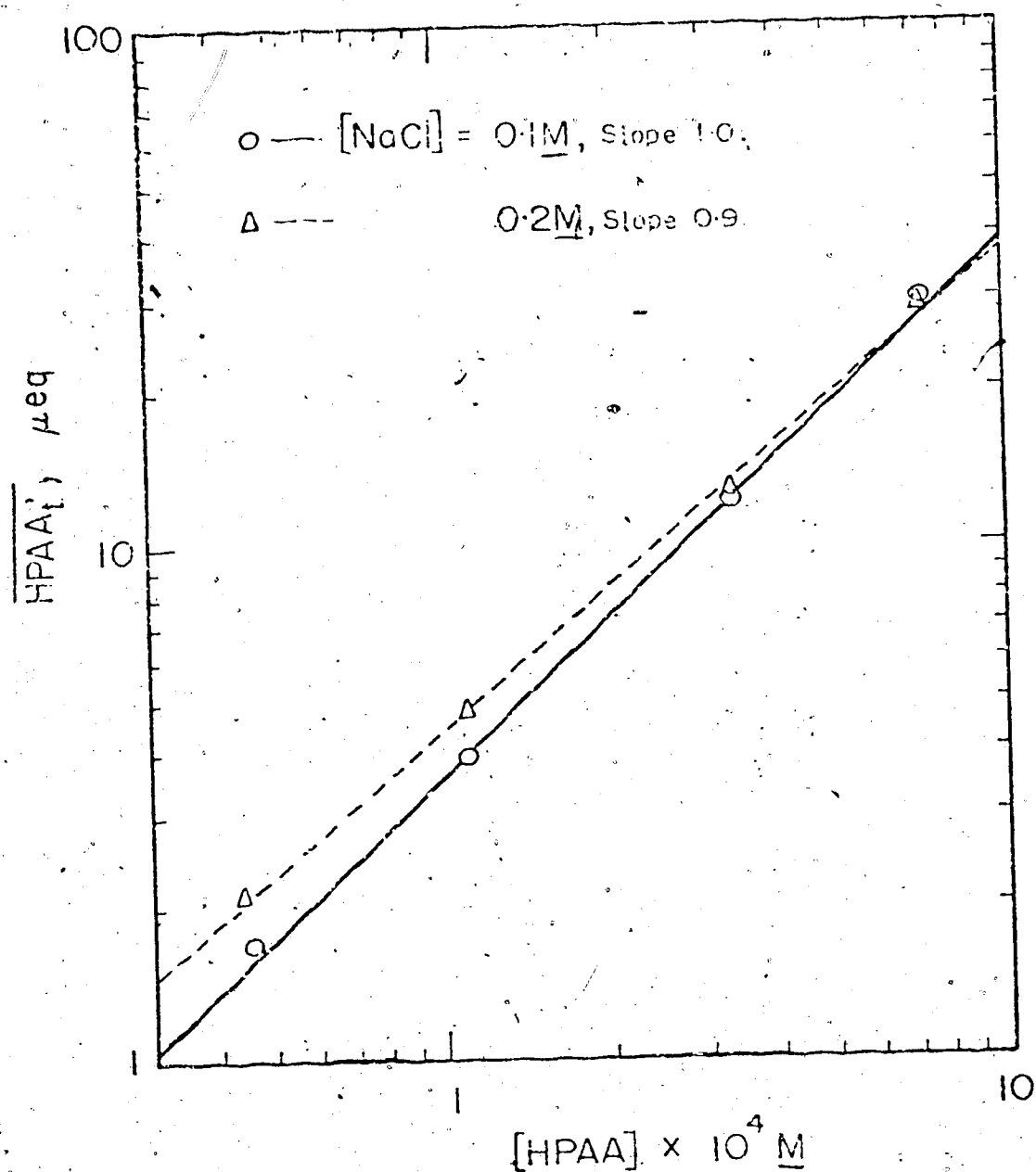


Figure 25a. The total sorption of HPAA on 16.25 meq of Dowex 50W x 8 at various concentrations of HPAA and NaCl

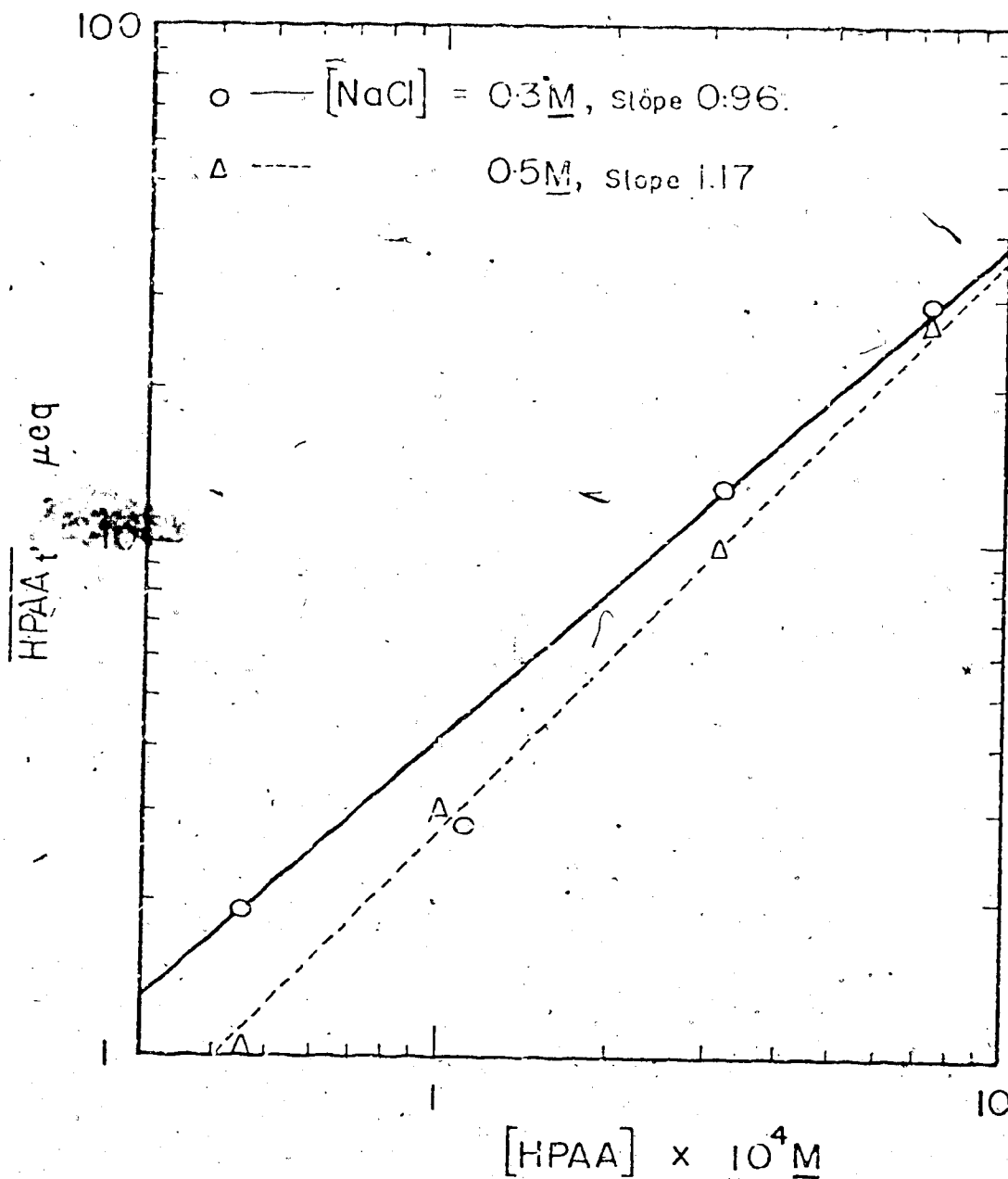


Figure 25b. The total sorption of HPAA on 16.25 meq of Dowex 50W  $\times$  8 at various concentrations of HPAA and NaCl

The dead volume,  $V_m$ , the exchanged  $H^+$ ,  $H^+$ , and the amount of sorbed material,  $HPAA_t$ , all contribute to the total acid content,  $H_t^+$ , measured in the NaCl washings by coulometry. The magnitude of  $H^+$  at fixed NaCl concentrations is determined only by  $[H^+]$  in solution, as is indicated by the study of HBSA sorption; and by the independence of  $HPAA_t$  on  $[NaCl]$  observed in the spectroscopic data.  $H^+$  is affected by neither the organic coion  $PAA^-$  nor by the sorbed molecules in the resin; therefore  $H^+$  at a given  $[H^+]$  can be estimated from the HCl/NaCl exchange data in Chapter III, Figure 5. Then

$$\overline{HPAA}_t = \overline{H}_t^+ - (\overline{H}_t^+)_{HCl/NaCl}$$

where  $(\overline{H}_t^+)_{HCl/NaCl}$  is the amount of sorbed hydrogen ion, calculated from the NaCl/HCl exchange data. The values of  $\overline{HPAA}_t$  calculated in this way are listed in column 7 of Table 20 and can be compared with the values of  $\overline{HPAA}_t$  obtained by spectrophotometry (column 8, Table 20). The excellent agreement observed between those two values validates the use of  $H^+$  sorption data from HCl/NaCl exchange for weak acid exchange. It also reveals that HPAA sorption is quite labile and reversible, since this species can be easily removed from the column by 50 ml of 0.8 M NaCl solution. The value of  $(\overline{H}_t^+)_{HCl/NaCl}$  was corrected for dead volume and was used for the calculation of  $\overline{K}_1$ .

Calculation of  $\bar{K}_1$  necessitates information on  $K_1$  [HPAA] and  $K_5$  [PAA<sup>-</sup>], as well as data on  $H^+$ .  $K_1$  can be estimated using the same approach as given in section 1. A  $\mu$  value for  $\mu$  of 8% DVB resin in the sodium form is not available in the literature, but it can be considered to be approximately that of  $H^+$  resin, which is 110 atm<sup>159,87</sup>. Assuming  $\bar{V}_N$  for HPAA to be also around 60 ml/mole, then

$$K_1 = \exp[-110 \times 60 / 0.08205 \times 300 \times 1000]$$

$$\approx 0.8$$

The value for  $K_5$  is estimated to be unity, and  $\bar{Cl}^-$  is estimated from the Donnan invasion sorption equation in Chapter III (Equation (14a)) as

$$\bar{Cl}^- = 418 [Cl^-]^2$$

where  $\bar{Cl}^-$  is expressed in meq, and is calculated on the basis of 16.9 meq. Converted to a basis of 16.25 meq, it can be written as

$$\bar{Cl}^- = 402 [Cl^-]^2$$

The values of  $\bar{Cl}^-$  thus calculated are tabulated in column 5 of Table 21. Once  $\bar{Cl}^-$  is known,  $\bar{PAA}^-$  can be obtained from Equation (A5c), with  $K_5$  taken as 1.

$$\frac{\bar{PAA}^-}{[PAA^-]} \cdot \frac{[Cl^-]}{\bar{Cl}^-} = 1$$



The values of  $\overline{PAA^-}$  at different concentrations of  $[NaCl]$  and  $[PAA^-]$  are shown in column 6, Table 21. Using 0.8 for  $\underline{K}_1$ , values of  $[\overline{HPAA}]$  were estimated from Equilibrium (1), Scheme 3, by

$$[\overline{HPAA}] = \underline{K}_1 [\overline{PAA^-}]$$

and listed in column 7 of Table 21.  $\overline{K}_i$  was then calculated from

$$\overline{K}_i = \frac{[\overline{H^+}][\overline{PAA^-}]}{[\overline{HPAA}]} = \frac{\overline{H^+} \cdot \overline{PAA^-}}{\underline{V}_s^2 [\overline{HPAA}]} \quad (23)$$

and tabulated in column 11 of Table 21.

The exceedingly large values of  $\overline{K}_i$  and strong dependence of  $\overline{K}_i$  on the external salt concentration indicate significant uncertainty in the estimates made or in the postulated equilibrium steps. As pointed out in the conclusion of Chapter III, hydrogen ion behaves abnormally in exchange, and has a retention volume nearly double that predicted by  $\underline{K}_{H/Na}(\overline{X}_H=0)$ . The extra hold-up of  $H^+$  is believed to be due to association in terms of a homogeneous model. Using the same symbols as in Chapter III,  $\overline{H}_s^+$  is the amount of  $H^+$  hold-up by association, and belongs to the resin matrix, whereas  $\overline{H}_e^+$  calculated by  $\underline{K}_{H/Na}(\overline{X}_H=0)$  is actually in internal solution and responsible for the internal dissociation equilibrium. From Chapter III,  $\underline{K}_{H/Na}(\overline{X}_H=0)$  was found to be 0.87.

Then

$$\frac{H_e^+}{[H^+]} \frac{[Na^+]}{Na_e^+} = 0.87$$

and

$$\frac{H_e^+}{H_e^+} = 0.87 \frac{[H^+]_{eq}}{[Na^+]} = \frac{0.87 [H^+] 16.25}{[Na^+]}$$

$$14.1 \frac{[H^+]}{[Na^+]} \quad \text{in meq.}$$

The values of  $H_e^+$  obtained (column 10, Table 21) can be used to calculate  $\bar{K}_i$  by

$$\bar{K}_i = \frac{[H_e^+][PAA^-]}{[HPAA]} = \frac{H_e^+ \cdot PAA^-}{v_s^2 [HPAA]} \quad (24)$$

The  $\bar{K}_i$  thus measured has an average value of  $5.5 \times 10^{-5}$ , which agrees with  $K_i$  ( $5.2 \times 10^{-5}$ ) within the uncertainty introduced by the various assumptions. The following section gives additional support for this value.

The better value of  $\bar{K}_i$  obtained from Equation (24) by taking into account the association of  $H^+$  furnishes further support for the theory developed in Chapter III.  $H_s^+$  is strongly associated with the resin phase, and does not take part in any of the equilibria occurring in the internal solution.

#### HCAA-NaCl-H<sub>2</sub>O-Dowex 50W × 8 System

Attempts at the UV spectrophotometric measurement of the concentration of HCAA were unsuccessful

because absorption by the small amount of HCAA present (in the order of  $10^{-5}$  to  $10^{-4}$  M as calculated by the dead volume contribution) was interfered with seriously by 0.3 M NaCl, even though the molar absorptivity of the latter is much smaller. This measurement problem did not exist for HBA, though the measurements were made under the same conditions as for HCAA, owing to the stronger molar absorptivity of HBA. Therefore colorimetric determinations of the acid content,  $H_0^+$ , were used, and gave satisfactory results. The concentrations of  $[H^+]$  and  $[HCAA]$  in solution were calculated by Equation (22), section 5. The values of  $H_0^+$ , after conversion to a 16.9 meq basis (column 5, Table 22), were divided by the corresponding  $[H^+]$  and are listed in column 6 of Table 22. Then  $\log H_0^+/[H^+]$  was plotted against  $[H^+]$  (Figure 26) on the same graph as HCl/NaCl exchange (Figure 5, Chapter III) for comparison. The good agreement observed indicates that molecular sorption of HCAA on Dowex 50W-3 is very small.

Using Equation (24),  $\bar{K}_1$  can be calculated as follows:

$$\bar{K}_1 = \frac{\bar{H}_0^+ \cdot \bar{A}}{[HA]V_B}$$

$$[\bar{HA}] = \bar{K}_L[HA]$$

$$\bar{H}_0^+ = \bar{K}_{H/Na} (\bar{X}_H = 0) \frac{[H^+]}{[Na^+]} \bar{Na}_e^+$$

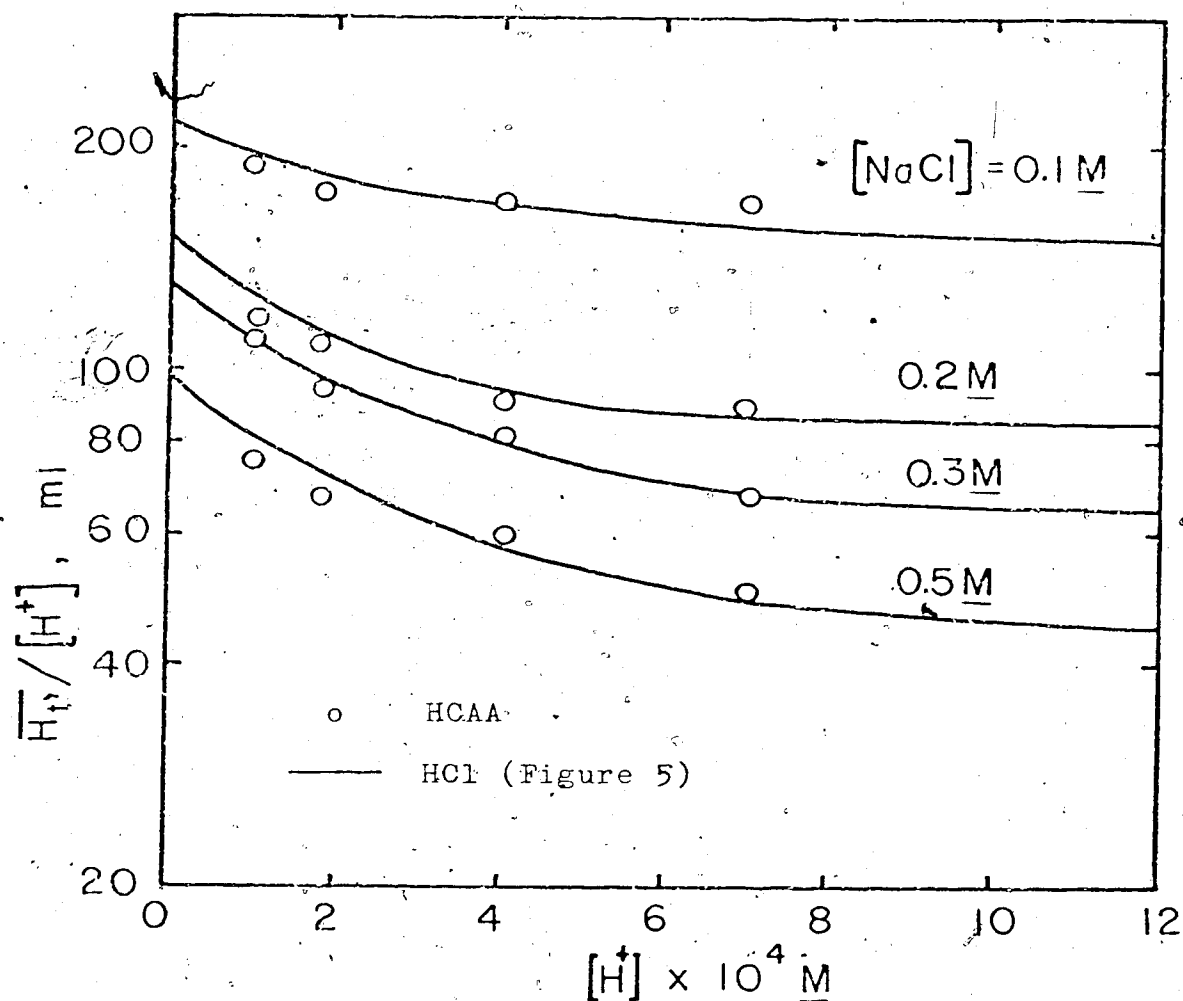


Figure 26. Comparison of the ratio of total sorbed HCAA on Dowex 50W x.8 over  $H^+$  concentration in equilibrium with HCAA in external solution at various  $H^+$  concentration and with that of HCl in Figure 5

$$\bar{A}^- \approx \frac{[A^-]}{[Cl^-]} \bar{Cl}^- \quad (AIII5c)$$

$$\bar{Cl}^- = 402 [Cl^-]^2 \quad (\text{Equation (14a)}) \text{ on } 16.25 \text{ meq basis}).$$

Substituting these values in Equation (24)

$$\begin{aligned} \bar{K}_i &= \frac{K_{H/Na} (\bar{X}_H=0)}{[Na^+]} \frac{Na_e^+ \cdot 402 [A^-] [Cl^-] \times 10^{-3}}{[HA] K_1 v_s^2} \\ &= \frac{K_{H/Na} (\bar{X}_H=0)}{[HA]} \frac{Na_e^+ \cdot 402 \times 10^{-3}}{K_1 v_s^2} \\ &= \frac{K_{H/Na} (\bar{X}_H=0) K_i}{K_1 v_s^2} \approx \frac{402 \times 10^{-3}}{K_1 v_s^2} \end{aligned}$$

If chloroacetic acid is considered sufficiently close to acetic acid in size that  $K_1$  can be assumed to be 0.8 (Chapter V, section 1), then

$$\begin{aligned} \bar{K}_i &= \frac{0.87 \times 16.9 \times 402 \times 10^{-3}}{0.8 \times 2.7^2} \times K_i \\ &= 1.00 K_i = 1.4 \times 10^{-3} \end{aligned}$$

The good agreement found between  $\bar{K}_i$  ( $1.4 \times 10^{-3}$ ) and  $K_i$  ( $1.4 \times 10^{-3}$ ) for HCAA supports the theory developed in this chapter. Internal dissociation does take place in the internal solvent, and the homogeneous model is appropriate for describing the internal equilibrium steps. It also provides indirect proof for association of  $H^+$  in the resin.

## CONCLUSIONS

The stoichiometric method described in Chapter II is effective in measuring ion exchange constants for all kinds of ion exchange materials in any physical form. It is rapid, simple and can readily be applied to routine analysis. The precision is obtained as a function of the loading factor  $\alpha$ , the optimum range of  $\alpha$  being from 0.4 to 1. Within this range the error is less than 1%.

The sorption isotherm for  $H^+$  on Dowex 50w resins was obtained as a function of  $[H^+]$  and  $[Na^+]$ . In ion exchange chromatography, where the solute contains trace amounts of  $H^+$ , the retention volume of  $H^+$  is doubled over that predicted by the ion exchange constant alone. The unexpectedly large uptake of  $H^+$  at trace levels is due to the association of  $H^+$  with either the sulfonate groups or with small amounts of carboxylate groups present as an impurity. The latter possibility is more likely.

The experiment described in Chapter V for weak acid sorption confirms the presence of an internal dissociation equilibrium for three different weak acid systems.  $\bar{K}$  was found not to be affected to any significant extent by the high charge density in the resin. Owing to internal dissociation, the sorptions of  $\bar{H}^+$ ,  $\bar{A}^-$ , and  $\bar{HA}$  are not independent.

Once the sorption of a weak acid HA and of  $H^+$  is known, the retention time of that acid in elution ion exchange chromatography can be predicted. The poisoning by organic acids and thus the life time of ion exchangers in desalination can also be estimated by the amount of weak acid sorbed. The sorption of weak acids is also important in treating waste water containing organic acid pollutants and salts. Ion exchange resins are known to catalyze reactions such as hydrolysis of esters and inversion of sugars. The catalytic power of ion exchangers should depend on the sorption of the reactants and products. An improved understanding of the sorption of weak bases and acids facilitates better understanding of catalytic mechanisms in the resin phase as well as the catalytic effectiveness of the resin itself.

To further support the arguments in the text, the individual species, such as  $\overline{HA}^*$ ,  $\overline{HA}$ ,  $\overline{A}^-$ , have to be measured independently. At the present stage, no instrumental technique is available for this purpose; it is hoped that technology will be developed in the future to permit such measurements.

Regarding future work, further study of exchange reactions involving carboxylate resins is recommended, so that the mechanism of  $H^+$  uptake may be elucidated by comparing the exchange constant with the association constant

measured in this work. It would also be of interest to study the sorption of weak acids on weak acid or weak base ion exchange resins, where association occurs in the external solution as well as in the internal solution and in the exchange groups.



## GLOSSARY

- $\bar{a}$  effective capacity for sorption of  $H^+$ ,  $\mu\text{eq.}$
- $\bar{a}_N, a_N$  the activity of molecular species in the resin phase and solution phase, respectively.
- $a'$  the maximum amount of solute that can be adsorbed on unit weight of resin (sites in Langmuir isotherm),  $\text{m mole/g.}$
- $B$  parameter in error equation  $H_O [\bar{V}_a / (\bar{V}_a + \bar{V}_O)]$ ,  $\underline{M.}$
- $\underline{c}$  exchange capacity of the resin sample,  $\text{meq.}$
- $\underline{c'}$  exchange capacity of the resin per unit external solution volume,  $\underline{M.}$
- $\underline{C}_O$  total acid concentration in solution,  $\underline{M.}$
- $\text{Cl}$  concentration of chloride ion in the external solution at equilibrium,  $\underline{M.}$
- $H$  concentration of hydrogen ion in the external solution at equilibrium,  $\underline{M.}$
- $H_O$  concentration of the acid added in stoichiometric method,  $\underline{M.}$
- $\bar{H}_t^+, \bar{H}_t^+$  total sorption of  $H^+$  (exchange and association), uncorrected and corrected for dead volume contribution respectively,  $\mu\text{eq.}$
- $\bar{H}_e^+, \bar{H}_e^+$  uptake of  $H^+$  due to exchange reaction, uncorrected and corrected for dead volume contribution respectively,  $\mu\text{eq.}$
- $\bar{H}_s^+$  additional uptake of  $H^+$  due to sorption mechanisms,  $\mu\text{eq.}$
- $\bar{H}_D^+$  amount of  $H^+$  sorbed due to Donnan invasion,  $\mu\text{eq.}$
- $\bar{H}R$  amount of resin in  $H^+$  form,  $\text{meq.}$

- $\overline{HA}_t$  total amount of acid sorbed in the resin phase as measured by UV spectroscopy,  $\mu\text{eq.}$
- $\overline{HA}^*, \overline{HA}$  amount of acid sorbed due to surface adsorption and true dissolution respectively,  $\mu\text{eq.}$
- $K_{A/B}$  ion exchange constant for the exchange reaction of A replacing B.
- $K_o$  homogeneous equilibrium constant, equal to  $(\underline{V}_s + \underline{k}_{Na} \underline{c}) / (\underline{k}_H + \underline{c} \underline{K})$ .
- $\overline{K}_i, \overline{\overline{K}}_i$  dissociation constant of weak acid in the external solution and resin phase.
- $(\overline{K}_i)_1, (\overline{\overline{K}}_i)_2$   $\overline{\overline{K}}_i$  calculated according to Schemes 1 and 2 respectively.
- $\underline{K}_4$  Donnan invasion coefficient in Step (4), i.e.  $[\overline{A}^-] / [A^-]^2$ .
- $\underline{k}_1, \underline{k}_2, \underline{k}_4$  heterogeneous rate constants, as defined by Equations (AII2), (A, II5).
- $\underline{k}_7$  molarity ratio of the neutral solute in resin phase to the solution phase due to true dissolution.
- $\underline{k}_{Na}, \underline{k}_H$  homogeneous rate constants for  $\text{Na}^+$  and  $\text{H}^+$ .
- $\underline{k}$  adsorptivity in Langmuir isotherm.
- $\text{Na}$  concentration of sodium ion in the external solution at equilibrium,  $\underline{M}$ .
- $\overline{\text{Na}}_D^+$  amount of  $\text{Na}^+$  sorbed due to Donnan invasion,  $\mu\text{eq.}$

$\overline{Na_c^+}, \overline{Na_c^+}$	uptake of $Na^+$ due to exchange reaction, uncorrected and corrected for the dead volume contribution respectively, meq.
$\overline{NaR}$	amount of resin in $Na^+$ form, meq.
$S_x$	standard deviation of the quantity concerned, $x$ , ( $x = Cl, H, H_2O, V_a, c$ ).
$S_K$	standard deviation of $K$ obtained by stoichiometric method.
$V_a$	volume of acid added, ml.
$V_m, V_m$	void volume (dead volume), ml.
$V_o$	volume of water retained in the resin, ml.
$V_R$	retention volume, ml.
$\overline{V}_N$	partial molal volume of the neutral species, ml/mole.
$V_s$	internal 'gel' water in the resin phase.
$\alpha$	loading factor, $B/c'$

## BIBLIOGRAPHY

1. R. Kunin, A.G. Winger. *Agnew. Chem. Intern. Ed.*, 1, 149 (1962).
2. F.L. Moore. *Anal. Chem.* 29, 1660 (1957).
3. K. Sollner, G.M. Shean. *J. Am. Chem. Soc.* 86, 190 (1964).
4. C.B. Amphlett. ) "Inorganic Ion Exchangers". Elsevier, N.Y., 1964.
5. W.J. Maecck, M.E. Kussy, J.E. Rein. *Anal. Chem.* 35, 2086 (1963).
6. G.T. Kerr, G.T. Koktails. *J. Am. Chem. Soc.* 83, 4675 (1961).
7. J.R. Miller, D.G. Smith, W.E. Marr, T.R.E. Kressman. *J. Chem. Soc.* 2740 (1964).
8. K. Kun, R. Kunin. *J. Polym. Sci.* 2, 587 (1964).
9. K.A. Kun, R. Kunin. *J. Polym. Sci. Part C* 16, 1457 (1967).
10. J.J. Kirkland. "Modern Practice of Liquid Chromatography", John Wiley and Sons, Inc., 1971, Chap. 1, p. 40.
11. C. Horvath, B. Preiss, S.R. Lipsky. *Anal. Chem.* 39, 1422 (1967).
12. C. Horvath, S.R. Lipsky. *Anal. Chem.* 41, 1227 (1969).
13. H.G. Cassidy, K.A. Kun. *Oxidation-Reduction Polymers, Polymer Reviews*, Vol. 11, N.Y., Interscience, 1965.
14. G. Manecke. *Angew. Makromol. Chem.* 45, 26 (1968).
15. M.J. Hatch, J.A. Dillon, H.B. Smith. *Ind. Eng. Chem.* 49, 1812 (1957).
16. F. Wolf, H. Mlytz. *J. Chromatog.* 34, 59 (1968).
17. G. Nickless, G.R. Marshall. *Chromatog. Rev.* 6, 154 (1964).
18. E. Blasius, B. Brozio. "Chelating Ion Exchange Resins in Chelates in Analytical Chemistry". New York, M. Dekker Publishing Co., 1969.

19. R. Hering. *Z. Chem.* 5, 402 (1965).
20. J.A. Lott, W. Rieman. *J. Org. Chem.* 31, 561 (1966).
21. S. Romano, K.H. Wells, H.L. Rothbart, W. Rieman. *Talanta* 16, 581 (1969).
22. A.J.P. Martin, R.L.M. Synge. *Biochem. J.* 35, 1385 (1941).
23. E. Glueckauf. *Trans. Faraday Soc.* 51, 34 (1955).
24. E. Glueckauf. "Ion Exchange and its Applications". London, Society of Chemistry Industry, 1955, p.34.
25. S.H. Tang, W.E. Harris. *Anal. Chem.* 45, 1977 (1973).
26. W.E. Cohn. *Science* 109, 377 (1949).
27. S. Moore, W.H. Stein. *J. Biol. Chem.* 192, 663 (1951).
28. Biorad. Lab. private communication, 1969.
29. M. Uziel, C.K. Koh, W.E. Cohn. *Anal. Biochem.* 25, 77 (1968).
30. C.D. Scott, R.L. Jolley, W.W. Pitt, W.F. Johnson. *Am. J. Clin. Pathol.* 53, 701 (1970).
31. A.T. Rave, K.S. Bhatki. *Anal. Chem.* 38, 1598 (1966).
32. D.O. Campbell, S.R. Butox. *Ind. Eng. Chem. Process Design Develop.* 9, 89 (1970).
33. K.A. Kraus, F. Nelson. *ASTM Spec. Publ. No.* 195, 27 (1958).
34. R.M. Wheaton, W.C. Bauman. *Ind. Eng. Chem.* 45, 228 (1953).
35. R. Sargent, W. Rieman. *J. Phys. Chem.* 61, 354 (1957).
36. W.E. Harris, B. Kratochvil. "Chemical Separations and Measurements". W.B. Saunders Co., Philadelphia, 1974, p. 227.
37. Y. Marcus. "Ion Exchange". J.A. Marinsky (ed.), Marcel Dekker Inc., N.Y. (1966), v.1, Chap. 3, p. 101.

38. G. Eisenman. "Ion-Selective Electrodes". R.A. Durst (ed.), National Bureau of Standards Special Publication 314, NBS Washington, D.C., 1969, Chap. 1.
39. H. Krause, O. Nentwich. Chem. Ingr. Tech. 40, 301 (1968).
40. K. Dorfner. "Ion Exchangers Properties and Applications". Ann. Arbor Science Publ. Inc., 1972.
41. J.W. Fisher, A.J. Vivyurka. Conference on Ion Exchange. London, 1969.
42. Ass. Sci. and Techn. Soc. of South Africa. "Uranium in South Africa 1946-1956". Vol. I, II. Johannesburg, 1957.
43. D.J. Crouse, K.B. Brown. Ind. Eng. Chem. 51, 1461 (1959).
44. J. Davison, F.O. Read, F.D.L. Noakes, T.V. Arden. Bull. Inst. Mining Met. 651, 247 (1961).
45. T.V. Arden, M. Giddings. J. Appl. Chem. 11, 229 (1961).
46. J.A. Tallmadge. Ind. Eng. Chem. Process Design Develop. 6, 419 (1967).
47. W.E. Blake, J. Randle. J. Appl. Chem. 17, 358 (1967).
48. G. Borgotte. Chem. Ztg. 92, 621 (1968).
49. F.X. McGarvey. Am. J. Oenol. 9, 168 (1958).
50. J. Dehner. Weinberg Keller 12, 403 (1965).
51. R.L. Gustafson. Ind. Eng. Chem. Prod. Res. Dev. 7, 107 (1968).
52. Ref. 40, p. 112, table 20.
53. M.V. Glikina. Biokhimiya 37(3), 594 (1972).
54. V.A. Nikiforov. Khim. Farm.Zh. 7(8), 43 (1973).
55. W. Neier. Hydrocarbon Pro. 51(11), 113 (1972).
56. O.N. Sharma. Indian J. Technol. 10(6), 221 (1972).
57. F. Helfferich. "Ion Exchange". McGraw-Hill Book Co., N.Y., 1962, p. 519.

58. J. H. Hildebrandt. "Ion Transfer in Heterogeneous Catalysis". MIT, Cambridge, 1970.
59. O.D. Bonner, V. Rhett. J. Phys. Chem. 57, 254 (1953).
60. A.A. Krylova, V.S. Soldatov. Russ. J. Phys. Chem. 39, 1597 (1965).
61. H.P. Gregor, F.C. Collins, M. Pope. J. Colloid Sci. 6, 245 (1951).
62. F. Helfferich, C.H. Peterson. Science 142, 661 (1953).
63. W. Rieman, H.F. Walton. "Ion Exchange in Analytical Chemistry". Pergamon Press, 1970, p. 53.
64. V.V. Rachinskii. Teor. Ionogo. obmena Khromatogr. Tr.Vses.Nauch.Tekh.Konf, 1965 (pub. 1968), p. 141.
65. G.M. Kolosova, Zh. Fiz. Khim. 42, 2873 (1968).
66. J.S. Mackie, P. Meares. Discussion Faraday Soc. 21, 111 (1956).
67. E. Glueckauf. J. Chem. Soc. 3280 (1949).
68. K. Dorfner. Reference 40, p. 124.
69. J.J. Wunsche, R. Henze. Chem. Tech. 20, 219 (1968).
70. H. Gehlesen, E. Fürstenberg, Energietechnik 16, 123 (1966).
71. Ref. 10, p. 120.
72. R.F. Hollis, C.K. McArthur. Mining Eng. 9, 422 (1957).
73. V.W. Weckman. A.I.Ch.E.J. 20, 833 (1974).
74. M.R. Ghatge, A.R. Gupta, J. Shankar. Indian J. Chem. 4, 64 (1966).
75. W.E. Harris, B. Kratochvil, Reference 36, p. 49.
76. J. Mandel. "The Statistical Analysis of Experimental Data". John Wiley and Son, Inc., 1964, pp. 71 and 72.
77. H.A. Laitinen and W.E. Harris. "Chemical Analysis". McGraw-Hill Book Co., Inc., 2nd Ed., 1975, p. 538.

78. E.B. Wilson. "An Introduction to Scientific Research". McGraw-Hill Book Co., N.Y., 1952, pp. 232 to 253.
79. W.E. Harris, B. Kratochvil. "Teaching Introductory Analytical Chemistry". W.B. Saunders Company, Philadelphia, 1973, p. 75.
80. L.M. Schwartz. Anal. Chem. 47, 963 (1975).
- 80a. F. Helfferich. Reference 57, Chap. 1, pp. 107-116.
81. J.E. Gordon. J. Phys. Chem. 66, 1150 (1962).
82. T.E. Gough, H.D. Sharma, N. Subramanian. Can. J. Chem. 48, 917 (1970).
83. H.D. Sharma, N. Subramanian. Can. J. Chem. 49, 457 (1971).
84. R.H. Dinius, M.T. Emerson, G.R. Choppin. J. Phys. Chem. 67, 1178 (1962).
85. V.V. Mank. Russ. J. Phys. Chem. 46, 200 (1972).
86. A. Darickova et al. Polym. Letters 8, 259 (1970).
87. G.E. Boyd, B.A. Soldano. Z. Elektrochem. 57, 162 (1953).
88. V.S. Redhina, J.A. Kitchener. Trans. Fara. Soc. 59, 515 (1963).
89. G. Zundel, H. Noller, G.M. Schwab. Z. Elektrochem. 66, 122, 129 (1962).
90. P.R. Ismatullaev. Uzb. Khim. Zh. 12, 29 (1968).
91. T. Yamabe. Kogyo. Kagaku. Zasshi. 70, 1839 (1967).
92. H.P. Gregor. J. Am. Chem. Soc. 70, 1293 (1948); 73, 642 (1951).
93. H. Kakihana, T. Nomura, H. Ohtaki. Bull. Tokyo Inst. Techn. Ser. B, No. 1, 14 (1960).
94. G.E. Boyd, J. Schubert, A.W. Adamson. J. Am. Chem. Soc. 69, 2818 (1947).
95. E. Glueckauf. Proc. Roy. Soc. (London). A214, 207 (1952).



96. L.A. Rice, F.E. Harris. *Z. Physik. Chem. (Frankfurt)* **B**, 207 (1956).
97. A. Euteneier. *J. Polym. Sci.* **23**, 683 (1957).
98. L.E. Arkhangelskii. *Termodinam. i kinetika khim. reaktsii* **60** (1963); 49 (1963).
99. J.B. Pauley. *J. Am. Chem. Soc.* **76**, 1422 (1954).
100. G. Eisenman. *Biophys. J. Suppl.* **2**(2), 259 (1962).
101. G. Eisenman. *Biol. Inst. Estud. Med. Biol., Mex.*, **21**, 155 (1963).
102. G. Eisenman. "Membrane Transport and Metabolism," A. Kleinzeller; A. Kotyk (ed.), Academic Press, N.Y., 1961, p. 163.
103. G.N. Ling. *J. Gen. Physiol., Suppl.* **43**, 149 (1960).
104. G.N. Ling. "A Physical Theory of Living States", Blaisdell, N.Y., 1962, Chap. 4.
105. E.M. Kuznetsova. *Russ. J. Phys. Chem.* **45**, 10 (1971).
106. A.M. Filimonova. *Zh. Fiz. Khim.* **43**, 1249 (1969).
107. E.D. Kalinina. *Russ. J. Phys. Chem.* **45**, 9 (1971).
108. T.L. Gulevskaya. *Vesti. Akad. Nauk. Belarus. SSR, Ser. Khim. Nauk* (1967), No. 4, 106.
109. F. Helfferich. Ref. 57, p. 78.
110. V.I. Gorshkov, O.N. Vorontsova, M.S. Safonov. *Russ. J. Phys. Chem.* **43**, 102 (1969).
111. J.J. Lingane. *Anal. Chem.* **26**, 622 (1954).
112. A.A. Krylova, V.S. Soldator, G.L. Starobinets. *Russ. J. Phys. Chem.* **39**, 1597 (1965).
113. J.J. Lingane. *Anal. Chim. Acta* **11**, 283 (1954).
114. K.W. Pepper, D. Reichenberg, D.K. Hale. *J. Chem. Soc.*, 3129 (1952).
115. F. Helfferich, Reference 57, p. 142.
116. F.G. Donnan, E.A. Guggenheim. *Z. Physik. Chem.* **A62**, 346 (1932).

117. D.H. Freeman. J. Phys. Chem. 64, 1049 (1960).
118. E. Glueckauf. Proc. Roy. Soc. (London), A268, 350 (1962).
119. G.E. Boyd, K. Bunzl. J. Amer. Chem. Soc. 89, 1776 (1967).
120. L.S. Frankel. Anal. Chem. 45, 1570 (1973).
121. P. Meares, J.F. Thain. J. Phys. Chem. 72, 2789 (1968).
122. G.L. Gaines, H.C. Thomas. J. Chem. Phys. 21, 714 (1953).
123. I.A. Legendchenko. Russ. J. Phys. Chem. 45, 1598 (1971).
124. E.M. Kuznetsova. Russ. J. Phys. Chem. 46, 1462 (1972); ref. 105.
125. G.E. Myers, G.E. Boyd. J. Phys. Chem. 60, 521 (1956).
126. R.W. Creekmore. Anal. Chem. 42, 570 (1970).
127. H.C. Thomas. Ann. N.Y. Acad. Sci. 49, 161 (1948).
128. A.O. Grigorov, L.K. Arkhangel'skii, E.A. Materova. Russ. J. Phys. Chem. 48, 1096 (1974).
129. H.P. Gregor, F. Gutoff, J.I. Bregman. J. Colloid Sci. 6, 245 (1956);  
H.P. Gregor, J.I. Bregman. J. Amer. Chem. Soc. 70, 2370 (1948).
130. I.M. Abrams. Ind. Eng. Chem. 48, 1469 (1956).
131. F.F. Cantwell, D.J. Pietrzyk. Anal. Chem. 46, 344 (1974).
132. F.F. Cantwell, Ph.D. Thesis, 1972, University of Iowa. "Heterogeneous acid-base titrimetry in ion exchange: Aqueous solution medium".
133. D. Reichenberg, D.J. McCauley. J. Chem. Soc., 2731 (1955).
134. L.S. Frankel. Anal. Chem. 43, 1506 (1971).

135. Rohm and Haas Co., Technical Bulletin, Ion Exchange Department EX-IE-29 (1967).
136. R.H. Doremus. "Ion Exchange". J.A. Marinsky (Ed.), M. Dekker, Inc., N.Y., v.2, Chap. 1, p. 1, 1969.
137. G. Eisenman (Ed.). "Glass Electrode for Hydrogen and Other Cations". M. Dekker, N.Y., 1966.
138. G.W. Morey. "The Properties of Glass". Reinhold, N.Y., 2nd Ed., 1954, p.69.
139. Stankevich, Vesti. Akad. Navuk Belarus SSR Ser. Khim. Navuk (4) 166 (1966).
140. F.X. Pollio, Environ. Sci. Technol. 1, 160 (1967).
141. R. Komer. Collect Czech. Chem. Commun. 37, 774 (1972).
142. V.O. Reikhsfeld. Zh. Prikl. Khim. (Leningrad) 45, 2487 (1972).
143. D. Reichenberg, W.F. Wall. J. Chem. Soc., 3364 (1956).
144. Y. Marcus, A.S. Kertes. "Ion Exchange and Solvent Extraction of Metal Complexes." Wiley Interscience, p. 267, 1969.
- 
145. L. Lazare, B.R. Sundheim, H.P. Gregor. J. Phys. Chem. 60, 641 (1956).
146. I. Langmuir. J. Amer. Chem. Soc. 38, 221 (1916).
147. D.O. Hayward, B.M.W. Trapnell. "Chemisorption". 2nd Ed., Butterworths & Co., London, 1964.
148. C.W. Davies, G.G. Thomas. J. Chem. Soc., 2624 (1951).
149. V.A. Vakulenko, E.P. Kuznetsova, I.V. Samborskii. Russ. J. Phys. Chem. 48, 569 (1974).
150. R.A. Stokes, H.F. Walton. J. Amer. Chem. Soc. 76, 3327 (1954).
151. F. Helfferich. Nature 189, 1001 (1961).
152. M. Ziegler. Agnew. Chem. 71, 283 (1959).

153. J. Aveston, D.A. Everest. Chem. Ind. (London) 1238 (1957).
  154. J.J. Pesek. Anal. Chem. 45, 1762. (1973).
  155. I.K. Tsitovich, E.I. Semenova. Russ. J. Anal. Chem. 27, 668 (1972).
  156. B.V. Moskvichev, G.V. Samsonov. Russ. J. Phys. Chem. 47, 1161 (1973).
  157. J. Feitelson. "Ion Exchange". J. Marinsky (ed.), M. Dekker, N.Y., vol. 2, 1969, p. 139.
  158. E.M. Savitskaya, P.S. Nys. Termodin. Ionogo. Obmena. 187 (1968); Chemical Abstracts 71:54301h.
  159. H.P. Gregor, B.R. Sundheim, K.M. Held, M.H. Waxman. J. Colloid Sci. 7, 511 (1952).
  160. J.C.R. Turner, C.B. Snowdon, D.C. Jones, J.W.C. Ward. Trans. Instn. Chem. Engrs. 46, T232 (1968).
  161. F. Helfferich, reference 57, p. 141.
  162. R.M. Silverstein, G.C. Bassler. "Spectrometric Identification of Organic Compounds." 2nd Ed., John Wiley and Son, N.Y., 1967.
  163. L. Lang. "Absorption Spectra in the UV and VIS region". Academic Press Inc., N.Y., vol. 12, 1969, pp. 23-4.
-

# Appendix I

Evaluation of the uncertainty,  $\Delta K/K$ , in the determination of  $K$ .

A) The uncertainty in  $K$  due to measurement errors in  $H^+$ ,  $(\Delta K/K)_H$ , can be derived as follows:

Differentiation of Equation (1) with respect to  $H$  gives

$$\left(\frac{\partial K}{\partial H}\right)_H = \frac{H \cdot \overline{NaR} \left\{ \overline{HR} \frac{\partial Na}{\partial H} + Na \frac{\partial \overline{HR}}{\partial H} \right\} - \overline{HR} \cdot Na \left\{ \overline{NaR} \frac{\partial H}{\partial H} + H \frac{\partial \overline{NaR}}{\partial H} \right\}}{\overline{NaR}^2 H^2}$$

$$\frac{\partial Na}{\partial H} = -1 \quad \text{From (4b)}$$

$$\frac{\partial \overline{HR}}{\partial H} = \frac{\partial \overline{HR}}{\partial Na} \frac{\partial Na}{\partial H} = +(\underline{V}_a + \underline{V}_o) (-1) \quad \text{From (4a, 4b)}$$

$$\frac{\partial \overline{NaR}}{\partial H} = \underline{V}_a + \underline{V}_o = - \frac{\partial \overline{HR}}{\partial H} \quad \text{From (5a)}$$

$$\frac{\partial H}{\partial H} = 1$$

$$\therefore \left(\frac{\partial K}{\partial H}\right)_H = \frac{1}{\overline{NaR} H} \left\{ -\overline{HR} - Na(\underline{V}_a + \underline{V}_o) \right\} - \frac{K}{\overline{NaR} H} \left\{ \overline{NaR} + H(\underline{V}_a + \underline{V}_o) \right\}$$

$$\frac{1}{K} \left(\frac{\partial K}{\partial H}\right)_H = \frac{-\overline{HR} - Na\underline{V}}{\overline{HR} Na} - \frac{\overline{NaR} + H\underline{V}}{\overline{NaR} H}$$

where  $\underline{V} \equiv \underline{V}_o + \underline{V}_a$ , the total volume of external solution.

If the uncertainty is small,  $\partial K/\partial H$  can be approximated by  $\Delta K/\Delta H$ <sup>77</sup>.

Upon rearrangement,

$$\begin{aligned} \left(\frac{\Delta K}{K}\right)_H &= \Delta H \left\{ \frac{-\overline{HR} - NaV}{\overline{HR} \cdot Na} - \frac{\overline{NaR} + HV}{\overline{NaR} H} \right\} \\ &= -\Delta H \left\{ +\frac{1}{Na} + \frac{V}{\overline{HR}} + \frac{1}{H} + \frac{V}{\overline{NaR}} \right\} \end{aligned}$$

Substituting Eqs. (2) to (5) into this expression gives

$$\left(\frac{\Delta K}{K}\right)_H = \Delta H \left\{ -\frac{2}{Na} - \frac{1}{B-Na} - \frac{1}{C'-Na} \right\} = \Delta H \left\{ \frac{-2Bc' + (B+c')Na}{Na(B-Na)(C'-Na)} \right\} \quad (Ala)$$

(Ala) shows the relative uncertainty  $(\Delta K/K)_H$  caused by  $\Delta H$ , the error in the measurement of  $H^+$ . Expressed in relative error,  $\Delta H/H$ , the relation

$$\left(\frac{\Delta K}{K}\right)_H = \left(\frac{\Delta H}{H}\right) \left\{ \frac{-2Bc' + (B+c')Na}{Na(B-Na)(C'-Na)} \right\} = \left(\frac{\Delta H}{H}\right) \left\{ -\frac{B}{Na} - \frac{c'Na}{K(C'-Na)^2} \right\} \quad (Alb)$$

is obtained.

B) In a similar way, the uncertainty in  $K$  due to the error in measurement of  $Cl$ ,  $(\Delta K/K)_{Cl}$ , can be obtained using the same technique as in A above.

$$\left(\frac{\partial K}{\partial Cl}\right)_{Cl} = \frac{H \cdot \overline{NaR} \left\{ \overline{HR} \frac{\partial Na}{\partial Cl} + Na \frac{\partial \overline{HR}}{\partial Cl} \right\} - \overline{HR} \cdot Na \left\{ \overline{NaR} \frac{\partial H}{\partial Cl} + H \cdot \frac{\partial \overline{NaR}}{\partial Cl} \right\}}{(\overline{NaR} H)^2}$$

$$\frac{\partial \overline{HR}}{\partial Cl} = \frac{\partial \overline{HR}}{\partial Na} \frac{\partial Na}{\partial Cl} = \frac{V_a + V_o}{V} = \frac{V}{V}$$

$$\frac{\partial Na}{\partial Cl} = \frac{\partial (Cl - H)}{\partial Cl} = 1$$

$$\frac{\partial H}{\partial Cl} = 0$$

Since  $H$  and  $Cl$  are mutually independent, any error in measuring  $Cl^-$  will not be reflected in measuring  $H^+$ .

$$\frac{\partial \overline{NaR}}{\partial Cl} = - \frac{\partial \overline{HR}}{\partial Cl} = -(\underline{V}_a + \underline{V}_o) = -\underline{V}$$

$$\begin{aligned} \therefore \frac{1}{\underline{K}} \left( \frac{\partial \underline{K}}{\partial Cl} \right)_{Cl} &= \frac{1}{\overline{HR} Na} (\overline{HR} + Na \underline{V}) + \frac{\underline{V}}{\overline{NaR}} \\ &= \frac{1}{Na} + \frac{\underline{V}}{\overline{HR}} + \frac{\underline{V}}{\overline{NaR}} \\ &= \frac{2\underline{c}' - Na}{Na(\underline{c}' - Na)} \end{aligned}$$

$$\left( \frac{\Delta \underline{K}}{\underline{K}} \right)_{Cl} = \Delta Cl \cdot \frac{2\underline{c}' - Na}{Na(\underline{c}' - Na)} \quad (A2a)$$

$$\text{and } \left( \frac{\Delta \underline{K}}{\underline{K}} \right)_{Cl} = \frac{\Delta Cl}{Cl} \cdot \frac{B(2\underline{c}' - Na)}{Na(\underline{c}' - Na)} \quad (A2b)$$

c) The uncertainty in  $\underline{K}$  due to the error in measurement of  $\underline{c}$ ,  $(\Delta \underline{K}/\underline{K})_{\underline{c}}$ , can be obtained by differentiating Eq. (1) with respect to  $\underline{c}$ .

$$\frac{1}{\underline{K}} \left( \frac{\partial \underline{K}}{\partial \underline{c}} \right)_{\underline{c}} = \frac{1}{\overline{NaR}} = \frac{1}{\underline{c}' - Na \underline{V}}$$

because

$$\frac{\partial H}{\partial \underline{c}} = \frac{\partial Na}{\partial \underline{c}} = \frac{\partial \overline{HR}}{\partial \underline{c}} = 0$$

This expression is considered valid because  $c$  is only used in calculating  $\overline{NaR}$ , and therefore  $\Delta \underline{c}$  is only reflected in  $\overline{NaR}$ , and not in  $Na$ ,  $H$  or  $\overline{HR}$ .

$$\therefore \left( \frac{\Delta K}{K} \right)_{\underline{C}} = \frac{\Delta \underline{C}}{\underline{C} - NaV} = \frac{\Delta \underline{C}'}{\underline{C}' - Na} \quad (A3a)$$

$$\left( \frac{\Delta K}{K} \right)_{\underline{C}} = \frac{\Delta \underline{C}'}{\underline{C}'} \left( \frac{\underline{C}'}{\underline{C}' - Na} \right) \quad (A3b).$$

D) The uncertainty in  $\underline{K}$  due to the error in measurement of  $H_O$ ,  $(\Delta \underline{K}/\underline{K})_{H_O}$ , can be obtained by differentiating Eq. (7).

$$\left( \frac{\Delta \underline{K}}{\Delta H_O} \right)_{H_O} = \frac{(\underline{C}' - Na)(\underline{B} - Na)2Na \frac{\partial Na}{\partial H_O} - Na^2(\underline{B} - Na) \frac{\partial \underline{C}'}{\partial H_O} - Na^2(\underline{C}' - Na) \frac{\partial \underline{B}}{\partial H_O}}{(\underline{C}' - Na)^2 (\underline{B} - Na)^2}$$

$$\frac{\partial Na}{\partial H_O} = 0 \quad \text{since measurement of Na is not affected by } H_O.$$

$$\frac{\partial \underline{B}}{\partial H_O} = \frac{\partial \frac{H_O \underline{V}_a}{\underline{V}_a + \underline{V}_O}}{\partial H_O} = \frac{\underline{V}_a (\underline{V}_O + \underline{V}_a) - H_O \underline{V}_a \frac{\partial \underline{V}_O}{\partial H_O}}{(\underline{V}_a + \underline{V}_O)^2}$$

$$\frac{\partial \underline{V}_a}{\partial H_O} = 0$$

but  $\frac{\partial \underline{V}_O}{\partial H_O} \neq 0$  because the magnitude of  $\underline{V}_O$  depends on  $H_O$  (see Eq. (6b)).

$$\frac{\partial \underline{V}_O}{\partial H_O} = \frac{\underline{V}_a}{\underline{E}}$$

From Eq. (6b)

$$\therefore \frac{\partial \underline{B}}{\partial H_O} = \frac{\underline{V}_a}{\underline{V}} - \frac{\underline{V}_a}{\underline{V}} = 0$$

The explanation is uncertainty in  $H_O$  will not propagate to  $\underline{B}$  where  $\underline{B} = Cl$ .



$$\frac{\partial \underline{c}}{\partial H_O} = 0$$

But,  $\frac{\partial \underline{c}'}{\partial H_O} \neq 0$  for  $\frac{\partial \underline{V}_O}{\partial H_O} \neq 0$

$$\begin{aligned} \frac{\partial \underline{c}'}{\partial H_O} &= \frac{\partial \frac{\underline{c}}{\underline{V}_a + \underline{V}_O}}{\partial H_O} = \frac{\underline{V} \frac{\partial \underline{c}}{\partial H_O} - \underline{c} \frac{\partial \underline{V}_a}{\partial H_O}}{\underline{V}^2} = -\frac{\underline{c}}{\underline{V}^2} \frac{\partial \underline{V}_a}{\partial H_O} \\ &= -\frac{\underline{c}}{\underline{V}^2} \frac{\underline{V}_a}{\underline{B}} = -\frac{\underline{c}'}{\underline{H}_O} \end{aligned}$$

$$\therefore \left( \frac{\partial \underline{K}}{\partial H_O} \right)_{H_O} = \frac{-N_a^2 \left( -\frac{\underline{c}'}{\underline{H}_O} \right)}{(\underline{c}' - Na)^2 (\underline{B} - Na)} = \frac{\underline{K} \underline{c}'}{(\underline{c}' - Na) \underline{H}_O}$$

$$\left( \frac{\Delta \underline{K}}{\underline{K}} \right)_{H_O} = \frac{\Delta H_O}{H_O} \left( \frac{\underline{c}'}{\underline{c}' - Na} \right) \quad (A4)$$

E) The uncertainty in  $\underline{K}$  due to the error in measurement of  $\underline{V}_a$ ,  $(\Delta \underline{K}/\underline{K})_{\underline{V}_a}$ , can be obtained by differentiating Eq. (7) with respect to  $\underline{V}_a$ ,

$$\left( \frac{\partial \underline{K}}{\partial \underline{V}_a} \right)_{\underline{V}_a} = \frac{-N_a^2 (\underline{B} - Na) \frac{\partial \underline{c}'}{\partial \underline{V}_a} - Na^2 (\underline{c}' - Na) \left( \frac{\partial \underline{B}}{\partial \underline{V}_a} \right)}{(\underline{c}' - Na)^2 (\underline{B} - Na)^2}$$

where  $\frac{\partial Na}{\partial \underline{V}_a} = 0$  because  $Na = Cl - H$ .

$$\frac{\partial \underline{B}}{\partial \underline{V}_a} = \frac{\partial \frac{H_O \underline{V}_a}{\underline{V}_a + \underline{V}_O}}{\partial \underline{V}_a} = \frac{\underline{V} H_O - \underline{V}_a H_O - H_O \underline{V}_a \frac{\partial \underline{V}_O}{\partial \underline{V}_a}}{\underline{V}^2}$$

$$\frac{\partial \underline{V}_O}{\partial \underline{V}_a} = \frac{\underline{V}_O}{\underline{V}_a}$$

From Eq. (6b)

$$= 0$$

$$\left(\frac{\partial K}{\partial \underline{V}_a}\right) \underline{V}_a = - \frac{Na^2 (\underline{B}-Na) \frac{\partial \underline{C}'}{\partial \underline{V}_a}}{(\underline{C}'-Na)^2 (\underline{B}-Na)^2}$$

$$\frac{\partial \underline{C}'}{\partial \underline{V}_a} = \frac{-\underline{C}'(1 + \frac{\partial \underline{V}_o}{\partial \underline{V}_a})}{\underline{V}} = - \frac{\underline{C}'}{\underline{V}_a}$$

$$\therefore \left(\frac{\partial K}{\partial \underline{V}_a}\right) \underline{V}_a = K \frac{\underline{C}'}{(\underline{C}'-Na) \underline{V}_a}$$

$$\left(\frac{\Delta K}{K}\right) \underline{V}_a = \frac{\Delta \underline{V}_a}{\underline{V}_a} \left(\frac{\underline{C}'}{\underline{C}'-Na}\right) \quad (A5)$$

F) Uncertainty due to all measurement errors  $(\Delta K/K)$ .  
Total error can be calculated by a combination of individual errors which are from mutually independent sources.

$$\left(\frac{\Delta K}{K}\right)^2 = \left(\frac{\Delta K}{K}\right)_H^2 + \left(\frac{\Delta K}{K}\right)_{Cl}^2 + \left(\frac{\Delta K}{K}\right)_{\underline{V}_a}^2 + \left(\frac{\Delta K}{K}\right)_{H_2O}^2 + \left(\frac{\Delta K}{K}\right)_{\underline{C}}^2 \quad (A6)$$

Since measurement errors can be expressed in two different ways, either as absolute error  $\Delta X$  or relative error  $\Delta X/X$ , the error equation (A6) can also be written in two forms.

i) Relative error form:

All measurement errors are in the form of  $\Delta X/X$ .

First  $Na$  is calculated from Eq. (7).

$$\underline{K} = \frac{Na^2}{(\underline{B}-Na)(\underline{C}'-Na)}$$

$$\underline{B}\underline{C}' - (\underline{B}+\underline{C}')Na + (1 - \frac{1}{\underline{K}}) Na^2 = 0$$

Since  $\underline{K}_H/Na = 0.8 \approx 1$  and  $Na \ll \underline{B}+\underline{C}'$ , then  $(1 - \frac{1}{\underline{K}})Na^2$

can be considered negligible and so  $\underline{Bc}' \approx (\underline{B} + \underline{C}')Na$ .

Therefore,

$$Na = \frac{\underline{Bc}'}{\underline{B} + \underline{C}'} \quad (A7a)$$

and

$$\underline{C}' - Na = \frac{\underline{C}'^2}{\underline{B} + \underline{C}'} \quad (A7b)$$

$(\Delta K/K)$  can be obtained by substituting Eqs. (A1b), (A2b), (A3b), (A4), (A5) and (A7a,b) into Equation (A6)

$$\begin{aligned} \left(\frac{\Delta K}{K}\right)^2 = & \left(\frac{\Delta H}{H}\right)^2 \left\{ \frac{\underline{B} + \underline{C}'}{\underline{C}'} + \frac{(\underline{B} + \underline{C}')\underline{B}}{K\underline{C}'^2} \right\}^2 + \left(\frac{\Delta Cl}{Cl}\right)^2 \left\{ \frac{(\underline{B} + \underline{C}')(\underline{C}' + \underline{B})}{\underline{C}'^2} \right\}^2 \\ & + \left(\frac{\Delta \underline{C}}{\underline{C}}\right)^2 \left(\frac{\underline{B} + \underline{C}'}{\underline{C}'}\right)^2 + \left(\frac{\Delta V_a}{V_a}\right)^2 \left(\frac{\underline{B} + \underline{C}'}{\underline{C}'}\right)^2 + \left(\frac{\Delta H_o}{H_o}\right)^2 \left(\frac{\underline{B} + \underline{C}'}{\underline{C}'}\right)^2 \end{aligned}$$

Rearranging into a more convenient form,

$$\begin{aligned} \left(\frac{\Delta K}{K}\right)^2 = & \left(\frac{\Delta H}{H}\right)^2 (1+\alpha)^4 + \left(\frac{\Delta Cl}{Cl}\right)^2 (1+\alpha)^2 (2+\alpha)^2 \\ & + (1+\alpha)^2 \left\{ \left(\frac{\Delta \underline{C}}{\underline{C}}\right)^2 + \left(\frac{\Delta V_a}{V_a}\right)^2 + \left(\frac{\Delta H_o}{H_o}\right)^2 \right\} \end{aligned} \quad (A8a)$$

where

$$\alpha = \frac{K}{1} \approx 1$$

$$\alpha = \frac{\underline{B}}{\underline{C}'} = \frac{\text{amount of acid added, meq}}{\text{capacity of the resin, meq}}$$

ii) Absolute error form

Using Eqs. (A1a), (A2a), (A3a), (A4), (A5)

and (A7a,b), it can be shown that

$$\begin{aligned}
\left(\frac{\Delta K}{K}\right)^2 &= (\Delta H)^2 \left\{ \frac{-2B\underline{c}' + (B+\underline{c}')Na}{Na(B-Na)(\underline{c}'-Na)} \right\}^2 + (\Delta Cl)^2 \left\{ \frac{2\underline{c}'-Na}{Na(\underline{c}'-Na)} \right\}^2 \\
&+ (\Delta \underline{c}')^2 \left\{ \frac{1}{\underline{c}'-Na} \right\}^2 + (\Delta H_O)^2 \left\{ \frac{\underline{c}'}{H_O(\underline{c}'-Na)} \right\}^2 + (\Delta \underline{V}_a)^2 \left\{ \frac{\underline{c}'}{\underline{V}_a(\underline{c}'-Na)} \right\}^2 \\
&= (\Delta H)^2 \left\{ \frac{(B+\underline{c}')^3}{(B\underline{c}')^2} \right\}^2 + (\Delta Cl)^2 \left\{ \frac{(2\underline{c}'+B)(B+\underline{c}')}{B\underline{c}'^2} \right\}^2 + (\Delta \underline{c}')^2 \frac{(B+\underline{c}')^2}{\underline{c}'^4} \\
&+ \left\{ \frac{(\Delta \underline{V}_a)^2}{\underline{V}_a^2} + \frac{(\Delta H_O)^2}{H_O^2} \right\} \left( \frac{B+\underline{c}'}{\underline{c}'} \right)^2 \\
&= (\Delta H)^2 \left\{ \frac{(1+\alpha)^6}{\alpha^4 \underline{c}'^2} \right\} + (\Delta Cl)^2 \left\{ \frac{(2+\alpha)^2 (1+\alpha)^2}{\alpha^2 \underline{c}'^2} \right\} + \frac{(\Delta \underline{c}')^2}{\underline{c}'^2} (1+\alpha)^2 \\
&+ \left\{ \frac{(\Delta \underline{V}_a)^2}{\underline{V}_a^2} + \frac{(\Delta H_O)^2}{H_O^2} \right\} (1+\alpha)^2 \quad (A8b)
\end{aligned}$$

## APPENDIX II

A) Heterogeneous model of ion exchange resins

In this model, it is assumed that  $\text{Na}^+$  counter ions are all held by electrostatic force, and thus localized in the resin, whereas the  $\text{Na}^+$  ion sorbed by Donnan invasion can move freely in the internal water. The latter form is designated as "non exchange-able  $\text{Na}^+$ " or "sorbed  $\text{Na}^+$ ", while "exchange  $\text{Na}^+$ " refers to the  $\text{Na}^+$  associated with the fixed charge groups. The amount of sodium ion sorbed may be considered under the conditions described to be equivalent to the sorption capacity, which is much smaller than the exchange capacity. The former changes with the concentration of the eluting electrolyte  $\text{NaCl}$ , and is described by Donnan exclusion theory<sup>116</sup>, while the latter is a constant depending only on the type of resin.  $\text{H}^+$  can replace not only "exchange  $\text{Na}^+$ " but also

"sorbed  $\text{Na}^+$ ". The replacement of sorbed  $\text{Na}^+$  contributes to the additional hold-up of  $\text{H}^+$  in chromatography.

The total  $\text{H}^+$  and  $\text{Na}^+$  present in the resin phase,  $\overline{\text{H}}_t^+$  and  $\overline{\text{Na}}_t^+$ , can each be divided into two terms

$$\overline{\text{H}}_t^+ = \overline{\text{H}}_s^+ + \overline{\text{H}}_e^+ = \overline{\text{H}}_s^+ + \frac{[\text{H}^+]}{[\text{Na}^+]} \frac{Kc}{\quad} \quad (\text{AIII})$$

$$\overline{\text{Na}}_t^+ = \overline{\text{Na}}_s^+ + \overline{\text{Na}}_e^+ \approx \overline{\text{Na}}_e^+ \approx c$$

where the subscripts s and e refer to sorption and exchange.

Thermodynamics makes no distinction between electrolyte in the sorption sites and in the exchange sites; the internal phase is treated as a concentrated solution containing fixed charged groups, counter ions and coions. The arbitrary distinction between these two kinds of electrolytes is thermodynamically ill-defined, just as is the definition of water of hydration.

Nevertheless, from a microscopic point of view those ions "belonging to" exchange sites experience a strong electrostatic field, such that a covalent bond may even exist in some cases<sup>126</sup>, whereas  $\text{Na}^+$  in sorption sites can move freely. In this case the adoption of a two-site model proves advantageous.

Assuming the replacement mechanism in the sorption site follows mixed first and second order kinetics<sup>127</sup>, the rate of electrolyte transport can be expressed as follows:

$$\left(\frac{dH}{dt}\right)_{s_1} = k_1 [\text{H}^+] \overline{\text{Na}}_s^+ \quad (\text{AII2})$$

$$\left(\frac{dH}{dt}\right)_{s_2} = k_2 \overline{\text{H}}_s^+ + k_4 [\text{Na}^+] \overline{\text{H}}_s^+ \quad (\text{AII3})$$

$$\left(\frac{d\text{Na}}{dt}\right)_{s_1} = k_4 [\text{Na}^+] \overline{\text{H}}_s^+ + k_5 \overline{\text{Na}}_s^+ + k_2 \overline{\text{H}}_s^+ \quad (\text{AII4})$$

$$\left(\frac{d\text{Na}}{dt}\right)_{s_2} = k_5 \overline{\text{Na}}_s^+ + k_1 [\text{H}^+] \overline{\text{Na}}_s^+ \quad (\text{AII5})$$

Subscript 1 refers to the species going from solution to the resin, and 2 refers to the species going from resin to the solution. The rate constants  $k_1$ ,  $k_2$ ,  $k_4$ , and  $k_5$  vary but little with concentrations of individual species. Equation (A112) contains only a second order term, which represents the situation that hydrogen ions in the external solution can go into the resin only by replacing sorbed  $\text{Na}^+$ . The direct entrance of  $\text{HCl}$  would result in a building up of electrolyte concentration in the internal solution, and is forbidden because of the high Donnan exclusion potential. Because the concentration of  $\text{NaCl}$  eluent is approximately  $10^2$  to  $10^4$  times greater than that of the  $\text{HCl}$  solute, the number of ions that can be accommodated by the internal solvent is essentially completely determined by the concentration and charge of the more concentrated species,  $\text{NaCl}$ . Thus the sorption capacity is nearly independent of  $\text{HCl}$  concentration.

Equation (A113) shows that the rate of hydrogen ion release by the resin is described by a first order, and a second order term. It can either leave the resin freely as  $\text{HCl}$  (first term), or by replacement (second term). Unlike replacement of  $\text{Na}^+$  in an exchange site, sorption replacement is not necessarily stoichiometric, that is,  $\text{H}^+$  can enter the exterior solution as  $\text{HCl}$  without the necessity of replacement by an equal amount of  $\text{Na}^+$ . The same interpretation applies to Equation

(AII5). Equation (AII4) is analogous to (AII3) but for two additional terms that account for the fact that as NaCl and HCl leave the resin, the "void space" is immediately re-occupied by NaCl from the external solution. The sorption level thus always remains constant for a given ionic strength.

At equilibrium, as determined by the column effluent having a constant pH (same pH as the solution being added), the following relationships exist:

$$\left(\frac{dH}{dt}\right)_{s_1} = \left(\frac{dH}{dt}\right)_{s_2} \quad \left(\frac{dNa}{dt}\right)_{s_1} = \left(\frac{dNa}{dt}\right)_{s_2}$$

Both relationships lead to the result

$$k_1 [H^+] \overline{Na_s^+} = k_2 \overline{H_s^+} + k_4 [Na^+] \overline{H_s^+}$$

Letting  $\underline{a}$  be the effective sorption capacity of the resin at  $[Na^+] = m$ , then  $\overline{Na_s^+} + \overline{H_s^+} = \underline{a}$ . By simple substitution

$$\frac{[H^+]}{\overline{H_s^+}} = \frac{[H^+]}{\underline{a}} + \frac{k_2 + k_4 [Na^+]}{k_1 \underline{a}} \quad (AII6)$$

If  $\overline{H_t^+}$  and  $\overline{Na_t^+}$  are known at given concentrations of NaCl and HCl in dynamic equilibrium on a column, then  $\overline{H_s^+}$  and  $\overline{Na_s^+}$  can be calculated by Equation (AII1) and  $\underline{K}$  can be measured accurately. Then a plot of  $[H^+]/\overline{H_s^+}$  vs.  $[H^+]$  should give a straight line with a slope equal to  $\underline{a}^{-1}$  if the proposed mechanism is correct. The ratios  $k_2/k_1$



and  $k_4/k_1$ , can be determined from a plot of the intercept-slope ratio  $I/S$  against  $[Na^+]$

$$\frac{I}{S} = \frac{k_2 + k_4 [Na^+]}{k_1} \quad (AII7)$$

#### B) Homogeneous models of ion exchange resins

In this model exchanged ions and Donnan sorbed ions are assumed to move freely in the internal solution, and are considered identical in every respect. Since a high charge density exists in the resin, some counter ions<sup>o</sup> will associate with the fixed ionic groups and result in additional uptake of  $H^+$ . The same notation as that introduced in the heterogeneous model is used here. The physical meaning of  $\overline{H_e^+}$  and  $\overline{H_t^+}$  is the same in both models; however  $\overline{H_s^+}$  is quite different here, being the hydrogen ion associated with the sulfonate groups or carboxylate groups.

The groups capable of hydrogen ion association may either be the sulfonate groups itself or carboxylate groups present in the resin as an impurity. Association with either one or both of these groups will cause increased uptake of  $H^+$  at low hydrogen ion concentration. The same mathematical treatments can be applied to either group, and the results are the same in either case. To be able to distinguish between these two homogeneous models by mathematical means is unlikely. The following approach is general, with a referring to either sulfonate groups capable of hydrogen ion association or carboxylate groups.

Since both  $\overline{H_e^+}$  and  $\overline{Na_e^+}$  (in the internal water phase) compete for effective groups, it can be described by a simple competitive adsorption isotherm<sup>146,147</sup>

$$\frac{\overline{H_e^+}}{H_s^+} = \frac{ak_H[\overline{H_e^+}]}{1 + k_H[\overline{H_e^+}] + k_{Na}[\overline{Na_e^+}]}$$

where  $a$  is the number of effective groups that can be associated at a specified ionic strength. The value of  $a$  depends on the internal ionic strength, that is, on the internal water content, and is a constant at any given ionic strength. The terms  $k_H$  and  $k_{Na}$  are apparent association constants.

$$\frac{[\overline{H_e^+}]}{H_s^+} = \frac{1 + k_H[\overline{H_e^+}] + k_{Na}[\overline{Na_e^+}]}{ak_H}$$

Since

$$[\overline{Na_e^+}] = c/V_s$$

and

$$[\overline{H_e^+}] = \frac{K[H^+][Na_e^+]}{[Na^+]}$$

then

$$\begin{aligned} \frac{[H^+]}{H_s^+} &= \left( \frac{1 + k_{Na}[\overline{Na_e^+}]}{ak_H} \right) \frac{[Na^+]}{[Na_e^+]K} + \frac{[H^+]}{a} \\ &= \left( \frac{V_s + k_{Na}c}{ak_H} \right) \frac{[Na^+]}{cK} + \frac{[H^+]}{a} \end{aligned} \quad (AII8)$$

and

$$\frac{I}{S} = \left( \frac{V_s + k_{Na}c}{k_H c K} \right) [Na^+] + \frac{[H^+]}{a} \quad (AII9)$$

## • APPENDIX III

In a thermodynamic treatment of electrolyte distribution between two phases, where transfer of charge from one phase to the other is involved, the electric potential  $\phi$  which is experienced by the ions has to be considered in addition to the chemical potential  $\mu$ . A collective term, called the electrochemical potential  $\eta$ , is used in dealing with such systems<sup>161</sup>.

$$\eta_i = \mu_i + z_i F \phi$$

Subscript  $i$  refers to the species  $i$ ;  $z_i$  to the charge on  $i$ ; and  $F$  to the Faraday constant. If the standard state is defined on pure  $i$  at pressure  $\underline{P}^\circ$  (usually 1 atm) at a certain temperature, then the chemical potential of the resin phase is

$$\overline{\mu}_i = \mu_i^\circ + RT \ln \overline{a}_i + (\overline{P} - \underline{P}^\circ) \overline{v}_i$$

Here  $\overline{v}_i$  is the partial molal volume of  $i$  and  $\overline{a}_i$  is the internal activity. (Because the standard state is defined at  $\underline{P}^\circ$  and the resin is under high pressure (osmotic pressure  $\pi$ ), the chemical potential due to pressure other than  $\underline{P}^\circ$  expressed by the  $(\overline{P} - \underline{P}^\circ) \overline{v}_i$  term, has to be added.

$$\pi = \overline{P} - \underline{P}^\circ$$

Then

$$\overline{\mu}_i = \mu_i^O + RT \ln \overline{a}_i + \pi \overline{V}_i \quad (\text{AIIII1})$$

and

$$\eta_i = \overline{\mu}_i + z_i F \bar{\phi} = \mu_i^O + RT \ln \overline{a}_i + \pi \overline{V}_i + z_i F \bar{\phi}$$

The chemical potential in the external solution can be written as

$$\mu_i = \mu_i^O + RT \ln \underline{a}_i$$

where the same standard state is used in the external solution. No pressure-volume term is added because the external solution is always at 1 atm, where the standard state is defined.

$$\eta_i = \mu_i^O + RT \ln \underline{a}_i + z_i F \bar{\phi} \quad (\text{AIIII2})$$

If equilibrium has been attained, the electrochemical potential in the two phases should be equal and the following equality can be written:

$$\mu_i^O + RT \ln \underline{a}_i + z_i F \bar{\phi} = \mu_i^O + RT \ln \overline{a}_i + z_i F \bar{\phi} + \pi \overline{V}_i$$

Rearranging,

$$\bar{\phi} - \phi = E_{\text{Don}} = \frac{RT}{z_i F} \ln \frac{\overline{a}_i}{\underline{a}_i} - \frac{\pi \overline{V}_i}{z_i F} \quad (\text{AIIII3})$$

$E_{\text{Don}}$  is the Donnan potential between the resin and external solution phases. In the system studied, HA-NaCl-H<sub>2</sub>O-Dowex 50W × 8, there are a total of four species, Na<sup>+</sup>, Cl<sup>-</sup>, H<sup>+</sup> and A<sup>-</sup>, which carry charge.

Correspondingly, four equations can be written

$$\frac{E_{\text{Don}}}{F} = \frac{RT}{F} \ln \frac{a_{\text{Na}}}{a_{\text{Na}}} - \frac{\pi \bar{v}_{\text{Na}}}{F} \quad (\text{AIII4a})$$

$$\frac{E_{\text{Don}}}{F} = \frac{RT}{F} \ln \frac{a_{\text{H}}}{a_{\text{H}}} - \frac{\pi \bar{v}_{\text{H}}}{F} \quad (\text{AIII4b})$$

$$\frac{E_{\text{Don}}}{F} = \frac{RT}{F} \ln \frac{a_{\text{A}}}{a_{\text{A}}} + \frac{\pi \bar{v}_{\text{A}}}{F} \quad (\text{AIII4c})$$

$$\frac{E_{\text{Don}}}{F} = \frac{RT}{F} \ln \frac{a_{\text{Cl}}}{a_{\text{Cl}}} + \frac{\pi \bar{v}_{\text{Cl}}}{F} \quad (\text{AIII4d})$$

The distribution ratio of any two species can be gotten by solving the two corresponding equations above.

Case 1 (AIII4a and b)

$$\frac{RT}{F} \ln \frac{a_{\text{Na}}}{a_{\text{Na}}} - \frac{\pi \bar{v}_{\text{Na}}}{F} = \frac{RT}{F} \ln \frac{a_{\text{H}}}{a_{\text{H}}} - \frac{\pi \bar{v}_{\text{H}}}{F}$$

$$\therefore \frac{a_{\text{Na}}}{a_{\text{Na}}} \frac{\bar{v}_{\text{H}}}{\bar{v}_{\text{Na}}} = \exp \left[ -\frac{(\bar{v}_{\text{Na}} - \bar{v}_{\text{H}})}{RT} \right] = \tilde{K}_{\text{H/Na}} \quad (\text{AIII5a})$$

The ion exchange constant obtained,  $\tilde{K}_{\text{H/Na}}$ , is a thermodynamic constant. The quantities  $\bar{v}_{\text{Na}}$  and  $\bar{v}_{\text{H}}$  are not easily defined; their physical meaning is that of the volume increase obtained upon the addition of a mole of  $\text{Na}^+$  or  $\text{H}^+$  to the resin phase. Since cations and anions cannot be separated,  $\bar{v}_{\text{Na}}$  and  $\bar{v}_{\text{H}}$  are not measurable, and have only thermodynamic significance. Nevertheless, values for these terms can be approximated

through use of hydrated ionic volumes, as is done in Gregor's model<sup>128,129</sup>.

Case 2 (AIII4a and d)

$$\frac{RT}{F} \ln \frac{\overline{a_{Na}}}{a_{Na}} - \frac{\pi \overline{v_{Na}}}{F} = \frac{RT}{F} \ln \frac{\overline{a_{Cl}}}{a_{Cl}} + \frac{\pi \overline{v_{Cl}}}{F}$$

$$\therefore \ln \frac{\overline{a_{Na} a_{Cl}}}{a_{Na} a_{Cl}} = \frac{-\pi (\overline{v_{Na}} + \overline{v_{Cl}})}{RT} = \frac{-\pi \overline{v_{NaCl}}}{RT}$$

$$\frac{\overline{m_{Na} m_{Cl}}}{m_{Na} m_{Cl}} = \left( \frac{\gamma_{\pm}}{\gamma_{\pm}} \right)^2 \exp \left[ - \frac{\pi \overline{v_{NaCl}}}{RT} \right]$$

In the case of single electrolyte sorption, where there is NaCl present but no HA, or where the ratio of [NaCl] to [HA] is large (as in the system under study), then  $\overline{m_{Na}} = \overline{m_R}$ , where  $\overline{m_R}$  is the capacity of the resin per unit weight of internal solvent. Then

$$\overline{m_{Cl}} = \frac{[Cl^-]^2}{\overline{m_R}} \left( \frac{\gamma_{\pm}}{\gamma_{\pm}} \right)^2 \exp \left[ - \frac{\pi \overline{v_{NaCl}}}{RT} \right] \quad (\text{AIII5b})$$

This is known as Donnan exclusion sorption.

Sorption of the major electrolyte present,  $Cl^-$ , is unaffected by the minor component HA so long as its concentration is low.

Case 3 (AIII4c and d)

$$\frac{\overline{a_A a_{Cl}}}{a_A a_{Cl}} = \exp \left[ \frac{\pi (\overline{v_A} - \overline{v_{Cl}})}{RT} \right] = K'_5$$

The distribution of  $\text{Cl}^-$  and  $\text{A}^-$  is determined by the partial molal volume difference, or roughly by the difference in hydrated ionic radii. Providing the sizes of two ions are nearly equal, or the osmotic pressure is low,  $K_5'$  will have a value of 1, which means that the resin shows no preference for either species. Neglecting activity effects, the above equation can be put into the more useful form:

$$\frac{[\text{A}^-][\overline{\text{Cl}}^-]}{[\overline{\text{A}}^-][\text{Cl}^-]} = K_5 \quad (\text{AIII5c})$$